Catalytic hydrotreating of solvent refined coal (SPC-II) : the effect of metal combinations, impregnation technique and water addition on catalyst activity

by Turgut Sahin

A thesis submitted in partial fulfillment of the requirements for the degree of Doctor of Philosophy in Chemical Engineering

Montana State University

Abstract:
Solvent refined coal (SRC-II) must be catalytically hydrotreated at elevated temperatures and pressures to improve its stability and meet the feedstock requirements of conventional petroleum refineries and boilers. Once the operating conditions are set, the development of catalysts is the primary problem.

Four transition metals, cobalt (Co), nickel (Ni), molybdenum (Mo) and tungsten (W), were selected as the catalytic agents and impregnated on a γ-alumina support having large surface area and pore size. In the first stage, seven different combinations of the metals were impregnated by a stepwise impregnation technique to test their hydrotreating activity. In the second stage, the most active metal combinations, Ni-Mo and Co-Mo, were subjected to three different impregnation techniques to test the effect of impregnation method on catalytic activity. The effect of the presence of 2 % water in the feed on the catalytic activity was tested for every catalyst.

The most active metal combinations among the seven were Ni-Mo for hydrodenitrogenation (HDN) and hydrogenation (HYD), and Co-Mo for hydrocracking (HYC). Water enhanced HDN activity of the catalysts containing Ni-Mo and Co-W combinations, but inhibited activity of the catalysts containing Co-Mo and Ni-W combinations. In general, HYC activities of the catalysts prepared by stepwise impregnation were improved by water addition.

Batchwise impregnation of Co after batchwise Mo impregnation reduced the interaction of Mo with the support giving more surface CoMoO, type phase and produced the most active catalyst. HDN and HYD activities of Ni-Mo catalysts were not greatly affected by the impregnation technique. In general, batchwise impregnation of Mo reduced Mo-support interaction and improved HYC activity of both Ni-Mo and Co-Mo catalysts. When both step size and order of metal impregnation were changed, the enhancing effect of water on HDN and HYC activities of the Ni-Mo catalysts disappeared and the inhibiting effect on HDN activities of the Co-Mo catalysts became more inhibiting.

CATALYTIC HYDROTREATING OF SOLVENT-REFINED COAL (SRC-II): THE EFFECT OF METAL COMBINATIONS, IMPREGNATION TECHNIQUE AND WATER ADDITION ON CATALYST ACTIVITY

by

Turgut Sahin

A thesis submitted in partial fulfillment
of the requirements for the degree

of

Doctor of Philosophy

in

Chemical Engineering

MONTANA STATE UNIVERSITY
Bozeman, Montana

December 1983

APPROVAL

of a thesis submitted by

Turgut Sahin

This thesis has been read by each member of the thesis committee and has been found to be satisfactory regarding content, English usage, format, citations, bibliographic style, and consistency, and it is ready for submission to the College of Graduate Studies.

Nov. 7, 1983
Date

Lloyd Berg
Chairperson, Graduate Committee

Approved for the Major Department

Nov. 7, 1983
Date

John T. Sears
Head, Major Department

Approved for the College of Graduate Studies

11-16-83
Date

Michael Malone
Graduate Dean

STATEMENT OF PERMISSION TO USE

In presenting this thesis in partial fulfillment of the requirements for a doctoral degree at Montana State University, I agree that the Library shall make it available to borrowers under rules of the Library. I further agree that copying of this thesis is allowable only for scholarly purposes, consistent with "fair use" as prescribed in the U.S. Copyright Law. Request for extensive copying or reproduction of this thesis should be referred to University Microfilms International 300 North Zeep Road, Ann Arbor, Michigan 48106, to whom I have granted "the exclusive right to reproduce and distribute copies of dissertation in and from microfilm and the right to reproduce and distribute by abstract in any form."

Signature _____

Date Nov. 7, 1983

This thesis is dedicated to my son, Koray, and my wife, Hatice

VITA

The author, Turgut Sahin, was born in Hisarardi, a small mountain village in a south-western province (Mugla) of Turkey, on March 1954 to Mr. Mustafa and Mrs. Gullu Sahin.

His elementary education was acquired in the same village: He attended the Middle School in the nearby town of Cine. He was graduated from Mugla Turgutreis Lysee (high school) in September 1972. In July 1979, he received his Bachelor of Science Degree in Chemical Engineering from Middle East Technical University in Ankara, Turkey.

In August 1979, he passed the Turkish Government's Scholarship Test and obtained a scholarship for Master of Science Study in Chemical Engineering with a research project in the synthetic fuels area. He enrolled in Montana State University's College of Graduate Studies to work toward the degree of M.S. in Chemical Engineering. After receiving his M.S. degree in March 1982, he continued his study for the Ph.D.

He was married to the former Hatice Aslan in May 1979 and they have a son, Koray.

ACKNOWLEDGEMENTS

The author wishes to thank the staff of the Chemical Engineering Department at Montana State University for their help and encouragement. A special thanks goes to Dr. Lloyd Berg and Dr. F.P. McCandless for their guidance with this research. The author would like to extend his thanks to the United States Department of Energy for their financial support that made this study possible.

Special appreciation goes to Lyman Fellows for his help in the maintenance of the equipment, and Dr. G.J. Lapeyre, Dr. J.R. Anderson and Dr. D.J. Frankel who helped in using XPS and analyzing the data. Many thanks must go to Tim Ward for his valuable time spent in elemental analyses.

The author would like to thank I-Hsing Tsoa and Jack Pan for their participation and cooperation in the group that made it possible to finish this study in a short period of time.

Finally, a special thanks goes to the author's wife, Hatice, and son, Koray, for their patience and encouragement.

TABLE OF CONTENTS

TABLE OF CONTENTS--Continued

LIST OF TABLES

LIST OF TABLES--Continued

LIST OF FIGURES

LIST OF FIGURES--Continued

LIST OF FIGURES--Continued

ABSTRACT

Solvent refined coal (SRC-II) must be catalytically hydrotreated at elevated temperatures and pressures to improve its stability and meet the feedstock requirements of conventional petroleum refineries and boilers. Once the operating conditions are set, the development of catalysts is the primary problem.

Four transition metals, cobalt (Co), nickel (Ni), molybdenum (Mo) and tungsten (W), were selected as the catalytic agents and impregnated on a γ-alumina support having large surface area and pore size. In the first stage, seven different combinations of the metals were impregnated by a stepwise impregnation technique to test their hydrotreating activity. In the second stage, the most active metal combinations, Ni-Mo and Co-Mo, were subjected to three different impregnation techniques to test the effect of impregnation method on catalytic activity. The effect of the presence of 2 % water in the feed on the catalytic activity was tested for every catalyst.

The most active metal combinations among the seven were Ni-Mo for hydrodenitrogenation (HDN) and hydrogenation (HYD), and Co-Mo for hydrocracking (HYC). Water enhanced HDN activity of the catalysts containing Ni-Mo and Co-W combinations, but inhibited activity of the catalysts containing Co-Mo and Ni-W combinations. In general, HYC activities of the catalysts prepared by stepwise impregnation were improved by water addition.

Batchwise impregnation of Co after batchwise Mo impregnation reduced the interaction of Mo with the support giving more surface $CoMoO_4$ type phase and produced the most active catalyst. HDN and HYD activities of Ni-Mo catalysts were not greatly affected by the impregnation technique. In general, batchwise impregnation of Mo reduced Mo-support interaction and improved HYC activity of both Ni-Mo and Co-Mo catalysts. When both step size and order of metal impregnation were changed, the enhancing effect of water on HDN and HYC activities of the Ni-Mo catalysts disappeared and the inhibiting effect on HDN activities of the Co-Mo catalysts became more inhibiting.

CHAPTER 1

INTRODUCTION

When the world oil crisis started in the early seventies, many nations around the world seriously started looking for alternative energy resources.

Among the several alternatives, coal is the most important one to the countries which have abundant coal reserves such as the United States. The United States has 3,600 billion metric tons of coal reserves and 200 billion metric tons of it is estimated to be currently economically recoverable [1]. According to the forecasts, it will be enough to supply the nation's liquid-fuel needs more than a century [2] if it is used only for liquefaction.

Coal as a solid fuel is not convenient to substitute for petroleum or natural gas, because the transportation sector exclusively depends on liquid fuels, the residential and commercial sectors depend heavily on gaseous fuels, and industry requires three quarters of its needs as liquid and gaseous fuels [3, 4]. Consequently, the conversion of coal to conventional forms (liquid or gas) is necessary.

The first gasification and liquefaction processes were developed in Germany during the 1900s and 1930s. They constitute the basis of the today's technology. Today, there are four basic coal liquefaction processes in the U.S., Solvent Refined Coal (SRC), Exxon Doner Solvent

(EDS), H-Coal, and Synthoil. They convert high sulfur coal to distillate liquids. The chemical composition and the physical properties of the coal liquids are considerably different from those of petroleum. They have a higher carbon-to-hydrogen ratio and higher heteroatom (S, N, O) concentrations.

Raw coal-derived liquids, as received from liquefaction units, must be further hydrotreated before being used either as a boiler fuel or refinery feed stock because of their high heteroatom content. Nitrogen, sulfur, and oxygen cause storage problems [5]. Sulfur and nitrogen content must meet the EPA emission standards [6]. In addition, basic nitrogen content must be minimized for refining processes to prevent catalyst poisoning.

The maximum requirement for nitrogen in refineries varies from process to process, but should not be more than 0.3 wt% in order to be processed in the existing refineries [7]. In this study, 0.3 wt% nitrogen in the product was taken as the minimum requirement.

The objective of this study was to develop catalysts which would be able to upgrade SRC-II Light Ends Column Feed (LECF) to a feed stock acceptable to present petroleum refineries.

CHAPTER 2

BACKGROUND

COAL AND COAL CONVERSION

Coal: Coal is a generic term applied to widespread and widely differing natural rocks that consists primarily of organic material admixed with smaller quantities of mineral matter [8].

Coal deposits were formed from plant materials by the action of heat and pressure for long periods of time . The first stage of coalification involves the heirarchial formation of peat, lignite, followed by subbituminous coal, bituminous coal, and finally anthracite. Coal is ranked differently in different countries and the classification method currently being used in the U.S. is shown in Table 1 [9].

Despite the years of research in this field, the chemical structure and chemical properties of coal are still not well understood today. The basic reason is the complexity of coal and dependence of chemical properties and structure on the geographical origin and rank [10]. The major elemental components of coal are carbon, hydrogen and oxygen; the minor elements include sulfur, silicon, nitrogen, aluminum, iron, calcium, magnesium, potassium, sodium, and titanium. Carbon is the most abundant element, and its molecular form in combination with small amounts of hydrogen and oxygen provides the structural integrity of coal. The organic compounds shown in Fig. 1 are thought to be among the important components in the organic portion of coal structure.

Table 1. Classification of Coals by Rank [9].

Class	ASTM classification method: Limits of fixed carbon[a] (% w/w)	Limits of heat content (Btu/lb)	Ultimate analysis ratio[b]: Carbon	Hydrogen	Oxygen
I. Anthracite	86-98	-	90-97	3-5	1-3
II. Bituminous			85-90	4-5	5-10
low-volatile	68-86	-			
medium-volatile	69-78	-			
high-volatile A	<69	≦14,000			
high-volatile B		13-14,000			
high volatile C		11,500-13,000			
III. Subbituminous		8,300-11,500	75-85	5	10-20
IV. Lignitic		6,300-8,300	70-75	4-5	20-25
(plants and trees)	25-30	4,000-5,000	50-60	5-6	35-40

a Mineral-matter-free (mmf) basis. To convert to MJ/kg, multiply by 0.00232.
b Dry-mineral-matter-free (dmmf) basis, normalized for exclusion of sulfur and nitrogen.

These organic structures are bonded together to form cross-linked polymers. These polymeric chains represent the molecule of coal. However, there is no unique structure found to represent a coal molecule. Among many proposed representative coal structures [13, 14, 15, 16], the one proposed by Solomon [17] is shown in Fig. 2.

Coal Utilization and Conversion: Commercial utilization of coal is directly linked to industrialization. When the British were faced with deforestation, they substituted coke from coal for wood charcoal [18]. Coal was used extensively in steam generation for steam engines and electricity production, as well as home heating, until the liquid distillate fuels from petroleum became more efficient for

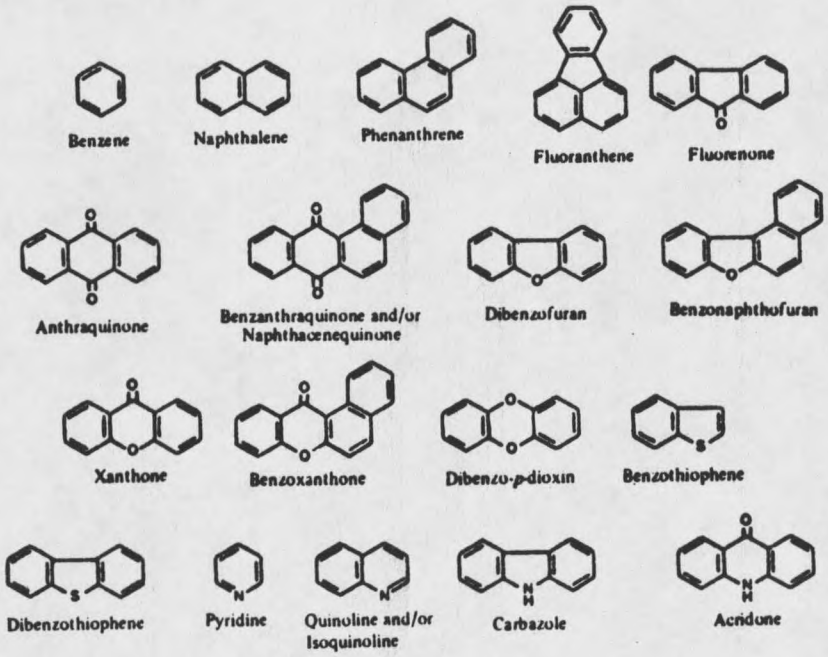

Figure 1. Aromatic Units Present in Coal Structure (adapted from the reference 12)

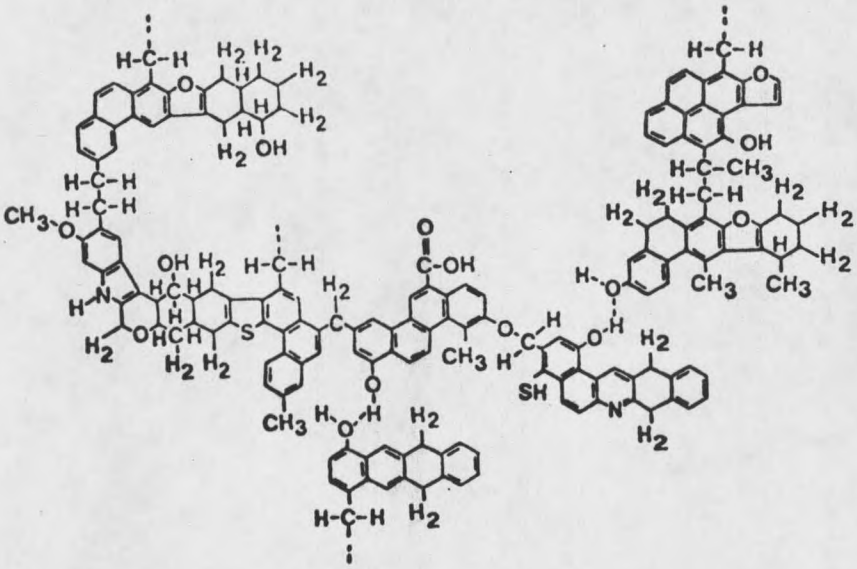

Proposed coal structure

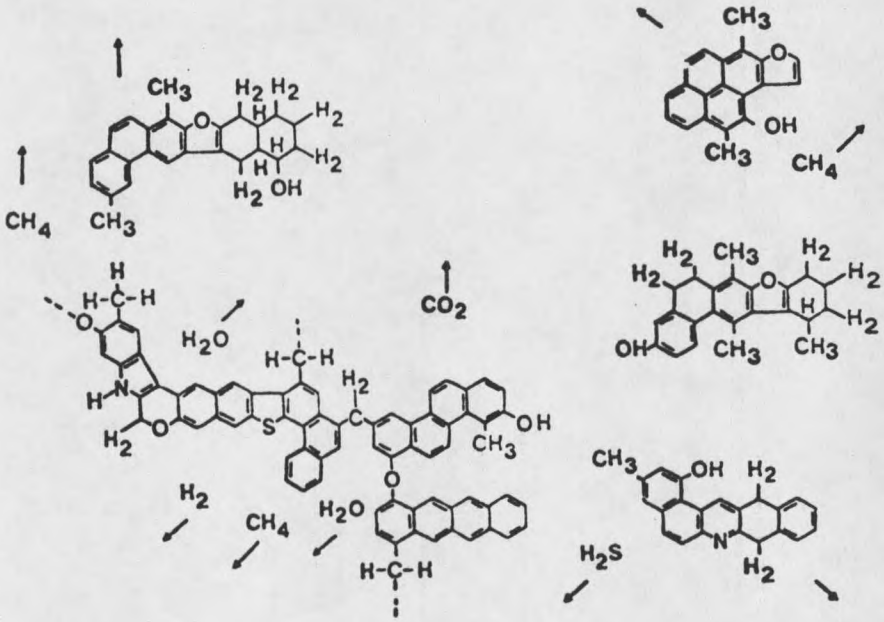

Possible racking of a coal molecule

Figure 2. Representative Structure of Coal Molecule

transportation, home heating and other forms of energy production. A factor in the decline of coal utilization was the extensive usage of natural gas in utilities after World War II [3].

The reasons behind these shifts include both convenience and cost. One measure of convenience is the concentration of energy per unit of fuel product. Approximately, wood contains 16 million Btu/ton, coal contains 26 million Btu/ton, and petroleum contains 40 million Btu/ton. This represents efficiency in transportation, storage and usage. The cost of crude oil was very low until 1973, and the natural gas prices were held at artificially low levels [3].

At present, the most common utilization of coal is metallurgical usage and combustion for energy production. For more extensive utilization of coal in today's technology, its conversion into gaseous or liquid fuels is required because of the dependence of users on these forms [3].

Conversion of coal is not a new idea. It extends far back to the early 18th century. When coke from coal was produced, the by-products were gaseous and liquid fuels from the pyrolysis ovens. However, only the gaseous products were used as fuel. The liquid products were utilized as chemicals.

After this initial stage, technological improvements were made for gasification of coal. Even though synthetic gas is not popular in the U.S., there are many commercial gasifiers around the world, especially in Europe. It is, however, reemerging in the U.S. today. There are about six major coal gasification processes; Descending

Bed, Fluidized Bed, Entrained Flow, Molten Bath, Tumbling Bed, and Underground Gasification.

In contrast to the gasification technology, the development of liquefaction technology waited until this century. Processes were pioneered in Germany during the 1920s and 1930s. Development of synthetic liquid fuels from coal followed two separate routes. First, the direct hydrogenation of coal was initiated by Bergius in 1913; and secondly, the production of liquids by the reaction of CO and H_2 was reported by Fischer and Tropsch in 1923 [19].

There were several commercial plants producing liquid fuels by using these two processes before and during the World War II. German capacity of the Bergius process was 70,000 bbl/day and that of Fischer-Tropsch process was 15,000 bbl/day [19]. Today, South Africa's SASOL process, based on the Fischer-Tropsch process, is the only commercial one producing liquid fuels from coal.

Coal liquefaction processes are usually classified as shown below [19];

Classification	Example
Pyrolysis	Coal-Oil-Energy-Development (COED)
	Lurgi-Ruhrgas
Direct Liquefaction	H-Coal and Bergius
Solvent Extraction	Solvent Refined Coal (SRC)
	Exxon Doner Solvent (EDS)
	Consolidation Synthetic Fuel (CSF)
Indirect Liquefaction	Fischer-Tropsch, Methanol

In the Pyrolysis Process, coal is heated in the absence of oxygen. This heating breaks down the coal molecules to form hydrogen rich gas, tar, and a hydrogen deficient char. The tar products are primarily aromatic in nature. This has been practiced industrially for decades.

In Direct Hydrogenation, a high purity hydrogen is used to react with coal at elevated temperatures and pressures in the presence of a catalyst. The products are primarily aromatic.

The Solvent Extraction Processes involve slurrying the pulverized feed coal in a coal-derived liquid and reacting at elevated temperatures and pressures. Hydrogen is added to the SRC and EDS processes. The products are primarily aromatic.

In Indirect Liquefaction, the feed coal is completely gasified to produce a synthesis gas consisting primarily of hydrogen and carbon monoxide. After purification, hydrogen and carbon monoxide are reacted at elevated temperatures and pressures in the presence of a catalyst. The products are aliphatic and olefinic in nature.

Thermal efficiency of these processes differ considerably from each other. In general the efficiencies of hydroliquefaction processes such as extraction, donor solvent, and direct hydrogenation are higher than those of complete pyrolysis and indirect liquefaction processes such as Fischer-Tropsch and methanol. Estimated efficiency of SRC-II is in the 63-77% range [19].

SRC Process: The SRC project was begun in 1962 when Spencer Chemical Company was awarded a research contract by the Office of Coal Research (OCR, subsequently a part of DOE) to study the technical feasibility of a coal deashing process (now called SRC process). In

1965, the process was successfully demonstrated with a 50-pound-per-hour continuous flow unit. During the term of contract, Gulf Oil Corporation acquired Spencer Chemical Company. After reorganization, the contract was assigned to the research department of Pittsburgh and Midway Coal Mining Company (P&M) [20].

Construction of a 50-ton-per-day pilot plant at Fort Lewis (Tacoma), Washington, was begun in 1972 and became fully operational in 1974. This early process is called SRC-I and produced a solid product. Later in 1977, the SRC-I process was modified to the SRC-II process to produce liquid products [20]. The SRC-II process flow diagram is shown in Fig. 3 [19].

In the SRC-II process, dried and pulverized coal is fed to the slurry mixing vessel where it is mixed with a slurry recycle stream and a filtered process solvent recycle. The entire slurry is pumped from the mixing vessel and the recycle plus make up hydrogen is injected in the stream ahead of the slurry heater. The mixture is heated to about 370°C in the slurry heater and then enters the dissolver at a pressure of about 13.8 MPa. The products come out of the reactor at about 425°C and are let down in pressure and cooled in several flash separations in the vapor/liquid separation section. The gases are sent to the acid gas removal unit to remove carbon dioxide and hydrogen sulfide to purify hydrogen. Part of the slurry stream is recycled back to the slurry mixing vessel; the rest is filtered to remove mineral residue and recover liquid products. The filtrate is vacuum distilled to produce distillate fuels overhead and SRC bottoms. The distillates are fractionated into light oil, light

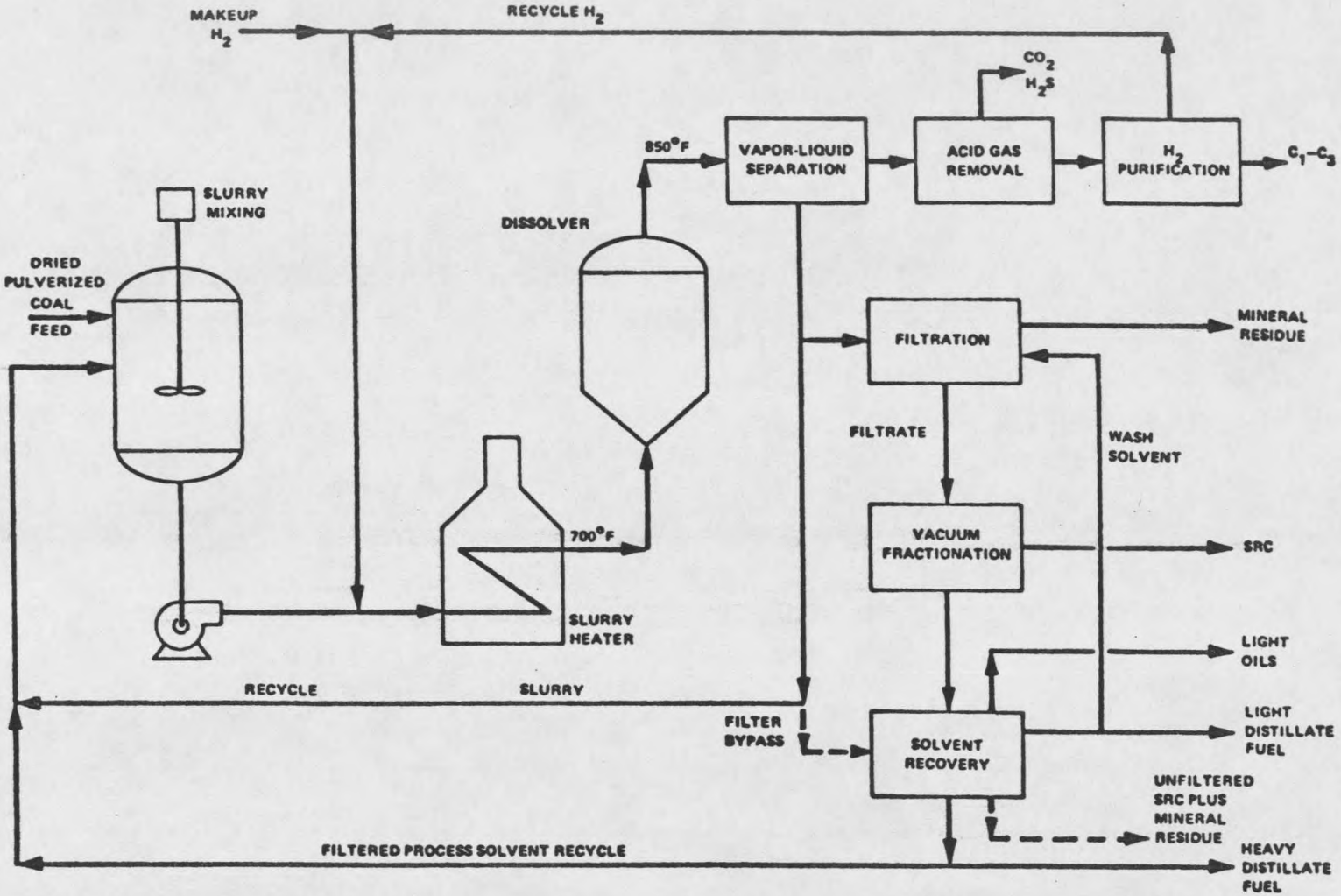

Figure 3. SRC-II Process Flow Diagram

distillate, and heavy distillate streams, including the wash solvent (part of the light distillate) and the filtered process solvent (part of the heavy distillate).

The feedstock used in this research, the Light Ends Column Feed (LECF), was distillate fuels obtained from the vacuum distillation overhead. The physical properties of LECF is shown in Table 2. It contains about 24 wt% light oil (naphtha), 65 wt% middle distillate and 11 wt% heavy oil. Hydrogen/Carbon atomic ratio is about 1.23. The heteroatom content is 1.21 wt% sulfur, and 0.67 wt% nitrogen. For the detailed analysis of the SRC-II product see Appendix A.

CATALYTIC UPGRADING OF COAL LIQUIDS

Coal liquids, as received from the liquefaction plants, are not suitable for conventional use. They contain very high concentrations of heteroatoms such as nitrogen, sulfur and oxygen, and H/C atomic ratio (see Fig. 4) is too low to meet the standards. The low H/C ratio is caused primarily by high percentage of condensed ring aromatic compounds present in the coal liquids. H/C ratio is a rough measure of aromaticity. In general aromatic compounds have lower H/C ratios than their aliphatic or olefinic counterparts.

Table 2. Properties of SRC-II Light Ends Column Feed

Elemental Analysis (wt %)		Distillation Fractions (wt%)	
Carbon	87.80	Light Oil (40-205°C)	24.09
Hydrogen	8.97	Middle Oil (205-298°C)	64.77
Sulfur	1.21	Heavy Oil (298+)	11.14
Nitrogen	0.67		
Oxygen*	2.25		
Ash	0.02		
Specific Gravity, 60/60°F = 0.96			

* By difference.

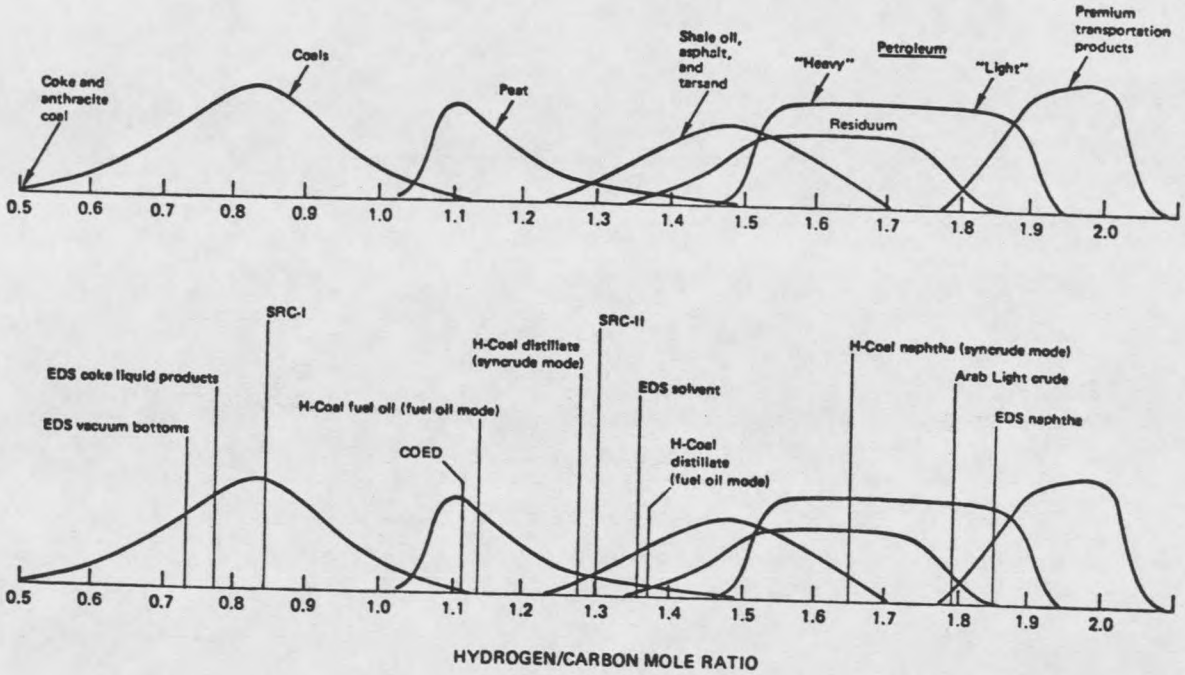

Figure 4. H/C Ratios for Various Hydrocarbon Sources and End Products

Heteroatoms, in general, reduce the stability of the coal liquids and cause storage problems [5]. Sulfur and nitrogen are very severe pollutants and must meet the current EPA standards. Basic nitrogen and sulfur compounds cause catalyst poisoning in the downstream refining processes such as catalytic cracking, hydrocracking and reforming. The tolerable nitrogen content varies from process to process. The maximum allowable nitrogen content in the existing petroleum refineries is 0.3 wt% [7].

Another problem with coal liquids is the presence of polycyclic organic compounds in high percentages. These compounds produce smoke upon burning and can not be cracked without hydrogenation. Hydrogenation of these polycyclic organic compounds reduces smoke production and eases cracking. However, hydrogenation is a very expensive process. If these compounds are entrained during combustion, they cause environmental and health problems. Some carcinogens have been identified among these products [21]. They also dissolve in the process water and cause cleaning problems [22]. Therefore, catalytic hydrotreating is a necessary step.

Catalysts:

The role of a catalyst, in general, is to control the rate and direction of a reaction. A catalyst increases the rate of a reaction by lowering the activation energy of a reaction by creating an alternative path or mechanism for the reaction.

In a multicomponent chemical environment such as coal liquids, the number of possible reactions are many. In this case a catalyst must selectively catalyze the desired reactions. Therefore, the

hydrotreating catalysts for coal liquids must be selective as well as active on certain desired reactions like Hydrodenitrogenation (HDN), Hydrodesulfurization (HDS), Hydrodeoxygenation (HDO), Hydrogenation (HYD), and Hydrocracking (HYC). An excessive hydrogenation is not desired because hydrogen is very costly; however, a certain level of hydrogenation activity is necessary to assure heteroatom removal and to minimize aromaticity and coking.

In both petroleum hydrotreating and coal-liquids hydrotreating, supported metal catalysts are usually used. The metals are transition metals, usually Co, Mo, Ni and W. Supported metal catalysts are prepared by impregnating the water soluble salts of the metals on a high surface area support. A gamma-alumina or gamma-alumina-silica are the supports most widely used.

Characteristics of the supported metal catalysts are not well understood today. Most technological patents and know-how are usually only accidental findings rather than a result of a scientific prediction [23]. This is due to the complexity of the processes of catalyst synthesis and testing. The most important of these is the catalyst synthesis, or in other words, catalyst preparation.

Catalyst preparation starts with selection of a proper support for the specific reactions involved. It must ensure [23] (1) a large enough pore diameter for the free passage of molecules involved in the reaction, (2) high dispersion of an active component (high surface area), (3) the required type of macro distribution of an active component along the radius and micro distribution on the surface, (4) absence of an unwanted interaction of the active component with the

support affecting the catalyst activity, (5) high mechanical and thermal stability of the catalyst under working conditions, (6) minimum heat and mass transfer resistance in the pellets and between them, and (7) absence of impurities or additives which reduce activity and selectivity of the catalyst for the desired reactions.

The pore diameter and pore size distribution is a very important physical property. Because of the very large molecules present in the coal liquids, a majority of the pores must be larger than the largest molecule. It must also be assured that the number of bottlenecks between the pores is minimum. This can be checked by the hysteresis in the adsorption-desorption curves.

The macro distribution of active components are dictated by the process, type of reaction, diffusion problems and the cost of the active components. It can be controlled by controlling the duration of the support in the solution, the rate and type of drying, and the type of impregnation (sorption, capillary and ion exchange). Details are given in references [23, 24, 25, 26, 27].

Once a proper support is selected, the impregnation technique becomes the most important step. The solution concentration, the pH of the solution [28], the sequence of metal impregnation [29, 30, 31, 32, 33, 34], the duration of the support in the solution, the percent metal load on the support, and the drying and calcining conditions are among the most important factors which must be carefully controlled to assure the desired activity and selectivity. The basic reason of the appearance of so many papers contradicting with each other is the complexity of controlling these factors.

Co-Mo/Al_2O_3 Catalysts: Chung and Massoth [29, 30] and Okamoto et al. [31] studied the effect of impregnation technique on the surface structure of Co-Mo/Al_2O_3 catalysts. The former investigators studied the effect of the sequence of metal loading, the calcining temperature and the solution concentration (in other words, stepwise and batchwise impregnation). The latter investigators studied the effect of the sequence of loading and the calcining temperature.

For Co+Mo (Mo impregnated after Co), the chemical state of Co depends on the method of Co impregnation. When Co is impregnated stepwise (1% each time), Co is present in the Al_2O_3 lattice. It is mostly $CoAl_2O_4$ (non-reducible, non-sulfidable) and with some octahedral CoO tightly bound to $CoAl_2O_4$ phase (non-reducible but sulfidable). The percent of the both phases increases with increasing Co concentration. No Co_3O_4 phase is detected up to 3.5 wt% Co, but no data was taken above this concentration. When Co is added batchwise, no Co_3O_4 phase is detected up to 1.5 wt% Co, and the phases present are the same as the Co-step catalyst. However, when the concentration of Co is more than 2 wt%, the octahedral Co_3O_4 (both reducible and sulfidable) starts to appear and increases linearly with increasing Co concentration. The concentrations of $CoAl_2O_4$ and CoO decreases with Co concentration after reaching a maximum at around 2 wt% Co. When the Co-batch catalyst is calcined at 750°C instead of 500°C, the phases present are similar to that of the Co-step catalyst. Calcining at high temperatures causes the migration of Co into the Al_2O_3 lattice. In this particular catalyst system (Co+Mo), Mo does not interact with the Co phase present on the support, and preexistence of Co limits

the Mo-Al_2O_3 interaction since most of the Al_2O_3 sites are occupied by Co. Usually, in all Co-Mo catalysts, Co limits the Mo-Al_2O_3 interaction and this is interpreted as the stablizing action of Co by some investigators [31, 35, 36] since it also limits the formation of a separate crystalline MoS_2 phase upon sulfiding.

In the case of Mo+Co catalyst (Co added after Mo), the chemical state of Co and Mo is different from the previous case. When Co is added stepwise on Mo, Co is present at tetrahedral sites resembling $CoAl_2O_4$ type structure (non-reducible but sulfidable to a certain extent), and there is no Co_3O_4 formed. Since the tetrahedral Co phase is sulfidable, it is not totally $CoAl_2O_4$, but probably a surface Co-Mo interaction where Co is strongly attached to the Al_2O_3 surface. This could be caused either by altering the surface acidity of Al_2O_3 [37] or Mo blocking Co-diffusion paths through the Al_2O_3 matrix [38]. However, when Co is added batchwise on Mo/Al_2O_3 (Mo+Co/Al_2O_3 catalyst), the less amount of the $CoAl_2O_4$ (T) phase is present than that is present in the Co+Mo/Al_2O_3 catalyst [29, 30, 39], and no Co_3O_4 is detected. The majority of Co is present in a surface CoMo complex (precursor to $CoMoO_4$) where Co occupies tetrahedral sites[29, 30, 40-42]. The rest of Co is present as CoO tetrahedral attached to the Al_2O_3 surface. Calcination of this catalyst above 650°C gives more $CoAl_2O_4$ by moving Co into the Al_2O_3 matrix. This shows the importance of the calcining temperature. Nevertheless, there are some disagreements on the presence of Co_3O_4 [31] and the sites occupied by Co in the surface CoMo complex [43], probably because of differences

in the preparation procedures other than the sequence of metal impregnation. Even though it is believed that the surface structure of the sulfided catalysts are similar to the oxidic precursors [31], the phases present are not certainly understood [30]. Upon sulfiding, CoO (O) and CoMo surface complex is sulfided to CoS, Co_9S_8 and MoS_2 respectively. Some MoS_2 may crystallize, but it has not been determined to be significant for the Mo concentrations less than 10 wt% [30].

When Co and Mo are coimpregnated, (Co-Mo)/Al_2O_3 catalyst, a discrete $CoMoO_4$ phase is observed when Co concentration is greater than 2 wt% [30, 44-48]. However, some investigators disagree with this finding [31, 36, 69, 43, 49-53]. Disagreement appears to be due to the differences in preparation technique. The major factor is the calcining temperature. When the catalysts containing $CoMoO_4$ are heated up to 750°C, the amount of $CoMoO_4$ decreases with increasing temperature [29, 41, 50]. The presence of other phases like Co_3O_4 are not known. Sulfiding gives some Co_9S_8, but a substantial fraction of Co remains unsulfided. Some investigators [54] give evidence for the presence of a two dimensional Co:MoS_2 structure.

Ni-Mo/Al_2O_3 Catalysts: It is interesting to note that there is no other supported metal catalyst that has received as much attention as Co-Mo, probably because of its extensive usage in petroleum hydrotreating. The Ni-Mo catalysts are one of the least studied catalysts. Only a few recent studies are concerned with the surface structure of the Ni-Mo catalysts [33, 55-59].

Even though some similarities with the Co-Mo catalysts can be devised it has a considerably different surface structure. Since Mo+Ni/Al_2O_3 (Ni added after Mo) is the only Ni-Mo catalyst studied, it will be given here.

For the concentrations up to 6 wt% Ni, no NiO phase is detected [58]. For low Ni content (Ni less than 3 wt% and Mo 14 wt%), the Ni and Mo species are well dispersed on the support as two independent two-dimensional layers, "$NiAl_2O_4$" and polymolybdate. They do not have any mutual interactions. The presence of this structure is very sensitive to the preparation technique [33, 55, 56, 60]. In this structure, the Mo and Ni species which are incorporated in the surface polymolybdate occupy octahedral sites and resemble a distorted octahedra [56]. As the Ni content increases (Ni > 3 wt%), formation of a new phase, a combination between the polymolybdate and [a] $NiMoO_4$ as an intermediate phase (not very well defined), takes place which results from interaction between the Ni and polymolybdate species. When the molar ratio Ni/Mo = 1/1, the [a] $NiMoO_4$ phase is distinctive [55]. Calcination temperatures between 350-550°C do not have any effect on the basic structure. However, when temperature is higher than 550°C, the Ni species migrate into the bulk of the Al_2O_3 lattice where a surface spinel with Ni in octahedral and tetrahedral positions is formed [41, 55, 56, 61]. This treatment leads to less distorted, two-dimensional monolayer of edge-sharing MoO_6 octahedra.

<u>Ni-W/Al_2O_3 Catalysts:</u> Even though Ni-W is a good hydrogenation and hydrocracking catalyst, it was not a subject of more than a few studies [62, 63]. Similarly to the Ni-Mo catalysts, there is no NiO

detected on the catalyst. Nevertheless, Ni is present on the catalyst as Ni_2O_3 and $NiAl_2O_4$, where Ni_2O_3 is not detected on Ni-Mo catalysts. Ni_2O_3 species are dispersed on top of the W monolayer. Separate WO_3, $NiWO_4$ and $Al_2(WO_4)_3$ phases are absent. However, in contrast to Mo, W interacts with Al_2O_3 support to form a monolayer of interaction complex which is not reducible but sulfidable. Upon sulfiding with H_2S, NiS, Ni_3S_2 and WS_2 are formed. If sulfiding is not complete, a W-surface complex intermediate is formed which has both a terminal oxygen and a terminal sulfur.

At this point a question may arise; what is the importance of knowing the surface structure to the catalyst performance? Since all of the reactions take place on the catalyst surface, the first few atomic layers of the catalyst surface determines activity and selectivity of a catalyst. That is why some catalysts are superior to the others even though they contain the same metals on the same support. The difference in the sequence of metal impregnation, the calcining temperature or other procedural changes make the activity and selectivity of a catalyst different, as in the case of Co-Mo [39, 64] and Ni-Mo [34, 60] catalysts. It is well known that Co or Ni added on Mo catalysts are more active for HDS than the others. Another finding is that, when Ni-Mo is calcined at high temperatures, it has low HDS activity. As discussed above, such a treatment causes the migration of Ni into the Al_2O_3 lattice.

Activity and Selectivity of Ni-Mo, Ni-W and Co-Mo Catalysts:

In general, the Co-Mo catalysts possess a lower hydrogenation activity than the Ni-Mo or Ni-W catalysts at the same or higher

degree of HDS [65, 66]. That is why the Co-Mo catalysts are preferred in the petroleum industry for HDS. The Ni-Mo catalysts possess a higher HYD activity and HDN activity than the Co-Mo and Ni-W catalysts [65, 66, 67]. If the primary objective is removal of nitrogen and hydrogenation of aromatic compounds in addition to HDS, as in the case of coal liquids upgrading, the Ni-Mo catalysts are preferred. The Ni-W catalysts are active for hydrocracking in addition to HDS and HYD [66, 68]. However, Ni-W is poorer for HDN reactions than the other two [69], even though there is some disagreement [66, 70, 71] (see discussion later). Catalyst activity or selectivity can be altered by some additives to the major metal lattice [65]. When phosphoric acid is added to the Ni-Mo catalysts with low metal content and medium phosphorus content (Ni < 3 wt%, Mo < 10 wt% and P < 3 wt%), HDS activity is increased: with high metals/high phosphorus catalyst the best HDN with the lowest hydrogenation and coke formation is obtained [55]. In the latter case, HDS is decreased.

Transport Phenomena in the Catalyst Pores:

Mass Transfer Effects: Mass transfer resistance within the catalyst pores has a significant role on the effectiveness of a catalyst and its life. Sometimes diffusion of reactants may control the global rate of a reaction if the pores are small compared to the size of reactant molecules involved. Therefore, during selection of a catalyst support or a commercial catalyst, this point must be considered as has been discussed above. For example, Cecil et al. [73] found that when the average pore diameter was increased from 7.8 to 10.3 nm, the effectiveness factor of a 1.6 mm cylindrical pellet was

increased from 0.4 to 0.8 in HDS of Middle Eastern residua. In addition to the average pore diameter, the critical pore diameter, diameter at the narrowest point, is important in diffusion effects as pointed out by Berg and Kim [74]. This effect is relatively easy to establish for simple molecules, but the importance of molecular configuration becomes increasingly important for higher molecular weight substances and complicates the study [75].

Heat Transfer Effects: Intraparticle heat transfer can have a significant effect on the reaction rate, activity and selectivity. If a reaction takes place in completely liquid filled pores, the temperature difference between the pellet center and the periphery will not be significant. However, if the pores are filled with vapor, a case which arises quite often for fast reactions with low flow rates, an exothermic reaction causes a large temperature difference [75]. As a result, catalyst performance is affected by transport phenomena. Therefore, selection of a catalyst support or a commercial catalyst and operating conditions must be made after carefully studying the specific reactions and reactants involved. This is another source of contradictory results reported in the literature.

Catalyst Aging: The catalyst aging is one of the most serious problems in all catalytic processes. Some catalysts last for years, some only a few months or days, and sometimes even a few hours, depending on the feed composition and reaction conditions. There are two general types of aging (or deactivation); permanent and temporary.

The permanent deactivation is usually caused by sintering of a catalyst or changing the surface structure (e.g. Ni-Mo and Co-Mo as

discussed above) because of excessive heat treatment or formation of volatile metal salts from the impurities in the feed (e.g. Cllorine ions) [76], deposition of metals (Ni, V, As, etc.) on the surface from demetallization reactions of organometallic compounds and deposition of solids (like iron and scale) [77, 78, 79]. These deposits cause pore blocking and restrict diffusion of reactants.

The temporary deactivation is caused mainly by coke deposition and other chemisorbed compounds depending on the feed composition and catalyst composition [77, 80]. Of these, coke deposition is the most serious problem. Its formation can be minimized by increasing the selectivity of the catalyst (e.g. phosphorus addition to Ni-Mo) or increasing H_2 pressure, but cannot be prevented in hydrocarbon processes. Coke deposition causes pore blocking. The chemisorbed compounds originate either from the feed or reaction products. Therefore, chemisorption can be minimized by purifying the feed or by altering the selectivity if the chemisorbed compounds are from the side reactions.

Coke is usually removed by air burnoff under strict temperature control. If temperature is not controlled very well, it may cause permanent loss of catalyst activity by sintering [76, 77] or changing the surface structure of the metals on the catalyst surface as discussed above [33, 56].

Catalysts for Petroleum and Coal Liquids Upgrading:

The types of catalysts to be used in both petroleum and coal liquids upgrading largely depend on the physical and chemical properties of the feedstock to be treated. In hydrotreating light

petroleum fractions, usually Co-Mo catalysts are the best because they have higher selectivity for HDS over HYD. However, if HDN and saturation of condensed ring aromatic compounds are desired prior to hydrocracking and where unsaturated aromatic compounds pass through without cracking and nitrogen compounds poison the noble metal molecular sieve catalysts, the desired catalyst is Ni-Mo [76] or Ni-W [21]. The composition of metals are in the range of 3-6 wt% for Co or Ni and 12-18 wt% for Mo or W. All catalysts are sulfided prior to use. As discussed before, the selection of support is important with respect to the feed. In general, heavier and highly aromatic feeds require larger pore diameters and pore volume, which is a compromise over larger surface area.

Similar catalysts will probably serve for the coal-liquids upgrading. However, the severity of conditions and composition and physical properties of the catalysts may be different since the chemical and physical composition of coal liquids are different from that of petroleum [81]. Coal liquids are more aromatic in nature and contain high molecular-weight condensed-ring aromatic compounds as well as insoluble organic and inorganic materials in varying concentrations, depending largely on the source of the coal liquids. They contain fairly large concentrations of heterocyclic nitrogen, sulfur and oxygen compounds. The reactivity of these compounds are relatively less than their counterparts in petroleum [21]. In practice, removal of nitrogen is generally more difficult than sulfur, especially in the condensed-ring compounds [21, 76, 81]. The reactions desired are HDN, HDS, HDO, HYD and HYC.

Therefore, the catalysts for coal liquids must be selective as well as active. Activity can be controlled and improved by changing the composition of metals on the support. Selectivity can be maintained or controlled by changing chemical structure or composition of the metals or by adding some promoters as discussed above. To prevent diffusion problems, physical properties of the catalysts must be very well controlled. Larger pore diameters and pore volumes are required while at the same time maintaining a large surface area [81]. As can be understood from this discussion, the catalysts should be bifunctional or multifunctional; selectively removing the heteroatoms with a minimum of hydrogen consumption.

Hydrotreating Coal Liquids and Representative Model Compounds:

Hydrotreating studies on coal liquids followed two different routes; (1) studies on model compounds to determine the mechanism of HDN, HDS, HDO, HYD and HYC, and (2) studies on actual coal liquids to determine the process variables, catalysts and operating conditions. The model compound studies are important to understand the intrinsic mechanisms involved. However, they possess a drawback and can be misleading sometimes since they do not consider the complex interaction of different compounds, functional groups and competing reactions that are present in actual coal liquids.

Chemistry of Hydrodenitrogenation (HDN): To understand the mechanism of HDN, the most studied compounds are pyridine [82-99], quinoline [66, 91, 100-103], acridine [66] and indole [85, 104]. Some of these studies considered the gas phase reactions and the others liquid phase reactions [67]. Since the reactions of coal liquids will

take place in liquid phase, the mechanisms derived from the liquid phase reactions will be closer to the coal liquids. The mechanism of quinoline HDN proposed by Shih et al. [66] is given below as an example.

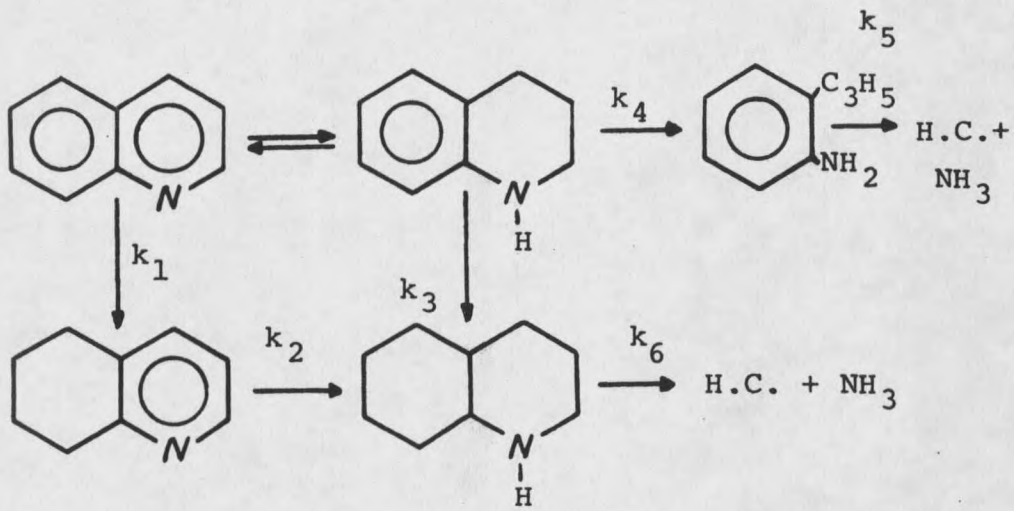

The most favored path is the lower one with every catalyst (Ni-Mo, Ni-W or Co-Mo). The rate constant k_4 is the smallest for every catalyst. Ni containing catalysts favor hydrogenation of benzonoid ring (k_1 and k_3), but Mo containing catalysts favor hydrogenation of the heteroaromatic ring (k_2). The cracking steps (k_4 and k_6) are more dependent on the source of the alumina than on the metals present which is reasonable since cracking requires acidic sites. Presulfiding has a marked influence on the rate of hydrogenation steps, increasing them several times. The cracking reactions are

not affected. Addition of H_2S to the system increases the C-N bond breaking rate constants (k_4 and k_6). This fact is true for most of the HDN reactions. Severe conditions make Ni-Mo catalysts more active compared to Co-Mo catalysts, probably because of excessive hydrogenation since high pressures make thermodynamic equilibrium favorable towards more hydrogenation for this system. Even though Co-Mo is less active than Ni-Mo, it is more selective in hydrogenating heteroatom rings which are required prior to C-N bond breaking [101]. The activity of each catalyst also depends on the heterocyclic nitrogen compounds studied [104]. For example, Co-Mo is more active for Pyrole and Carbozole HDN than Ni-Mo.

Chemistry of Hydrodesulfurization (HDS): This is the most studied reaction among hydrotreating reactions because of its importance in the petroleum industry. The most studied cyclic sulfur compound is thiophene [68, 77, 98, 105-115]. The other polycyclic thiophenes received attention in the recent years [116-123]. HDS of heterocyclic sulfur compounds differ with their molecular structure. From the easiest to the most difficult: thiophene > benzothiophene > benzo[b]naphtho[2,3-d]- thiophene > 7,8,9,10-tetrahydro-benzo[b]naphtho[2,3-d]- thiophene > dibenzothiophene > methyl substituted benzothiophenes [76, 118]. As an example, HDS mechanism of dibenzothiophene is given [116, 120],

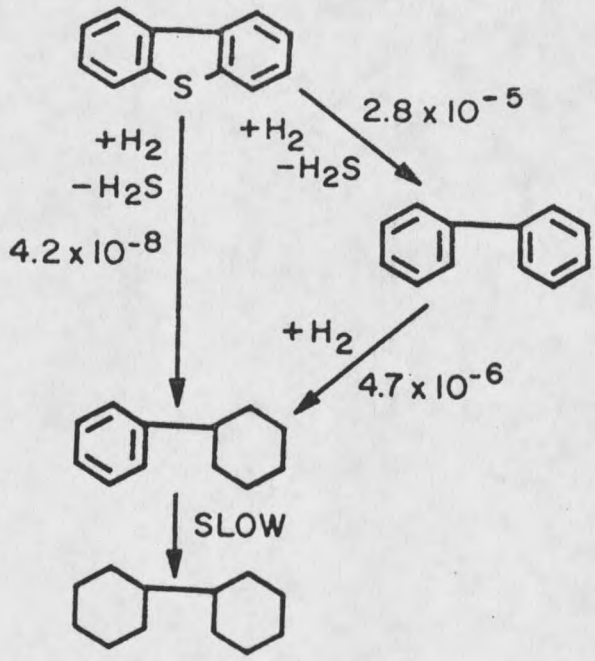

The lower path is favored with sulfided Co-Mo catalysts, and the fastest reaction is the removal of sulfur without any hydrogenation of benzene rings. This is the advantage of the Co-Mo catalysts over the Ni-Mo or Ni-W catalysts. Co-Mo is very selective for removing sulfur without spending any hydrogen other than necessary to remove sulfur. With Ni-Mo catalysts, the activity is about two times higher than Co-Mo, but the yield of cyclohexyl-benzene is three times higher. This shows how poorly selective is the Ni-Mo catalysts even though it is very active. Ni-W gives similar results to Ni-Mo, but stays intermediate between Ni-Mo and Co-Mo. Addition of H_2S suppresses HDS but

enhances hydrogenation of benzene ring. These results are true for the most of the HDS reactions of heterocyclic sulfur compounds.

Hydrogenation and hydrocracking also takes place on these catalysts at the same time because of their bifunctional character, and they follow similar mechanisms in both HDS and HDN. Cracking activity of catalysts depends more on the support than on metals. Silica containing gamma-alumina supports are more active [124]. Ni-W catalysts are more active for cracking than Co-Mo and Ni-Mo [124]. Studies with model compounds showed that HYD, HDN and HDS take place on different sites of the surface [124, 125]. Presence of heterocyclic nitrogen compounds hinders the HDS and HYD activity of Co-Mo catalysts. HDS is in general not sensitive to the basicity of a compound, but HYD is very sensitive to the basicity of the compounds. However, HDS deactivates more than HYD [124].

The first papers concerning coal-liquids upgrading appeared in the literature in the late seventies [126-135] and in the early eighties [67, 69, 136-159]. Their primary objective was to remove heteroatoms in the syncrude. They covered various operating conditions, tested almost every commercially known hydrotreating catalyst and developed new catalysts to achieve their objective. The common conclusion was the difficulty of removing nitrogen, especially from heavy syncrudes or syncrude fractions, and the necessity for continued research to develop new highly selective HDN catalysts.

It appears from some of these studies [69, 130-132, 140, 142] that the catalyst-support physical properties have a significant effect on the activity of the catalysts for HDN, HDS and HDO. The

catalyst with larger surface area and pore size distribution in the larger pore diameter range gave better HDN. HDS and HDO are less sensitive to pore size distribution [69]. One reason for poor performance of some good commercial hydrotreating catalysts for heavy coal liquid fractions is their pore size distribution even though they have large surface area [131, 132, 142]. The commercial catalysts have been developed for petroleum hydrotreating and their pore volume distribution is usually in the small pore diameter range.

The catalytic factor comes from the metals present. Metal content and composition have a pronounced effect on the catalyst activity and selectivity. However, if a right catalyst support is not selected, the effect of metals appears to be negligible. There is some disagreement about which metal combinations are most active; Ni-Mo, Co-Mo or Ni-W. The common conclusion is, however, that the Ni-Mo catalysts are more active for HDN and HYD than either Co-Mo or Ni-W [67, 79, 128, 132, 140]. The reasons for the disagreement appear to be originating either in the physical properties [131, 150] or in the impregnation methods [144, 132, 153]. Increasing the concentration of Mo on the catalyst increases the HDN activity [131, 132, 152]. Increasing Ni or Co at fixed Mo concentration (12-16%) increases the HDN activity [69]. Adding phosphorus as a promoter increases the HDN activity of Ni-Mo [69, 128]. Ni-Mo catalysts produce more saturated hydrocarbons, alicyclics or naphthenes, but Co-Mo produces more aromatics. The operating conditions have a marked effect on HDN, HDS, HDO and HYD. HDN, HDS and HDO are improved by increasing temperature [67, 127, 128, 130, 131, 138, 141, 146, 150, 153, 155, 157, 159]. However the

effect of temperature on HDS is not great [67, 138, 154]. The effect of temperature on hydrogenation depends on pressure, and sometimes high temperatures decrease hydrogenation because of thermodynamic equilibrium [127]. Low space velocities or short residence times give better HDN, HDS, HDO and HYD [128, 131, 138, 141, 146, 155, 159]. Nevertheless, selectivity is best at a low residence time and high temperature [141]. Generally, higher pressures and temperatures and lower space velocities (high severity conditions) are required for heavier feeds. Light fractions of coal liquids can easily be hydrotreated under mild operating conditions. The operating conditions will be, however, more severe than petroleum hydrotreating [67]. High severity conditions produce more gaseous and hydrogenated products, but less coke [67, 148, 150]. Usually, most of nitrogen is left in the heavy fractions indicating the difficulty of removing these heavy molecular weight nitrogen compounds [143].

One of the most serious problems in coal liquids upgrading is the very short catalyst life. Catalyst deactivation is very fast compared with petroleum processes. Deactivation rate depends largely on the composition of the feed, the operating conditions, the catalyst physical properties and the reactor type. Heavier feedstocks cause more rapid catalyst deactivation than the lighter feedstocks [145-147, 153, 154]. Heavy feedstocks tend to form more coke. Stability of the feed under high temperatures is also an important factor [147, 148]. Feeds containing mineral and particulate matter cause severe catalyst aging [139, 146]. Mineral matter deposits on the outer surface and combines with the metals. It also causes more coke formation [139].

Catalysts with pore volume distribution in the smaller pore-diameter range tend to deactivate faster because coke blocks the small pores [69]. The type of reactors plays a role in catalyst deactivation. For example, catalysts in upper portions of a trickle bed reactor start to deactivate first and most of the metal deposition and coke formation take place in this section [146, 147]. In the other reactor types, deactivation is more homogeneous.

The type of reactor to be used is usually determined by the feed composition and properties. Heavy and high boiling point feeds, and feeds causing operational problems in the trickle bed reactors are usually tested or processed in a batch, a slurry or a fluidized bed reactor [147, 151]. However, the batch reactors are not suitable for bench scale or pilot plant operations. Data evaluation is also difficult for these because of difficulty in controlling residence time. Using trickle bed reactors for liquid feeds is common. Handling and data interpretation is easier for trickle bed reactors.

Trickle Bed Reactors:

In a trickle bed reactor, a liquid phase and a gas phase flow concurrently downward through a fixed bed of catalyst particles while reaction takes place. The first commercial trickle bed reactors were developed by the Shell Companies and the British Petroleum Company. They are extensively used in the petroleum industry for hydrotreating, hydrocracking and hydrogenating units [75, 160].

Hydrodynamics: The two most important hydrodynamic factors in the lab-scale trickle-bed reactors are liquid distribution and pressure drop. A poor liquid distribution causes low conversions. Usually,

liquid tends to flow along the wall and the catalysts are left poorly wetted. Higher ratio of reactor-to-particle diameter is required to assure a good liquid distribution. Particle shape also affects good liquid distribution. They are from the best to the worst: granular, spherical and cylindrical [75, 161]. That is why the upper sections of reactors are sometimes packed with inert spherical or granular particles. Therefore, for a good liquid distribution, small catalyst particles are needed in small size lab reactors. However, small particles cause excessive pressure drop through the bed. When there is a problem with coking in the upper sections of the catalyst bed, this causes serious pressure drops, even reactor plug ups [147, 148].

Mass Transfer: External mass transfer limitations to hydrogen will not be significant since the limiting reactant is in the liquid phase in hydrotreating reactions [162].

Contacting Effectiveness: In most practical laboratory-scale trickle-bed reactors, the total external area of the catalyst is not wetted. The wetted fraction increases with increasing liquid velocity [163, 164]. The effect of gas velocity is negligible [165]. However, measurements are extremely difficult. One way of overcoming this problem is catalyst dilution [165]. By catalyst dilution with inert particles, axial dispersion is reduced, and plug flow is approached, catalyst wetting and heat transfer is improved.

X-RAY PHOTOELECTRON SPECTROSCOPY (XPS) IN CATALYST CHARACTERIZATION

Surface analysis by x-ray photoelectron spectroscopy (XPS), more commonly known as electron spectroscopy for chemical analysis (ESCA),

is accomplished by irradiating a sample with monoenergetic soft x-rays and energy analyzing the electrons emitted. MgKα x-rays (1253.6 ev) or AlKα x-rays (1486.6 ev) are used. The penetrating power of these photons in a solid is in the order of 1-10 micrometers. They interact with atoms in this surface region by photoelectric effect, causing electrons to be emitted. The emitted electrons have kinetic energies given by:

$$KE = h\nu - BE - Q$$

where hv is the energy of a photon, BE is the binding energy of the atomic orbital from which the electron originates, and Q is the spectrometer work function.

The binding energy can be regarded as an ionization energy of the atom for the particular shell involved. Therefore, every shell of an atom or different atoms will emit at different energy levels depending on the energy level of the shell.

Even though the photons can penetrate to a depth of a few micrometers, only those electrons that originate within tens of Angstroms below the solid surface can leave the surface without energy loss. It is these electrons which produce peaks in spectra. A more detailed theory and uses of ESCA is given in the references [167-171].

The electrons leaving the sample are detected by an electron spectrometer according to their kinetic energy. The analyzer operated as an energy "window", accepting only those electrons having an energy within the range of this fixed window, referred to as the pass

energy. Scanning for different energies is accomplished by applying a variable electrostatic field before the analyzer is reached.

Application of ESCA to catalyst characterization is new, and has been applied only for a decade. The basic applications to determine the chemical state of catalytic compounds, for example, transition metal oxides and sulfides, started in the early seventies [172-183].

When it was understood that ESCA had great potential applications in determining the chemical state of the metals on the catalyst, it found an extensive application in this field. Most of the applications were done on the Co-Mo catalysts since this catalyst was very important to the petroleum industry [31, 35, 40, 42, 52, 56, 181, 184-192]. Recently some nickel-containing catalysts, such as Ni-Mo, Ni-W, Ni or some tungsten catalysts, were studied by ESCA [55, 62, 193-197].

From the shifts in the BE of an element on the catalyst surface, its chemical environment can be qualitatively obtained. Usually the BE shifts range from 0.2 to 5 eV. See Fig. 5 for example.

It is also possible to obtain quantitative results on the quantities of metal ions present, dispersion of metals on the surface, etc. [198-200].

RESEARCH OBJECTIVE AND PLAN

The objective of this research was to develop catalysts which would be able to upgrade the SRC-II Light Ends Column Feed to a feedstock acceptable to the conventional petroleum refineries or a boiler fuel.

To achieve this objective the following research plan was proposed.

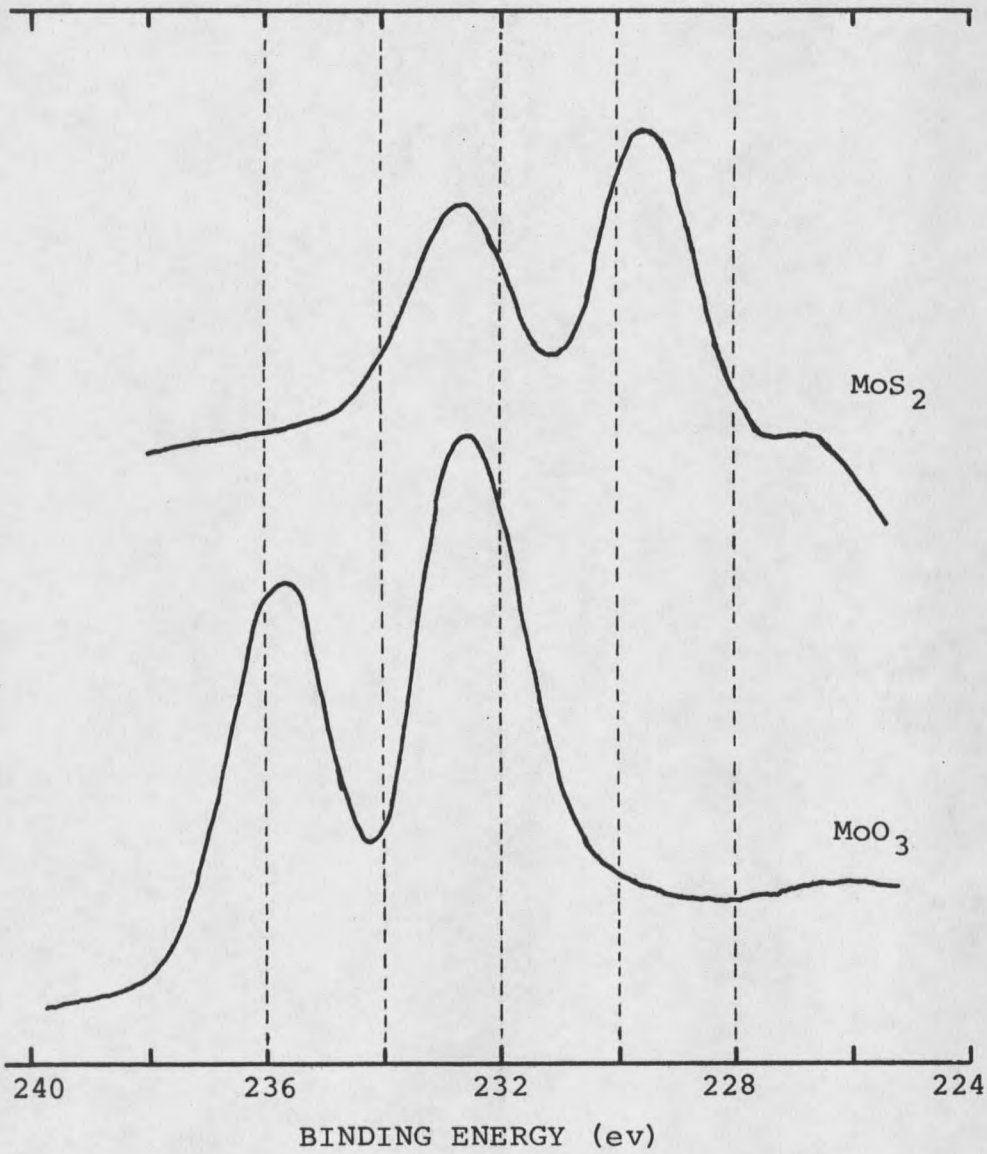

Figure 5. An example of XPS (ESCA) Binding Energy Shifts

Phase I:

a) Selection of a proper catalyst support (a large surface area and a pore volume distribution in the large pore diameter range),

b) Determining the effect of metal combinations on the catalyst activity and selectivity,

c) Determining the effect of water addition to the feed on activity and selectivity of the metals on certain reactions involved,

Phase II: A further study of the two best metal combina-tions in phase I.

a) Determining the effect of impregnation technique on the activity and selectivity of the catalysts,

b) Determining the effect of water on the activity and selectivity of the catalysts produced in part a.

Phase III: Consists of characterization of catalysts tested in phase I and II by ESCA, and correlation of catalyst activity and selectivity with the surface structure of the catalysts.

The effect of water on catalyst activity was also studied since water is present in coal liquids in certain amounts and it is always produced during the process from HDO reaction. Coal liquids contain approximately 3 wt% oxygen and the amount of water can reach a substantial amount in the catalyst pores to affect the activity of a catalyst. If its effect is known in advance some precautions can be taken or a catalyst resistant to the effect of water should be utilized if the effect is negative.

CHAPTER 3

EXPERIMENTAL

FEEDSTOCK AND MATERIALS USED

Solvent Refined Coal (SRC-II) Light Ends Column Feed (LECF) was used as a feed stock in this research. SRC-II LECF was obtained from the Tacoma (Washington) pilot plant of Pittsburgh & Midway Coal Mining Company. The properties of the feed are shown in Table 2.

The catalyst support was obtained from Katalco (serial no. 81-6731) which is a 0.794 mm γ-alumina extrudate. The support possesses a surface area of 223 m^2/g, a pore volume of 1.1 ml/g, and a pore diameter of 169 Å. See Appendix B for the detailed analysis of the support properties. The metal salts used to impregnate the metals were;

1. Ammonium Hepta Molybdate (from Baker Analyzed, reagent grade); $(NH_4)_6Mo_7O_{24}.4H_2O$ (F.W.= 1235.9 gm) with 81.4 % essay in MoO_3 (M.W.=143.94 gm).
2. Nickel Nitrate (from Baker Analyzed, reagent grade): $Ni(NO_3)_2.6H_2O$ (F.W.=290.82 gm) with 99.2 % essay in NiO (M.W.=74.71).
3. Cobalt Nitrate (from MCB, reagent grade): $Co(NO_3)_2.6H_2O$ (F.W.= 291.55 gm) with 99.5 % purity.

4. Ammonium Meta Tungstate (from MCB, technical grade): $(NH_4)_6H_2W_{12}O_{40}.xH_2O$ with 85 % essay in WO_3 (M.W.= 231.85 gm).

The reference compounds used for ESCA (XPS) analyses were;

1. Molybdenum (IV) Sulfide (from Aldrich); MoS_2 with 99+ % purity.
2. Cobalt (II,III) Oxide (from Aldrich); Co_3O_4 with 99.999 % purity.
3. Cobalt (II) Oxide (from Alfa); CoO with 95 % purity.
4. Cobalt (II) Molybdate (from Alfa); $CoMoO_4$ with 98 % purity.
5. Cobalt Aluminate (from Alfa); $CoAl_2O_4$ with 98 % purity.
6. Aluminum Molybdate (from Alfa); $Al_2(MoO_4)_3$ with 99 % purity.
7. Nickel Molybdate (from Alfa); $NiMoO_4$ with 98 % purity.
8. Molybdenum Trioxide (from Baker); MoO_3 with 100 % purity.
9. Nickel(ous) Oxide (from Fischer); NiO with 99.97 % purity.
10. Tungsten Oxide (from Fischer); WO_3, pure.
11. Ni_6S_5 and Co_9S_8 were synthesized in the lab as described in reference 201.

CATALYST PREPARATION TECHNIQUES

Catalysts were prepared by impregnating metal salts on a 0.794 mm (1/32 ") alumina-extrudate catalyst support by using the incipient wetness technique. In this study, the total metal load (as oxides) was kept at 20 wt% (which is percent weight increase over the support), with promoters (Ni and/or Co) and active metals (Mo and/or W) at 4 wt% and 16 wt% respectively. This enabled us to determine the effect

of metal combination on the activity of catalysts for upgrading SRC-II.

Stepwise Impregnation: Stepwise impregnation was used to impregnate the metals because of the difficulty in impregnating Mo and also to achieve better activity. In our earlier studies, when the concentration of Mo solution exceeded 4 wt%, the solution turned milky and a sticky white precipitate covered the outer surface of the particles a few minutes after soaking the support in the solution. Catalysts prepared this way were less active than their commercial counterparts [202, 153]. It was postulated that the precipitated material was plugging up the pores and also causing poor distribution of impregnated metals. In stepwise impregnation, the following procedure was used.

1. Wash the support,
2. Dry at room temperature until the particles can move freely, then oven dry for 8 hours at 110°C,
3. Calcine in an oven for 8 hours at 500°C,
4. Cool the support in a desiccator to room temperature,
5. Prepare a solution to impregnate 1 wt% metal oxide for Ni or Co and 3 wt% for Mo or W,
6. Soak the support in the solution while mixing the contents, and continue mixing for 1 minute,
7. Drain the excess solution (no excess solution in the case of Mo and W) and dry the catalyst by spreading it on a paper towel at room temperature,
8. Repeat steps 2-7 until the desired metal loading is reached.

9. Repeat steps 2-7 until the desired metal leading for Mo or W is reached. Follow the sequence of metal impregnation and the metal composition given in Table 3.

Seven catalysts (see Table 3), containing different metal combinations and compositions, were produced this way and tested for the effect of metal combinations.

Table 3. Metal Composition of Catalysts

Name of Catalyst	Metal Load as wt% increase over support				Impregnation Sequence and type
	Co	Mo	Ni	W	
TS-11	4	16	-	-	Co(s)+Mo(s)
TS-12	4	8	-	8	Co(s)+Mo(s)+W(s)
TS-13	4	-	-	16	Co(s)+W(s)
TS-14	2	8	2	8	Co(s)+Mo(s)+Ni(s)+W(s)
TS-15	-	-	4	16	Ni(s)+W(s)
TS-16	-	8	4	8	Ni(s)+Mo(s)+W(s)
TS-17	-	16	4	-	Ni(s)+Mo(s)
TS-18	4	16	-	-	Mo(b)+Co(b)
TS-19	-	16	4	-	Mo(b)+Ni(b)
TS-20	-	16	4	-	Ni(s)+Mo(b)
TS-21	4	16	-	-	Co(s)+Mo(b)

b = batchwise impregnation
s = stepwise impregnation

Single Step Impregnation: The best metal combinations from the stepwise impregnation technique (Co-Mo and Ni-Mo) were prepared with two different impregnation techniques as described below to test the effect of impregnation technique on the catalyst activity.

First, the order of impregnation of metals was reversed. Initially Mo and then Co or Ni were impregnated with calcination between each metal impregnation. The following procedure was used.

1. Follow steps 1-4 in the stepwise impregnation,
2. Prepare a solution to impregnate 16 wt% Mo,

3. Soak the catalyst support in the solution and keep under constant mixing for an hour,
4. Drain the excess solution and dry the catalyst by spreading on a paper towel at room temperature,
5. Sift the catalyst to remove the precipitate on the outer surface of the catalyst,
6. Oven dry at 110°C for 8 hours,
7. Calcine at 500°C for 8 hours,
8. Cool the catalyst to room temperature in a desiccator,
9. Prepare a solution to impregnate 4 wt% Co or Ni,
10. Soak the catalyst in the solution while mixing the contents and continue mixing for 5 minutes,
11. Repeat steps 4, 6, 7, and 8.

Second, the order of impregnation of the metals was the same (first Co or Ni then Mo), but Co or Ni was impregnated in two steps (2 wt% each time) and Mo in a single step. The following procedure was followed.

1. Follow steps 1-4 in stepwise impregnation,
2. Prepare a solution to impregnate 2 wt% Co or Ni,
3. Soak the support in the solution and mix for five minutes,
4. Follow steps 4, 6, 7, and 8 in the previous procedure,
5. Repeat steps 2-4 once more to make 4 wt% Co or Ni,
6. Prepare a solution to impregnate 16 wt% Mo,
7. Soak the catalyst in the solution and keep under constant mixing and blowing air at room temperature until the catalyst is dry,

8. Follow the steps 5-8 in the previous procedure,
9. Wash the catalyst with distilled water to remove the precipitate on the outer surface of the catalyst,
10. Repeat step 8.

The catalysts produced in this way are listed in Table 3 and given the names; TS-18 (Mo+Co), TS-19 (Mo+Ni), TS-20 (Ni:s+Mo:b), and TS-21 (Co:s+Mo:b).

Catalyst Pretreatment: Catalysts were sulfided before being used to improve their activity and reduce surface poisoning [77]. The reactor (will be explained later) was loaded with catalyst and heated to 400°C by an electric furnace while a stream of 10% H_2S/H_2 mixture passed through the catalyst bed for 12 hours (see Fig. 6). The spent gas from the sulfiding reactor was scrubbed by a series of impingers with 20% NaOH solution.

Extreme caution was taken during this operation because exposures of 800 to 1,000 ppm H_2S may be fatal in 30 minutes [203]. The low concentrations (20 to 150 ppm) of H_2S can be identified by a distinctive odor similar to a rotten egg. However, at higher concentrations it can not be detected by its odor.

CONTINUOUS TRICKLE BED REACTOR SYSTEM

For this study, a bench scale reactor fabricated by the Chemical Engineering Department at Montana State University was used. The reactor system is shown in Fig. 7. The reactor was a 101.6 cm long 2.54 cm diameter Schedule 80 Inconel pipe. A 0.635 cm stainless steel cross was welded to the top of the reactor to serve as liquid and gas

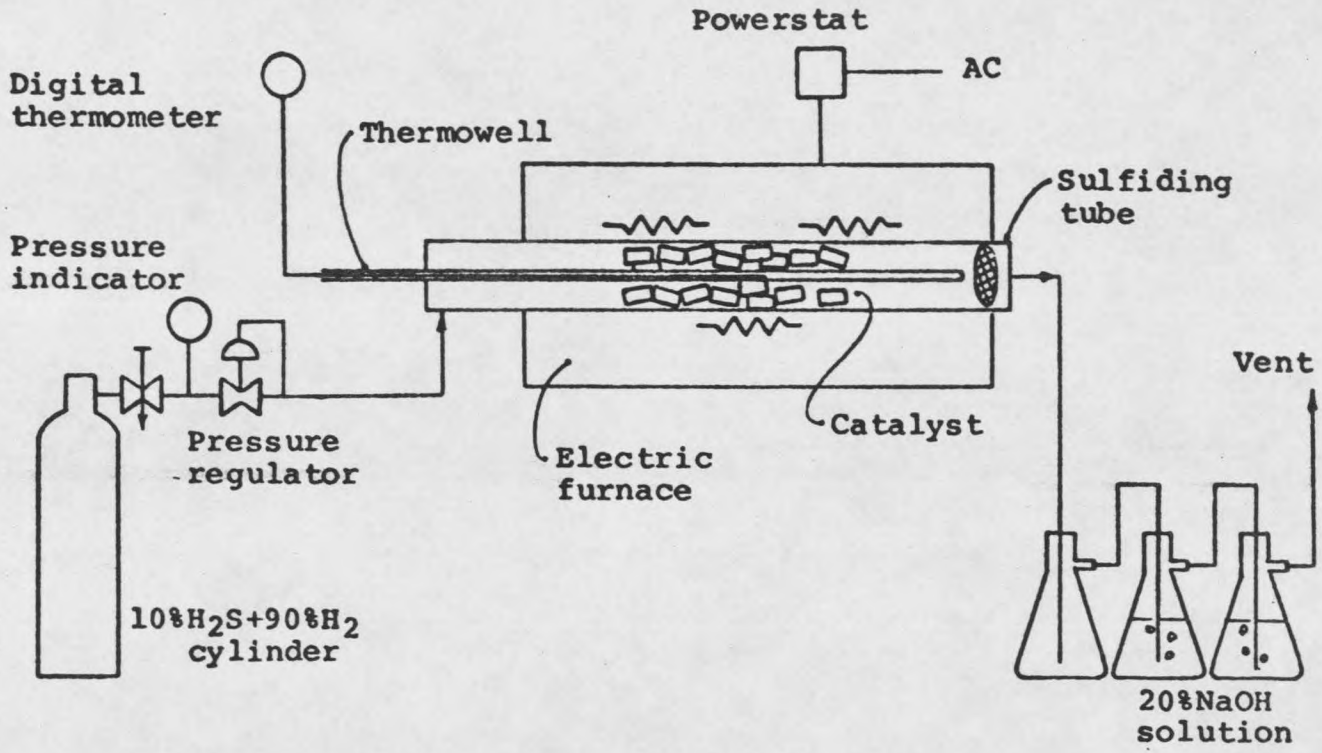

Figure 6. The Silfiding Equipment

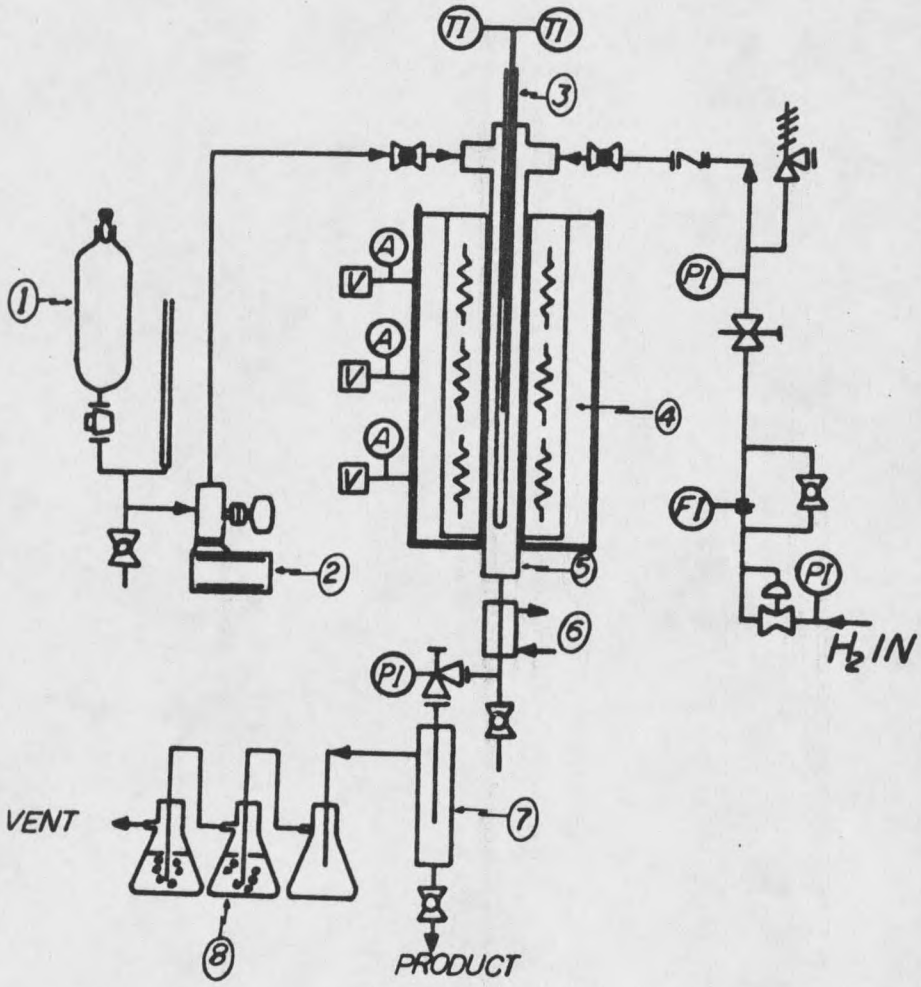

Figure 7. Trickle Bed Reactor System, (1) Feed Reservoir, (2) Milton Roy pump, (3) Thermowell, (4) Aluminum heating block and insulating material, (5) Reactor, (6) Condenser, (7) Gas-liquid seperator, (8) 20% NaOH solution and gas scrubber, (A) Amperemeter, (FI) Hydrogen flow meter, (PI) Pressure gage, (TI) Digital thermometer, (V) Variac, Pressure regulator, NiChrom heating wire, Back pressure regulator, Pressure relief valve, Check valve, micrometer valve.

feed ports to the reactor, and the fitting of a 95 cm long thermowell tubing. The reactor was placed into the bore of a 15.24 cm O.D. 91.44 cm long aluminum block wrapped with three sets of ceramic bead encased NiChrome wire heating coils. Each of the three coils was connected to a Powerstat variable transformer which is manually controlled for temperature. Two chromel-alumel (type K) thermocouple wires were placed in the thermowell to monitor temperatures at the end of the preheat section and at the center of the catalyst section. The temperatures were read by Cole-Palmer digital thermometers (Model 8520-40)

The upper section of the reactor was loaded with 175 ml of 0.635 cm spherical Denstone inert support [204] and 25 ml of 0.318 cm cylindrical Denstone inert support. The function of this section is mainly to preheat and uniformly distribute the feed. 44 gm of catalyst (based on oxide form and corresponding to approximately 60 ml) diluted [164] with 60 ml of 0.318 cm cylindrical Denstone inert support was loaded below the preheat section. The remainder of the reactor was filled with 0.318 cm cylindrical Denstone inert support (see Fig. 8). Finally, a stainless steel screen was placed to support the catalyst bed above the reactor plug which was threaded into the pipe.

The SRC-II LECF was pumped into the top of the reactor by a Milton-Roy simplex piston pump (Model A MR-1-23) through a 0.318 cm stainless steel tube. The pump is equipped with a manually controlled micrometer adjustment for feed rate control. Technical grade hydrogen was fed through a pressure regulator, a 0.318 cm stainless steel tube, a micrometer valve (to adjust the flow rate), a Brooks Thermal

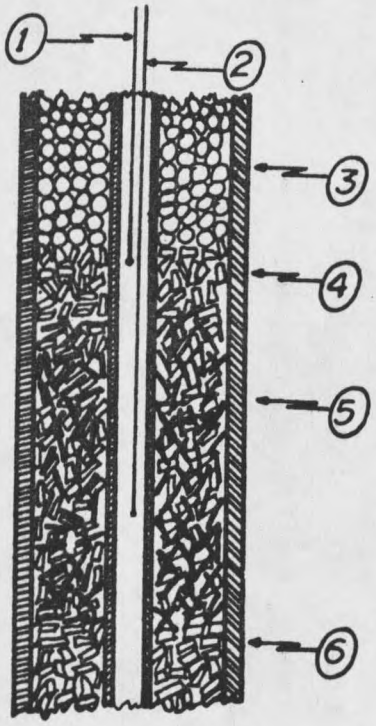

Figure 8. Cross Section of the Packed Reactor

(1) Thermocouple which monitors temperature at the catalyst section inlet, (2) Thermcouple which monitors temperature at the catalyst section, (3) Preheat section (0.635 cm serical inert support), (4) Inlet to the catalyst section (0.318 cm cylindrical inert upport), (5) Catalyst section (mixture of catalyst and 0.318 cm inert support), (6) Inert section (0.318 cm inert support).

Mass Flowmeter [205], and a ball check valve to the top of the reactor.

Hydrogen and the SRC-II feed was passed through the pressurized and packed reactor bed concurrently, to a condenser, and then to a gas-liquid separator through a Grove back-pressure regulator equipped with a corrosion-resistant Teflon diaphragm. The exit gases were scrubbed by a 10% NaOH solution and vented. The liquid product was collected in a bottle continuously.

EXPERIMENTAL PROCEDURES AND OPERATING CONDITIONS

The loaded and sealed reactor was placed in the heating unit and connected to the feed lines and product separator. The system was pressurized to 6.9 MPa (1000 psig) with nitrogen and the all connections were checked for leaks with Snoop liquid detergent. If there were no leaks, the heaters were turned on and the reactor was flushed with nitrogen for 10 minutes to remove air. The system was kept under nitrogen pressure until the desired starting temperature of 350 C was reached.

The cooling water valve for the condenser was opened and nitrogen pressure was released before connecting the hydrogen line to the system. When the system reached the desired hydrogen pressure of 6.9 MPa, the hydrogen flow rate was adjusted to 1,900 scm/min (10,000 scf/bbl of oil) with the micrometer valve. The feed reservoirs were filled with SRC-II LECF and the pump was turned on. Feed rate was measured by timing the change in the fluid level in the buret and

adjusted by the pump micrometer. The flow rate was checked every two hours to ensure a steady flow rate.

Every run was started at 350°C, and Liquid Hourly Space Velocity (LHSV) was kept at 15.0 hr^{-1} for the first 5 minutes to help prevent an initial rapid deactivation of the catalyst. The temperature was steadily raised to the steady state value of 400°C within 5 hours. The other operating conditions were: pressure of 6.9 MPa (1000 psig), Hydrogen flow rate of 1900 scm/min (10,000 scf/bbl of oil), and LHSV of 1 hr^{-1} (or WHSV of 1.3) (see Table 4). Water was added to the feed as 2% of the feed for the runs which applied this technique.

Table 4. Operating Conditions

Starting Temperature,	°C	350 ± 10
Starting LHSV*,	hr^{-1}	15 ± 1
Operating Pressure,	MPa	6.9 ± 0.6
Opreating Temperature,	°C	400 ± 10
Operating LHSV,	hr^{-1}	1.0 ± 0.1
WHSV**,	hr^{-1}	1.3 ± 0.2
Amount of Catalyst,	ml	60 ± 2
Amount of Catalyst***,	g	44.2 ± 0.2

* Liquid Hourly Space Velocity, for only the first three minutes.
** Weight Hourly Space Velocity.
*** Based on oxidic (unsulfided) form of the catalyst. It varies for every catalyst in sulfided form since every catalyst uptakes a different amount of sulfur.

The product was collected continuously in a bottle and the bottle was changed every 10 hours. Product samples for analysis were taken from these bottles so that every analyzed sample reflects the average value of 10 hours.

When the run was completed (either 140 or 100 hours), the pump was turned off and hydrogen was let flow for 30 minutes to make sure

that oil left in the reactor had enough time to react. Then, the hydrogen valve was closed, the heaters were turned off, and the system was depressurized.

ANALYTICAL PROCEDURES

Sample Pretreatment: After completion of a run, the amount of product in every bottle was measured and recorded. Water produced in the process was separated from the oil and the oil was washed with distilled water to remove water soluble nitrogen compounds. The oil was separated from the water again. Some samples were taken from the bottles containing the product for the periods 10-20, 50-60, 90-100, and 130-140 hours for nitrogen analysis.

Nitrogen Analysis: The nitrogen analysis for the product samples were done by Macro-Kjeldahl Method [206-208]. The percent Hydrodenitrogenation (HDN) was calculated with the following equation;

$$\% \text{ HDN} = \frac{(\text{wt\% N in the feed}) - (\text{wt\% N in the product})}{(\text{wt\% N in the feed})}$$

Where N is nitrogen present in the feed or the product.

Distillation: Product distillations were done in a column with three theoretical plates and a reflux ratio of three to determine the quality of the product obtained.

Elemental Analysis: The elemental analysis of the product samples was done by Carlo Erba Elemental Analyzer (model 116). Sample containers were cleaned with acetone, dried in an oven and then weighted. About 1.0 mg of sample was injected into the containers and the container mouth was sealed by squeezing with a pair of pliers.

After recording the weight of the sample the containers was placed in a rotating disc of the analyzer. Disc contains 22 sample holes. With every batch of sample analysis a couple of blank containers and standard chemicals were also analyzed as references [209]. Every sample was analyzed three times to get a reliable result. When enough consistency is reached the result was assumed to be the correct value.

ESCA (XPS) Analysis: The ESCA analyses of the catalysts were done by Leybold-Heraeus X-ray Photoelectron Spectrometer (L-H EA11). The catalyst particles were mounted on an Indium foil and evacuated in a separate evacuation chamber at 100°C under vacuum of 10^{-5} torr. A double-stick scotch tape was used for the reference compounds, the catalysts tested for the effect of impregnation technique and sulfided catalysts. The sulfided samples and the reference samples were prepared in a glove bag under inert atmosphere to avoid contact with oxygen. Then, the samples were mounted on the sample holder of the instrument as quickly as possible to avoid adsorption of moisture. The sample holder allows a quick insertion of the sample into preparation chamber and then to the analysis chamber. When vacuum in the chamber reached 10^{-7} or 10^{-8} torr, the x-ray source was turned on. The data was recorded both with an analog and a digital recorder. The latter was done by a Tektronix computer, and stored on a magnetic tape. For low signals such as Co 2p and Ni 2p spectra, a few scans were recorded by adding signal count rates on top of each other to magnify the signal.

When the analysis of all the catalysts were completed, the data were cleaned from noise (basically caused by the digital recorder) and smoothened by a second order smoothening function (see App. C for details). A copy of every scan was taken by a Tektronix Hard Copier or an X-Y recorder which is connected to the computer. The peak binding energies and intensities were determined and all binding energies were referenced to C 1s peak binding energy of 284.6 ev to account for the charging of insulating type catalyst samples.

CHAPTER 4

RESULTS

Results will be reported in three sections. The first section covers the effect of metal combinations on HDN, HYD and HYC activities of the seven catalysts fabricated with different combinations of Ni, Co, Mo and W. The second section includes the effect of impregnation technique on HDN, HYD and HYC activities of the Co-Mo and Ni-Mo combinations. The third section explains the results of ESCA (XPS) analysis of all catalysts evaluated in the first two sections.

EFFECT OF METAL COMBINATIONS

As explained in Chapter 3, seven catalysts were fabricated by impregnating different combinations of Co, Mo, Ni and W. Co and Ni were impregnated stepwise in 4 or 5 steps, and Mo or W were impregnated stepwise to an additional 3 wt% each time until the desired metal load was reached. Each catalyst was evaluated with respect to catalytic activity twice, once with and once without water addition to the feed to test the effect of water on the catalyst performance. In addition to the seven catalysts fabricated, the blank support was tested for its capability to upgrade SRC-II LECF, both with and without water addition to the feed, as a reference to the impregnated catalysts. HDN results are plotted in Fig. 9. Overall average nitrogen content of the product oil, average HDN, H/C atomic ratio, distillation

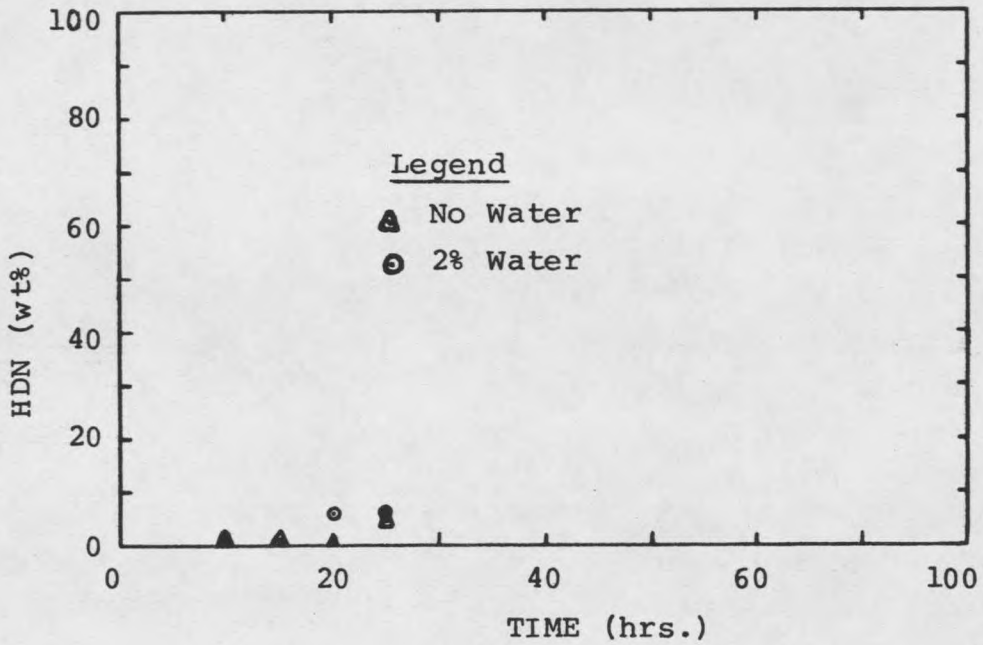

Figure 9. Hydrodenitrogenation vs. Time for the Blank Carrier (Alumina,Katalco)

fractions and percent carbonaceous material deposited on the catalyst are given in Table 5. As can be seen both from the Fig. 9 and Table 5, the blank support does not have any HDN activity and the water did not show any significant effect on HDN. Table 6 summarizes the difference between the H/C ratio and distillation fractions of the product oil and that of the feed. It also includes the relative percent change in these quantities over the feed. The effect of water on HDN, H/C ratio and distillation fractions are given in Table 7 as differences between the runs with and without water addition. Even though water did not have any effect on HDN, it enhanced the light oil production (see Table 7). In both cases, with and without water addition, the amount of light oil decreased, 2.1% and 7.1% respectively (see Table 6). The amount of middle oil increased, indicating some condensation of light hydrocarbons (see Fig. 10 and Fig. 11). Some hydrogenation occurs with the support but it is not great (Table 6 and Fig. 12).

Fig. 13 shows the HDN results of the catalyst TS-11 (4% Co, 16% Mo) as a function of time. HDN activity of the catalyst slowly decreased with time. However, the catalyst was operated for over 140 hours, and the time averaged HDN was 71 wt% and 74 wt% for the runs with and without water addition respectively. The effect of water on HDN was not significant (or may be slightly inhibiting) for this catalyst. The amount of light oil produced was 12.1 and 10.9 wt% over the feed with and without water addition respectively, and middle and heavy oil contents were reduced significantly (see Table 6 and Figures 10 and 11). This corresponds to 50% and 45% increase in light oil

Table 5. The Effect of Metal Combinations and Water on HDN, Product Quality (Distillation Fractions) and Catalyst Coking

Catalyst & Run	%N wt%	HDN wt%	H/C[a]	LO[b] wt%	MO[c] wt%	HO[d] wt%	%C[e] wt%
TS-10NW*(support)	0.71	0	1.25	22.4	66.3	11.4	10.03
TS-10W*	0.71	0	1.25	23.6	65.4	11.0	9.81
TS-11NW (Co+Mo)	0.18	74	1.38	35.0	55.7	9.4	13.06
TS-11W	0.19	71	1.38	36.2	55.0	9.1	11.61
TS-12NW (Co+Mo+W)	0.25	63	1.34	31.2	58.9	10.7	11.19
TS-12W	0.27	59	1.33	33.0	57.3	10.5	9.90
TS-13NW (Co+W)	0.35	49	1.33	33.0	56.8	10.2	9.45
TS-13W	0.25	63	1.32	35.2	57.8	6.9	12.63
TS-14NW (Co+Mo+Ni+W)	0.29	57	1.36	31.8	59.0	9.3	12.07
TS-14W	0.36	46	1.32	29.6	60.8	9.7	9.51
TS-15NW (Ni+W)	0.41	39	1.34	28.9	61.5	9.6	9.90
TS-15W	0.44	36	1.30	29.4	61.2	9.5	8.40
TS-16NW (Ni+Mo+W)	0.43	36	1.33	27.4	62.3	10.3	8.37
TS-16W	0.42	37	1.31	28.2	62.1	9.7	7.77
TS-17NW (Ni+Mo)	0.13	81	1.40	33.9	57.3	8.8	14.40
TS-17W	0.07	90	1.40	35.8	56.0	8.3	15.23

* NW = No water added, W = 2 % water added.
[a] Hydrogen to carbon atomic ratio.
[b] Light oil content in the boiling range 40 - 205 °C.
[c] Middle oil content in the boiling range 205 - 298 °C.
[d] Heavy oil content in the boiling range 298 - end point.
[e] Carbonaceous material deposited on the catalyst.

Table 6. Chenge in H/C Ratio, Light Oil (LO), Middle Oil (MO) and Heavy Oil (HO) from the Feed

Catalyst & Run	Composition Change From the Feed				Percent Relative Change From the Feed for Each Category			
	LO	MO	HO	H/C	LO	MO	HO	H/C
TS-10NW* (support)	-1.7	1.5	0.2	0.02	-7.1	2.3	2.7	1.6
TS-10W*	-0.5	0.7	-0.1	0.02	-2.1	0.9	- 0.9	1.6
TS-11NW (Co+Mo)	10.9	-9.1	-1.8	0.15	45.3	-14.0	-15.3	12.2
TS-11W	12.1	-9.8	-2.3	0.15	50.2	-15.3	-18.0	12.2
TS-12NW (Co+Mo+W)	7.1	-5.8	-1.3	0.11	29.5	- 9.1	- 3.6	8.9
TS-12W	8.9	-7.3	-1.6	0.10	37.0	-11.6	- 5.4	8.1
TS-13NW (Co+W)	8.9	-7.8	-1.1	0.10	36.9	-12.4	- 8.1	8.1
TS-13W	11.2	-7.0	-4.2	0.09	46.5	-10.8	-37.8	7.3
TS-14NW (Co+Mo+Ni+W)	7.7	-5.8	-1.9	0.13	32.0	- 9.0	-16.2	10.6
TS-14W	5.5	-4.0	-1.5	0.09	22.8	- 6.2	-12.6	7.3
TS-15NW (Ni+W)	4.8	-3.3	-1.6	0.11	19.9	- 5.1	-13.5	8.9
TS-15W	5.3	-3.6	-1.7	0.07	22.0	- 5.7	-14.4	5.7
TS-16NW (Ni+Mo+W)	3.3	-2.5	-0.8	0.09	13.7	- 3.9	- 7.2	7.3
TS-16W	4.1	-2.6	-1.5	0.08	17.7	- 4.2	-12.7	6.5
TS-17NW (Ni+Mo)	9.8	-7.5	-2.4	0.17	40.7	-11.6	-20.7	13.8
TS-17W	11.7	-8.8	-2.9	0.17	48.6	-13.6	-25.2	13.8

* NW = No water, W = 2 % water added.

Table 7. The Effect of Water on HDN, H/C ratio, and Light Oil (LO), Middle Oil (MO) and Heavy Oil (HO) Contents

Catalyst & Run	Difference in % Composition Between Runs NW and W (W-NW)*				
	H/C	LO	MO	HO	HDN
TS-10 (Support)	0.00	1.2	-0.9	-0.4	0.0
TS-11 (Co+Mo)	0.00	1.2	-0.7	-0.5	- 3.0
TS-12 (Co+Mo+W)	-0.01	1.8	-1.5	-0.3	- 4.0
TS-13 (Co+W)	-0.01	2.4	1.0	-3.3	14.0
TS-14 (Co+Mo+Ni+W)	-0.04	-2.2	1.8	0.4	-11.0
TS-15 (Ni+W)	-0.04	0.5	-0.3	-0.1	- 3.0
TS-16 (Ni+Mo+W)	-0.01	0.8	-0.2	-0.6	1.0
TS-17 (Ni+Mo)	0.00	1.8	-1.3	-0.6	9.0

* NW = No water added, W = 2% water added.

contents over the feed for these runs. Despite the insignificant effect of water on HDN, water enhances the light oil production (see Tables 6 and 7 and Fig. 10). The H/C ratio remained the same both with and without water addition (Fig. 12). This may indicate some contribution to HYC from water.

Fig. 14 shows HDN results of the catalyst TS-12 (4% Co, 8% Mo, 8% W). This catalyst was less active than the catalyst TS-11 (Co+Mo) which gave 74 wt% HDN vs. 63 wt% HDN for the present catalyst (see Table 5). Deactivation was faster for TS-12 (Co+Mo+W) than for TS-11 (the slope of the line gives the trend of deactivation). Quality of product was not as good using TS-12 (Co+Mo+W) as with TS-11 (Co+Mo). Going from the TS-12 (Co+Mo+W) to TS-11 (Co+Mo) catalyst, light oil production was lowered from 10.9% to 7.1% without water addition and from 12.1% to 8.9% with water addition (see Table 6 and Fig. 10); the H/C ratio was also lower (less HYD activity). The effect of water on HDN appeared slightly inhibiting (although not significant), but it

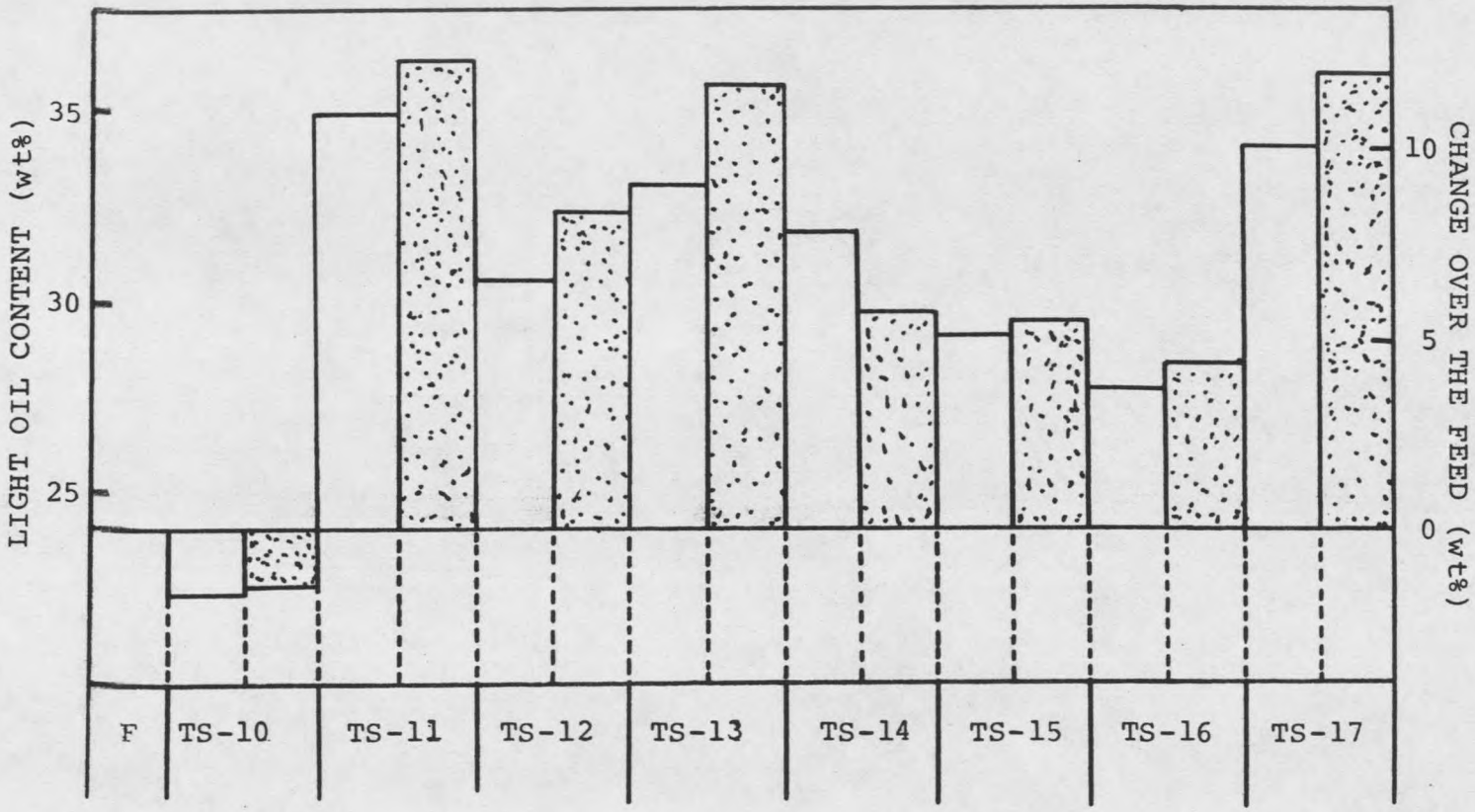

Figure 10. The Effect of Metal Combinations and Water Addition on Light Oil Yield

F = Feed, TS-10; blank carrier (alumina, Katalco), TS-11; Co+Mo, TS-12; Co+Mo+W, TS-13; Co+W, TS-14; Co+Mo+Ni+W, TS-15; Ni+W, TS-16; Ni+Mo+W, TS-17; Ni+Mo.

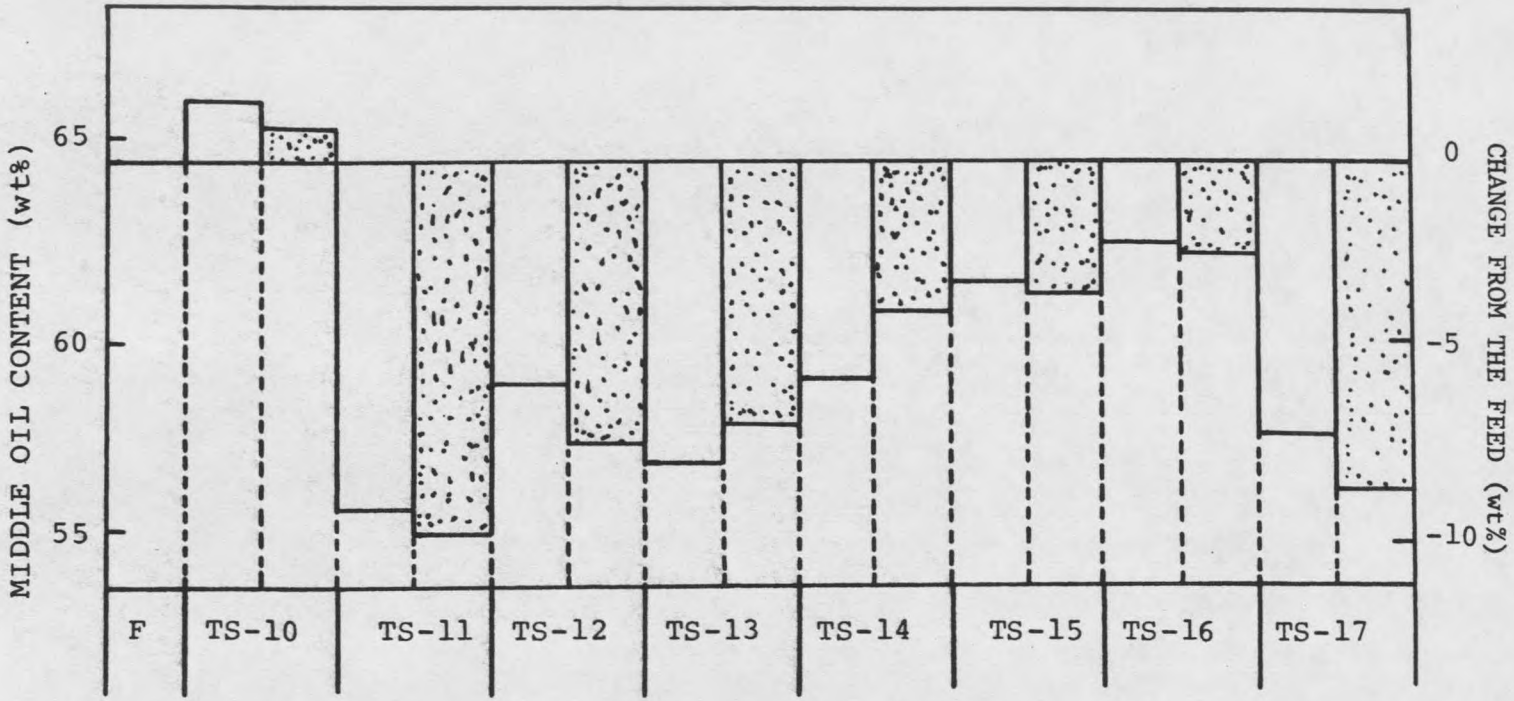

Figure 11. The Effect of Metal Combinations and Water Addition on Middle Distillate

F = Feed, TS-10; blank carrier (alumina, Katalco), TS-11; Co+Mo, TS-12; Co+Mo+W, TS-13; Co+W, TS-14; Co+Mo+Ni+W, TS-15; Ni+W, TS-16; Ni+Mo+W, TS-17; Ni+Mo.

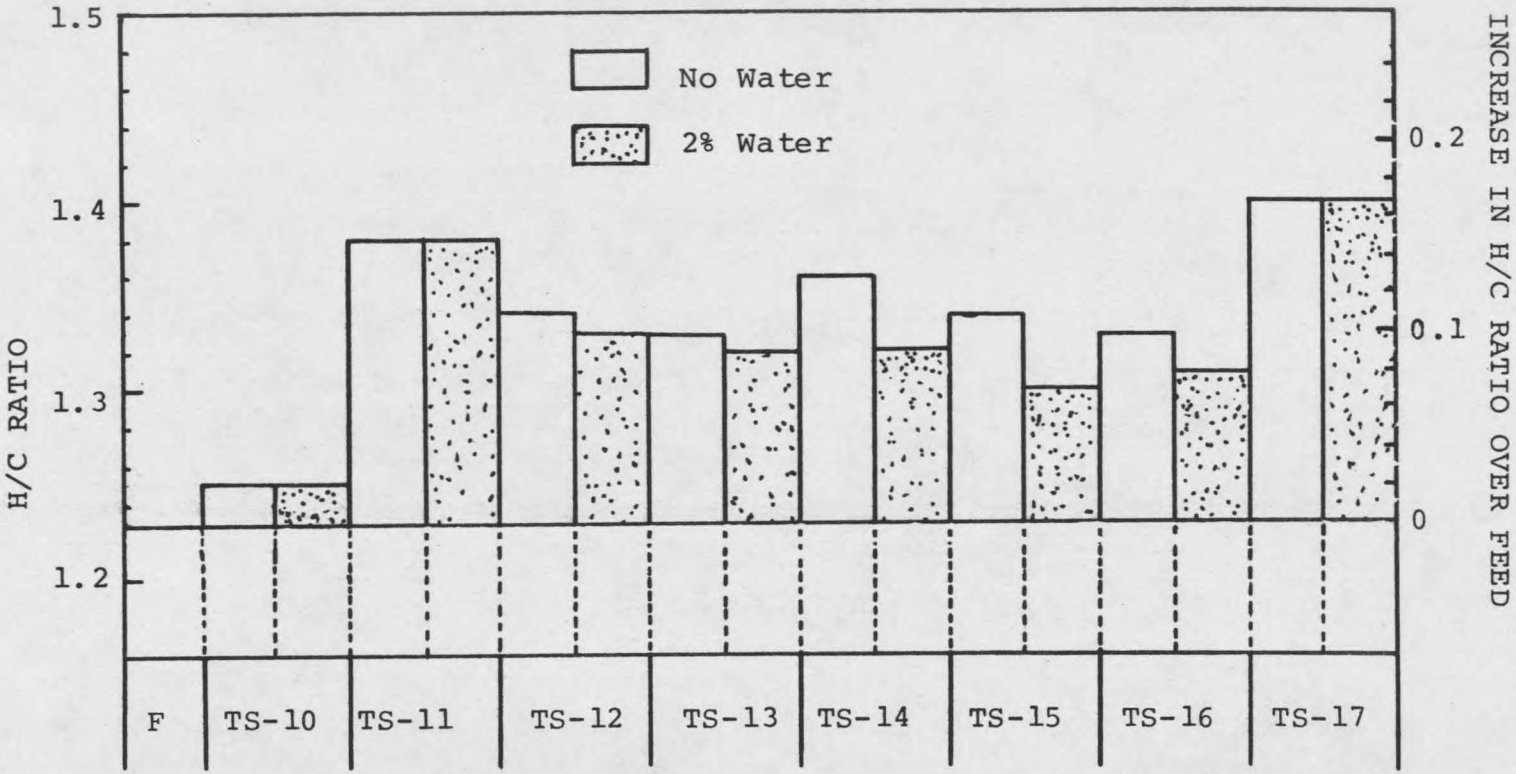

Figure 12. The Effect of Metal Combinations and Water Addition on H/C Ratio (atoms hydrogen per atom carbon)
F = Feed, TS-10; blank carrier (alumina, Katalco), TS-11; Co+Mo, TS-12; Co+Mo+W, TS-13; Co+W, TS-14; Co+Mo+Ni+W, TS-15; Ni+W, TS-16; Ni+Mo+W, TS-17; Ni+Mo.

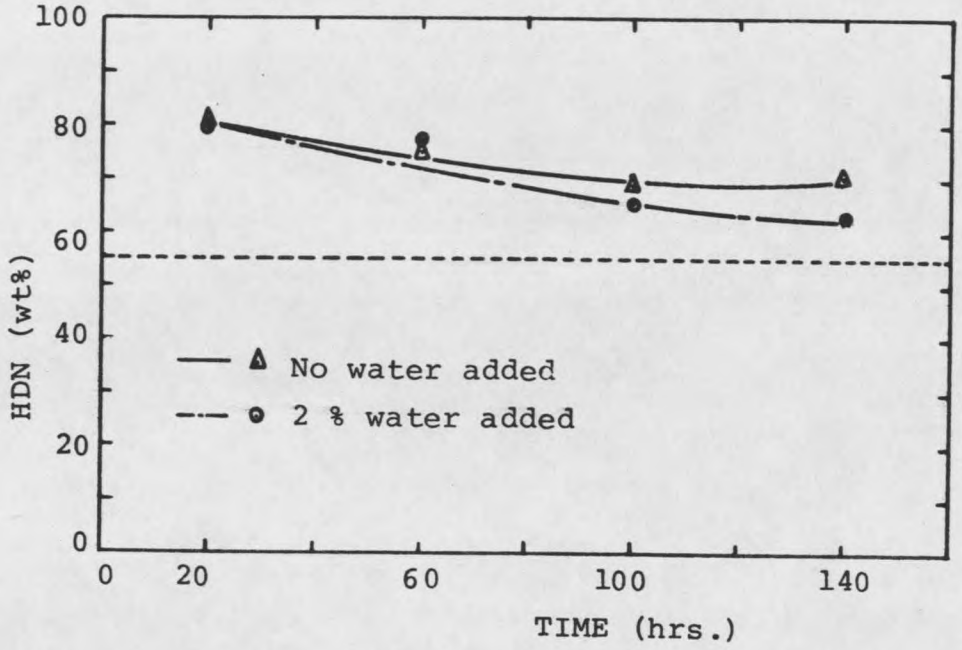

Figure 13. Hydrodenitrogenation vs. Time for the Catalyst TS-11 (4 wt% Co, 16 wt% Mo)

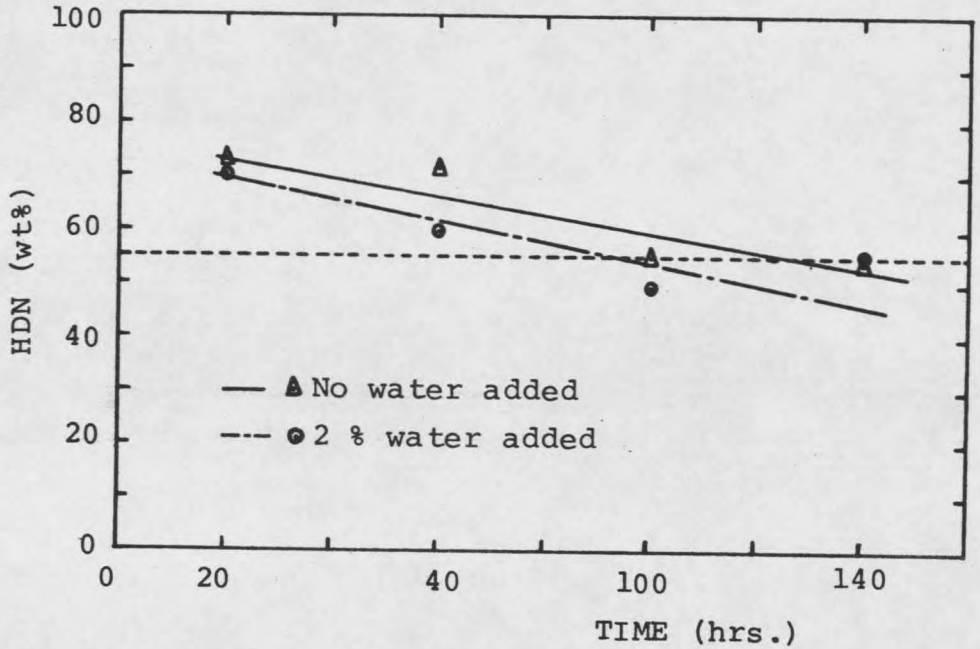

Figure 14. Hydrodenitrogenation vs. Time for the Catalyst TS-12 (4 wt% Co, 8 wt% Mo, 8 wt% W)

enhanced the product quality (see Table 7). H/C ratio remained about the same. Therefore, the improvement in light oil production may be because of enhancing effect of water on HYC activity of this catalyst. This catalyst produced specification grade product (less than 0.3 wt% N in the product oil) initially, but it started producing lower grade product at the end.

Fig. 15 shows the HDN results of the catalyst TS-13 (4% Co, 16% W). The activity of this particular catalyst was very low without water addition; however, water increased HDN from 49 wt% to 63 wt%. Without water addition, the catalyst was not able to produce specification grade product (see Table 5). A similar effect of water was observed for product quality. Light oil production increased from 8.9% to 11.2% (see Table 6 and Fig. 10), and a higher percentage of heavy oil was converted to lighter fractions. In contrast to the positive effect of water on HDN and the product quality, H/C ratio remained about the same (Tables 5 and 7 and Figures 10 and 12). This indicates the enhancing effect of water on HYC.

Fig. 16 shows the HDN results of the Catalyst TS-14 (2% Co, 8% Mo, 2% Ni, 8% W) as a function of time. HDN activity of the catalyst was moderately good without water addition even though deactivation was faster. However, water reduced HDN from 57 wt% to 46 wt%. The catalyst produced specification grade product when time averaged over 140 hours without water addition, but started producing non-specification grade product at the end of the run. The effect of water on the product quality was also inhibitive for this particular catalyst (see Tables 6 and 7 and Figures 10 and 11). Light oil production was

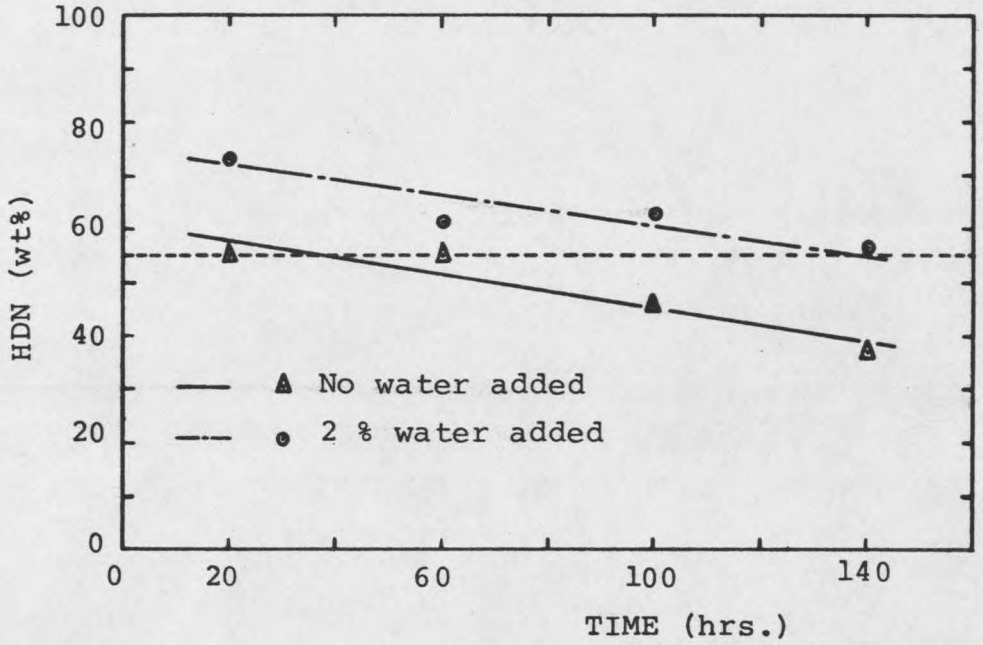

Figure 15. Hydrodenitrogenation vs. Time for the Catalyst TS-13 (4 wt% Co, 16 wt% W)

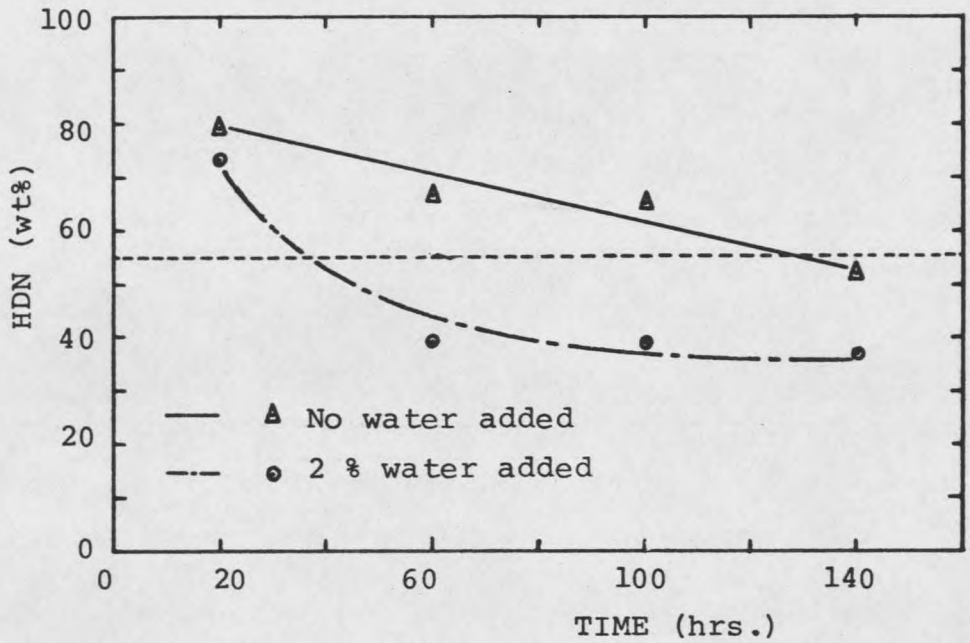

Figure 16. Hydrodenitrogenation vs. Time for the Catalyst TS-14 (12 wt% Co, 8 wt% Mo, 2 wt% Ni, 8 wt% W)

reduced from 7.7% to 5.5%. H/C ratio was reduced from 1.36 to 1.32 indicating that water inhibited HYD activity (Fig. 12).

Fig. 17 shows HDN results of the catalyst TS-15 (4% Ni, 16% W). This catalyst was one of the poorest for both HDN and product quality (Tables 5 and 6 and Figures 9 and 10). Catalyst deactivation was also faster than for the other catalysts. This catalyst did not produce a specification grade product with or without water addition. Water slightly inhibited HDN activity, 39 wt% vs. 35 wt%. The effect of water on product quality was not significant (see Tables 6 and 7 and Figures 10 and 11). H/C ratio for the run with water addition was lower, even though both runs produced about the same amount of light oil (Fig. 12). This indicates the enhancing effect of water on HYC for this catalyst.

Fig. 18 shows the HDN results of the catalyst TS-16 (4% Ni, 8% Mo, 8% W). This was the least active catalyst for both HDN and product quality. It did not produce specification grade product even at the beginning of the run, indicating extremely poor activity. The effect of water on HDN was insignificant, but light oil production slightly increased. Nevertheless, the production of light oil was the lowest of any catalyst tested (see Tables 6 and 7 and Fig. 10). The effect of water on H/C ratio was inhibitive (Fig. 12), therefore, it enhanced HYC activity.

Fig. 19 shows the HDN results of the catalyst TS-17 (4% Ni, 16% Mo). This catalyst had the highest HDN and HYD activity among the catalysts evaluated in this group. Catalyst deactivation was slower than for all the other catalysts except TS-11 (Co+Mo), especially

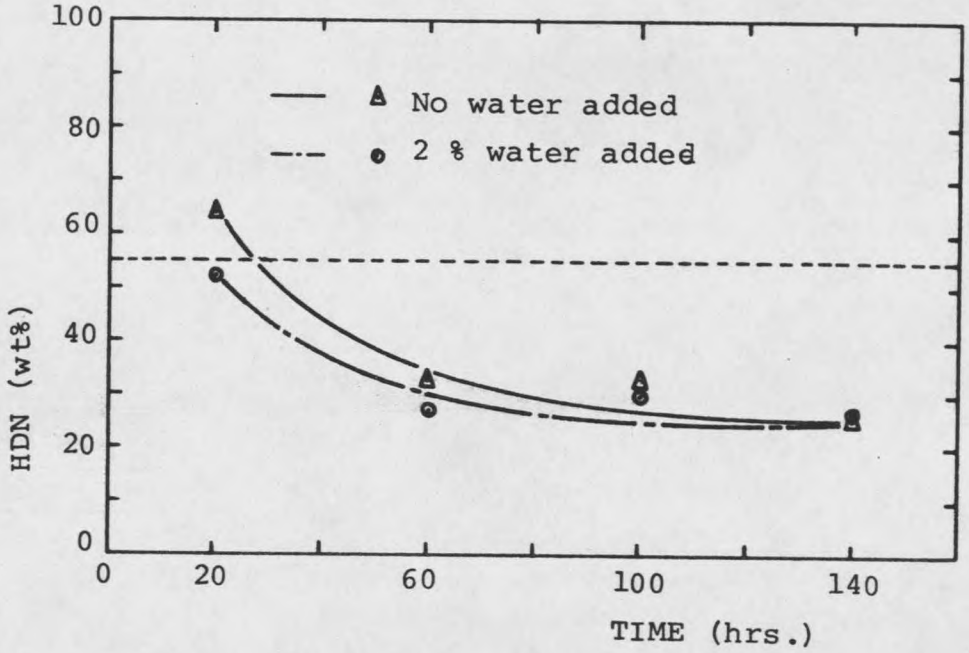

Figure 17. Hydrodenitrogenation vs. Time for the Catalyst TS-15 (4 wt% Ni, 16 wt% W)

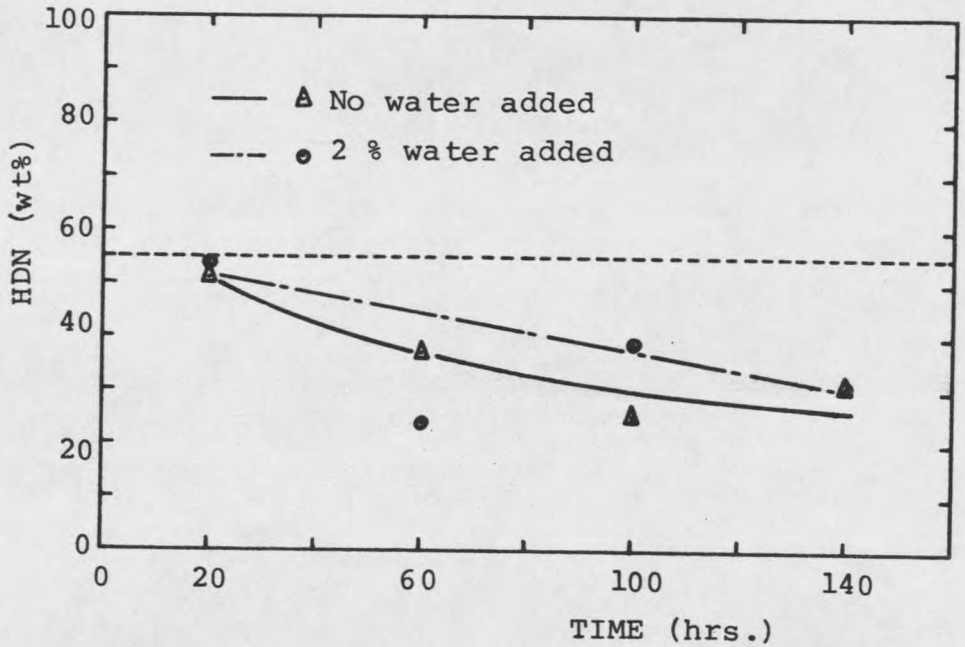

Figure 18. Hydrodenitrogenation vs. Time for the Catalyst TS-16 (4 wt% Ni, 8 wt% Mo, 8 wt% W)

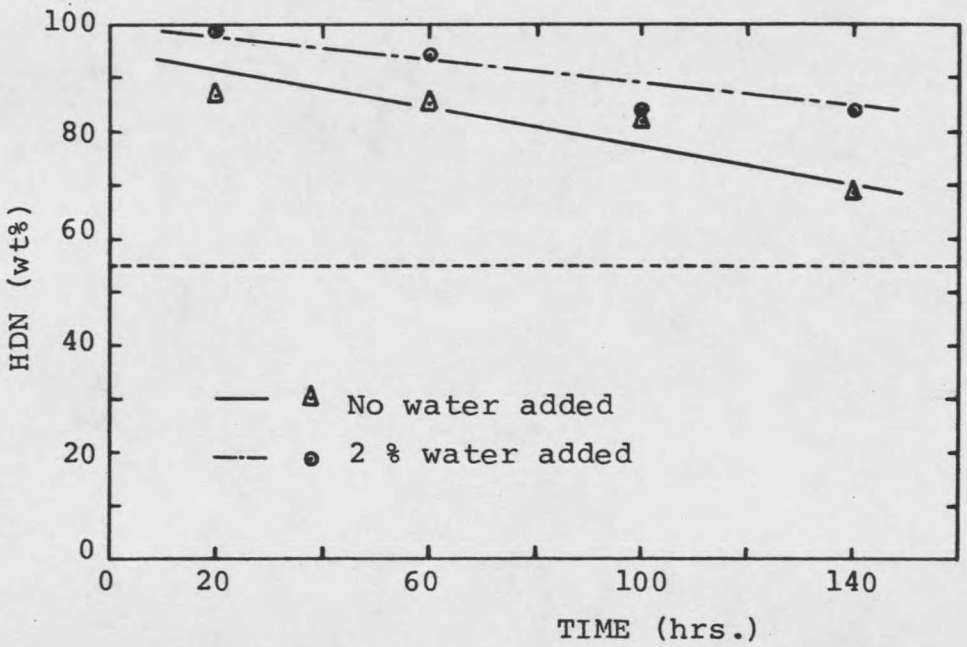

Figure 19. Hydrodenitrogenation vs. Time for the Catalyst TS-17 (4 wt% Ni, 16 wt% Mo)

when water was added to the feed. The effect of water on both HDN and the product quality was positive (Tables 6 and 7 and Figures 10 and 11). H/C ratio remained about the same for both runs. This indicates the positive effect of water on HYC since the light oil production was improved by water addition.

To see the relationship between activities of W and Mo, HDN results are plotted as a function of W/(W+Mo) ratio in Fig. 20. HDN activity decreased with increasing amount of W on the catalysts generally. However, when 2% water was added, HDN activity of Co-W catalyst increased significantly. With this exception in mind, in general Mo is preferable to W for HDN of SRC-II Light Ends Column Feed under the conditions of this study.

When all the catalysts evaluated in this group are compared, the most active metal combinations for HDN, product quality and H/C ratio (or HYD) can be given in the following order:

1. For HDN;

   a) No water,

      Ni+Mo > Co+Mo > Co+Mo+W > Co+Mo+Ni+W > Co+W > Ni+W > Ni+Mo+W

   b) With water,

      Ni+Mo > Co+Mo > Co+Mo+W = Co+W > Co+Mo+Ni+W > Ni+Mo+W = Ni+W

2. For product quality (or light oil production);

   a) No water,

      Co+Mo > Ni+Mo > Co+W > Co+Mo+Ni+W > Co+Mo+W > Ni+W > Mo+W

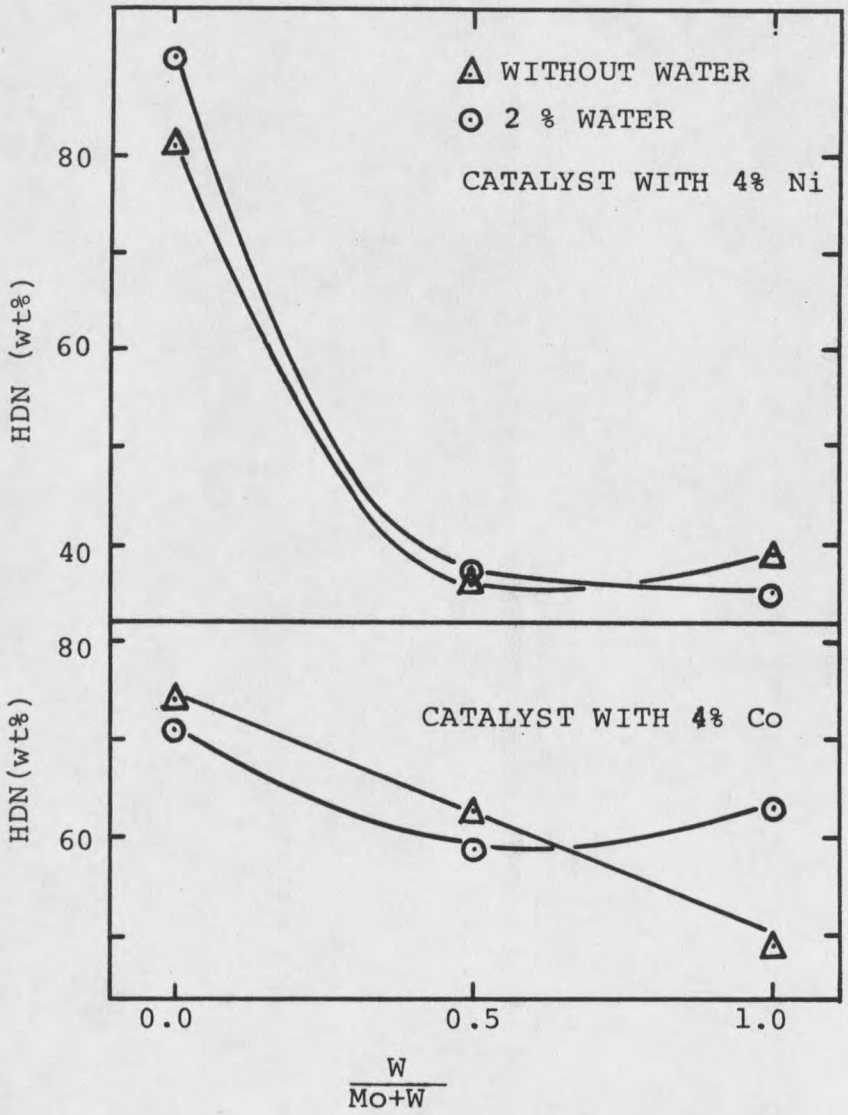

Figure 20. HDN activity of W as a function of metal load.

b) With water,

Co+Mo > Ni+Mo > Co+W > Co+Mo+W > Co+Mo+Ni+W > Ni+W > Ni+Mo+W

3. For H/C ratio (or HYD);

a) No water,

Ni+Mo > Co+Mo > Co+Mo+Ni+W > Co+Mo+W = Ni+W > Ni+Mo+W = Co+W

b) With water,

Ni+Mo > Co+Mo > Co+Mo+W > Co+W = Co+Mo+Ni+W > Ni+Mo+W > Ni+W

Carbonaceous material deposited on the catalyst was determined by air burnoff, and is given in Table 5. In general, water reduced the amount of carbonaceous material deposited. However, it is not easy to single this out from the data listed, because of the fact that the more active catalysts produced more carbonaceous material. When water enhanced the activity of a catalyst significantly, there was also an increased amount of carbonaceous material on the catalyst (see TS-13 and TS-17 in Table 5). This is probably due to the dual character of coke formation. Unreactive coke poisons reaction sites. Reactive coke is subsequently converted to reaction products [210]. Fig. 21 supports this proposition. The amount of coke on the catalyst significantly increased with increasing HDN activity. Indeed, water reduced the amount of carbonaceous material on the inert support, used as a diluent for every catalyst tested without any exception (not shown here).

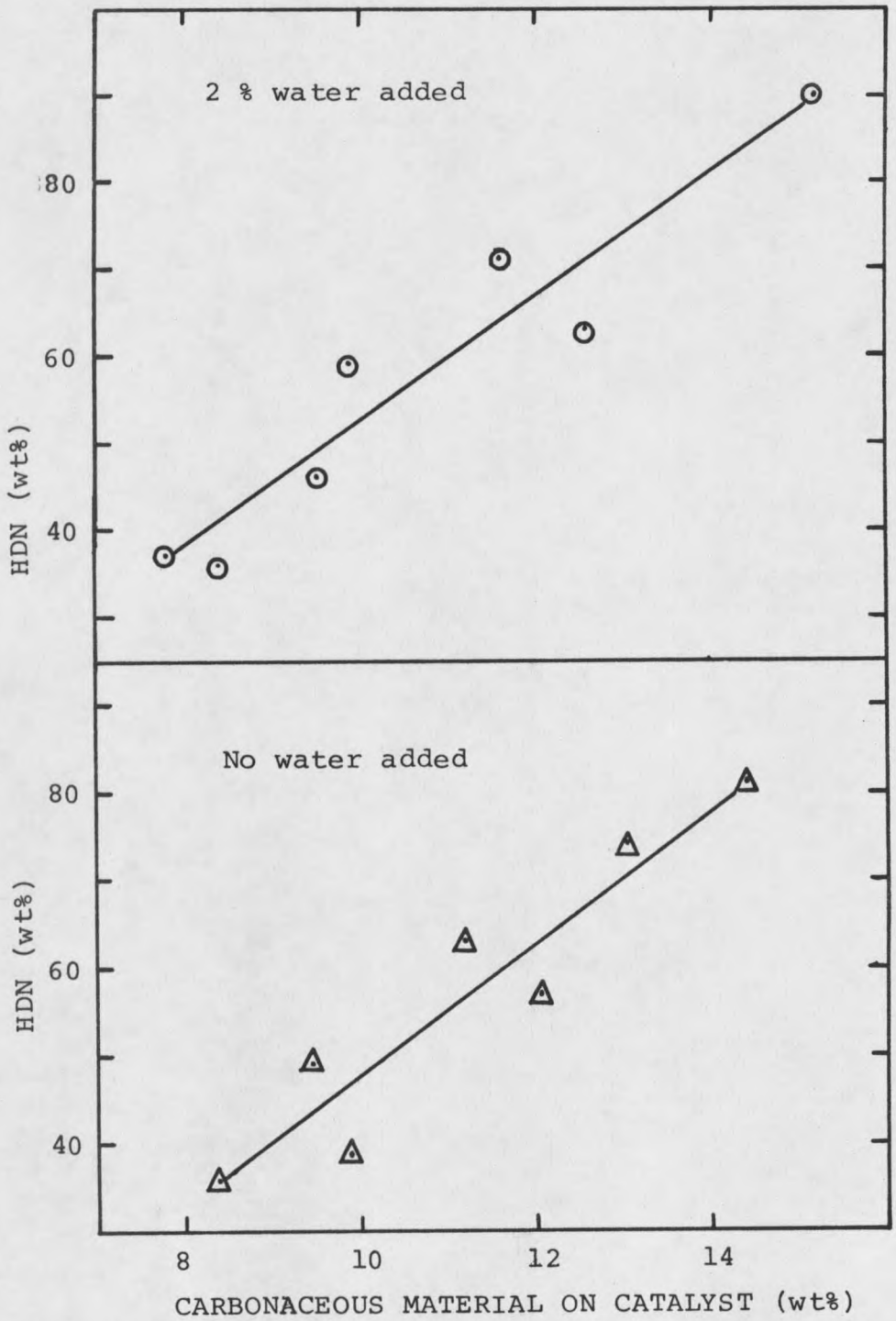

Figure 21. Relationship between HDN activity and carbonaceous material deposited on the Catalyst.

EFFECT OF IMPREGNATION TECHNIQUE

Two of the best catalysts, Co-Mo and Ni-Mo, evaluated in the previous section were subjected to two different impregnation techniques as described in Chapter 3. In both cases, Mo was impregnated in a single step (batchwise). Co or Ni was then impregnated in one case in two steps (TS-21 for Co-Mo and TS-20 for Ni-Mo) and in a single step (batchwise) in the other case (TS-18 for Co-Mo and TS-19 for Ni-Mo). The catalysts TS-18 (Mo+Co) and TS-19 (Mo+Ni) were prepared by Co and Ni impregnation on Mo, respectively. The catalysts TS-20 (Ni:s+Mo:b) and TS-21 (Co:s+Mo:b) had a reverse sequence of metal deposition. Activities of these catalysts are compared in the following paragraphs.

Ni-Mo Catalysts: Since TS-17 (Ni+Mo, step) was discussed in the previous section, it will not be discussed here. Instead, only comparative references will be made to it.

Fig. 22 shows HDN results of the catalyst TS-19 (16% Mo, 4% Ni) as a function of time. This catalyst was as active as TS-17 for HDN. In contrast to catalyst TS-17 (Ni+Mo, step), water did not have any significant effect on HDN for TS-19 (Mo+Ni). When the results given in Tables 8, 9, and 10 and Figures 23, 24 and 25 are compared, H/C ratio for TS-19 (Mo+Ni) is slightly higher than TS-17 (Ni+Mo, step), and the light oil production is significantly higher. Light oil production was 12.7% and 12.3% with and without water addition, respectively. The effect of water on both product quality and H/C ratio was not significant. As a result, HYC activity was not affected by water.

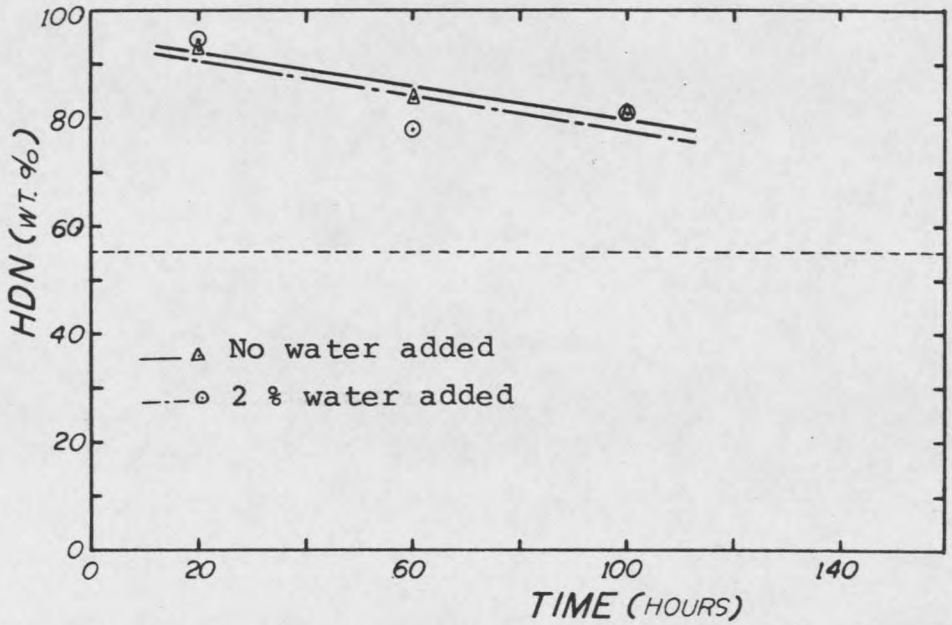

Figure 22. Hydrodenitrogenation vs. Time for the Catalyst TS-19 (16 wt% Mo, 4 wt% Co)

Table 8. The Effect of Impregnation Technique and Water Addition on HDN, Product Quality (Distillation Fractions) and Catalyst Coking

Catalyst & Run	Product Nitrogen (wt%)	HDN (wt%)	H/C[a] (wt%)	LO[b] (wt%)	MO[c] (wt%)	HO[d] (wt%)	C[e] (wt%)	RON[f] for LO
TS-11NW*(Co+Mo, step)	0.17	75	1.38	35.0	55.5	8.9	13.06	89.0
TS-11W*	0.17	74	1.38	36.2	55.0	9.1	11.61	
TS-18NW (Mo+Co)	0.09	87	1.38	39.2	53.0	7.9	14.29	85.4
TS-18W	0.12	82	1.36	38.0	54.2	7.8	15.53	
TS-21NW (Co:s+Mo:b)	0.15	78	1.37	36.9	55.0	8.1	14.53	89.4
TS-21W	0.20	71	1.37	36.8	54.7	8.5	14.24	
TS-17NW (Ni+Mo, step)	0.10	86	1.40	33.9	57.3	8.8	14.40	82.0
TS-17W	0.05	92	1.40	35.8	56.0	8.3	15.25	
TS-19NW (Mo+Ni)	0.10	86	1.41	36.8	54.5	8.7	16.25	82.4
TS-19W	0.11	84	1.40	36.4	54.8	8.8	15.53	
TS-20NW (Ni:s+Mo:b)	0.11	82	1.41	37.0	54.4	8.7	14.89	82.3
TS-20W	0.12	82	1.41	36.5	55.4	8.1	15.80	

* NW = No water addition, W = 2 % water added.

[a] Hydrogen to carbon atomic ratio.

[b] Light oil fraction in boiling range 40 - 205 °C.

[c] Middle oil fraction in boiling range 205 - 298 °C.

[d] Heavy oil fraction in the boiling range of 298°C to the end point.

[e] Carbonaceous material deposited on the catalyst.

[f] Research octane number.

Table 9. Change in H/C Ratio, Light Oil (LO), Middle Oil (MO), and Heavy Oil (HO) from the Feed

Catalyst & Run	Composition Change From the Feed				Percent Relative Change From the Feed for Each Category			
	H/C	LO	MO	HO	H/C	LO	MO	HO
TS-11NW* (Co+Mo, step)	0.15	10.9	- 9.1	-2.3	12.2	47.7	-14.4	-19.8
TS-11W*	0.15	12.1	- 9.8	-2.1	12.2	48.6	-15.1	-18.0
TS-18NW (Mo+Co)	0.15	15.1	-11.8	-3.2	12.2	62.7	-18.2	-28.8
TS-18W	0.13	13.7	-10.0	-3.3	10.6	57.7	-16.4	-29.7
TS-21NW (Co:s+Mo:b)	0.14	12.8	- 9.7	-3.1	11.4	53.1	-15.1	-27.0
TS-21W	0.14	12.7	-10.0	-2.7	11.4	52.7	-15.6	-23.4
TS-17NW (Ni+Mo, step)	0.17	9.8	- 7.5	-2.4	13.8	38.6	-11.7	-15.3
TS-17W	0.17	11.7	- 8.8	-2.9	13.8	48.6	-36.5	-25.2
TS-19NW (Mo+Ni)	0.18	12.7	-10.3	-2.5	14.6	52.7	-15.9	-21.6
TS-19W	0.17	12.3	-10.0	-2.3	13.8	51.0	-15.4	-20.7
TS-20NW (Ni:s+Mo:b)	0.18	12.9	-10.4	-2.5	14.6	53.5	-16.1	-21.6
TS-20W	0.18	12.4	- 9.3	-3.1	14.6	51.5	-14.5	-25.2

* NW = No water added, W = 2 % water added.

Table 10. The Effect of Water on HDN, H/C Ratio and Light Oil (LO), Middle Oil (MO) and Heavy Oil (HO) Contents for the Co-Mo and Ni-Mo Catalysts

Catalyst & Run	Difference in % Composition Between Runs NW and W (W-NW)*				
	H/C	LO	MO	HO	HDN
TS-11 (Co+Mo, step)	0.00	1.2	-0.7	-0.5	-1.0
TS-18 (Mo+Co)	-0.02	-1.4	1.0	0.4	-5.0
TS-21 (Co:s+Mo:b)	0.00	-0.1	-0.3	0.4	-7.0
TS-17 (Ni+Mo, step)	0.00	1.8	-1.3	-0.5	7.0
TS-19 (Mo+Ni)	-0.01	-0.4	0.3	0.2	-2.0
TS-20 (Ni:s+Mo:b)	0.00	-0.5	1.1	-0.6	0.0

NW = No water added, W = 2% water added

Fig. 26 shows HDN results of the catalyst TS-20 (4% Ni, 16% Mo). HDN activity of this catalyst was slightly lower than both TS-19 (Mo+Ni) and TS-17 (Ni+Mo, step) (see Table 8), and water did not show any significant effect on HDN, product quality and H/C ratio (see Tables 9 and 10 and Fig. 23 and 25). Light oil production was about the same as TS-19 (Mo+Ni).

Co-Mo Catalysts: Since TS-11 (Co+Mo, step) was discussed in the previous section, those results will not be given here. Some references will be made whenever necessary. Tables 8, 9 and 10 and Figures 23, 24 and 25 will provide necessary comparisons for Co-Mo catalysts.

Fig. 27 shows HDN results of the catalyst TS-18 (16% Mo, 4% Co) as a function of time. HDN activity of this catalyst was higher than TS-11 (Co+Mo, step) (see Table 8), and deactivation was reasonably slow. The effect of water on HDN activity was negative (see Table 10). The best product quality was obtained with this catalyst. The light oil production was over 15% (see Table 9 and Fig. 23). The

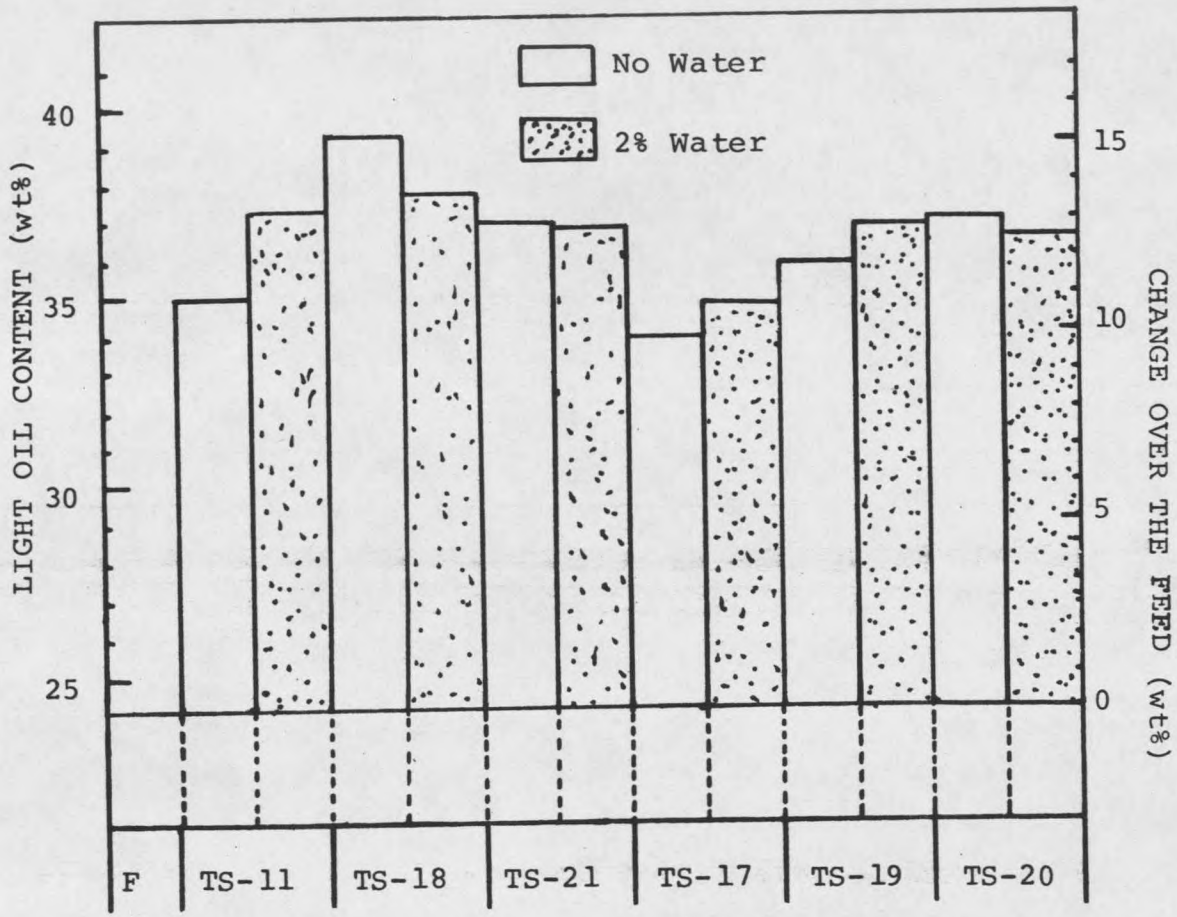

Figure 23. Light Oil (40 - 205°C) Yield for Ni-Mo and Co-Mo Catalysts
F = Feed, TS-11; Co+Mo, step, TS-18; Mo+Co, TS-21; Co:s+Mo:b, TS-17; Ni+Mo, step, TS-19; Mo+Ni, TS-20; Ni:s+Mo:b.

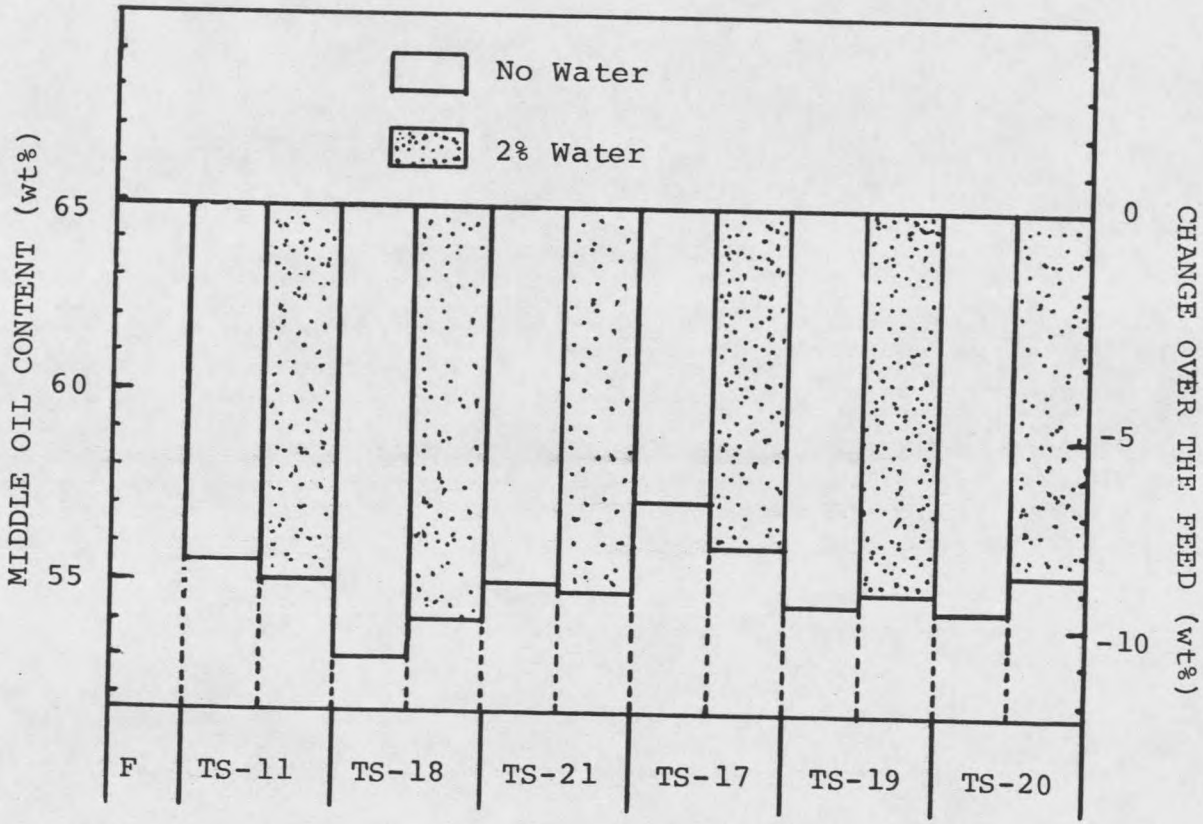

Figure 24. Middle Oil (205 - 298 ^{o}C) Yield for Ni-Mo and Co-Mo Catalysts

F = Feed, TS-11; Co+Mo, step, TS-18; Mo+Co, TS-21; Co:s+Mo:b, TS-17; Ni+Mo, step, TS-19; Mo+Ni, TS-20; Ni:s+Mo:b.

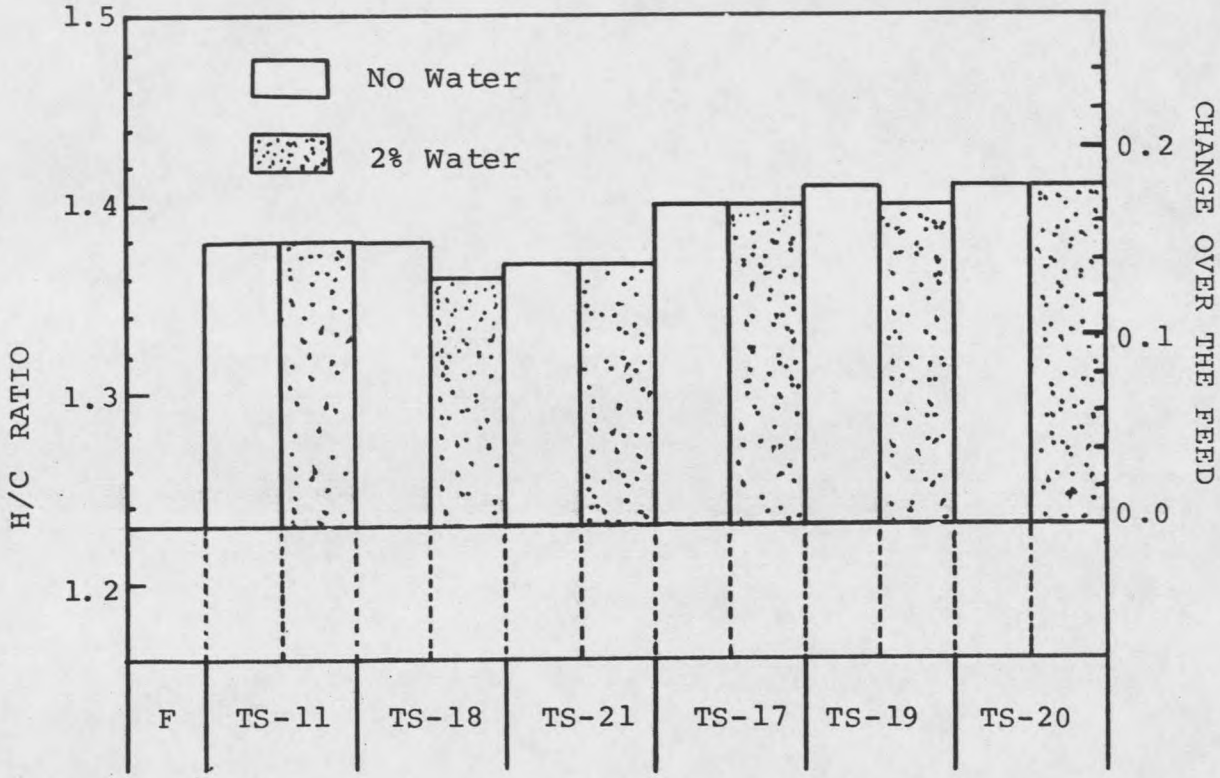

Figure 25. The Effect of Impregnation Technique and Water Addition on H/C Ratio for Ni-Mo and Co-Mo Catalysts

F = Feed, TS-11; Co+Mo, step, TS-18; Mo+Co, TS-21; Co:s+Mo:b, TS-17; Ni+Mo, step, TS-19; Mo+Ni, TS-20; Ni:s+Mo:b.

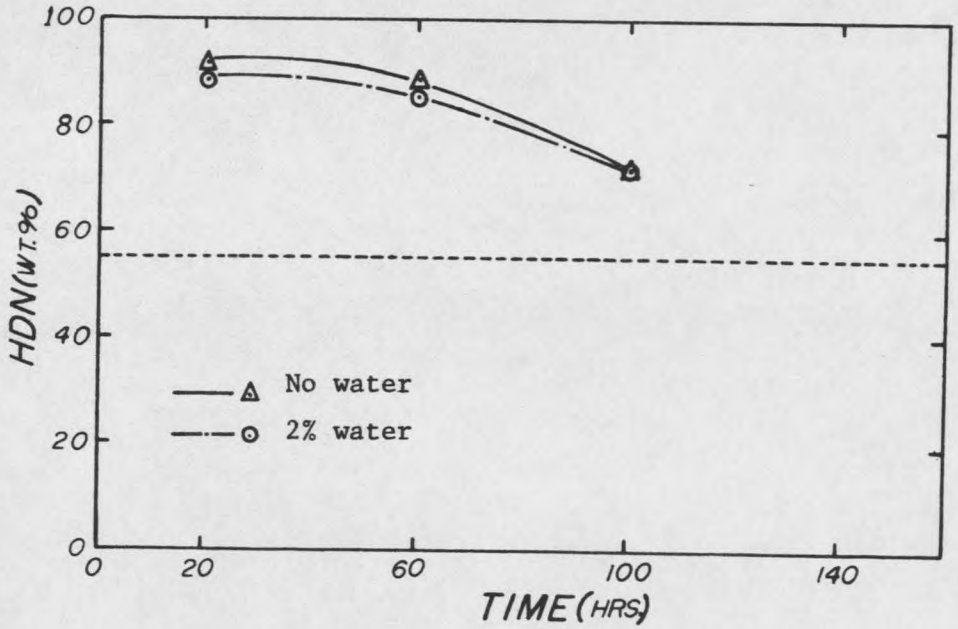

Figure 26. Hydrodenitrogenation vs. Time for the Catalyst TS-20
(4 wt%:s, 16 wt% Mo:b)

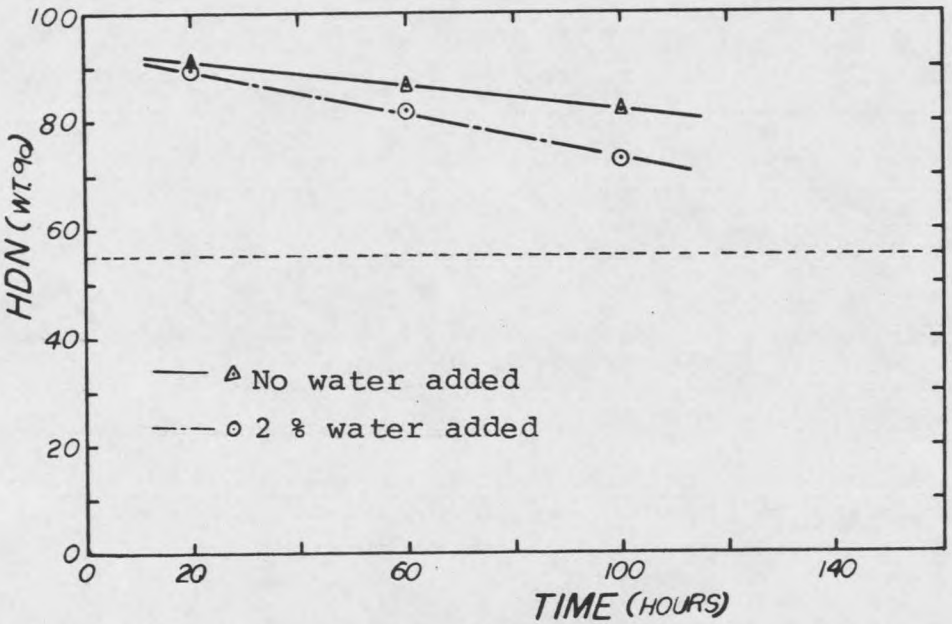

Figure 27. Hydrodenitrogenation vs. Time for the Catalyst TS-18 (16 wt% Mo, 4 wt% Co)

effect of water on the product quality and H/C ratio was negative, indicating an inhibitive effect of water on HYD activity. HYC activity was probably not affected since the heavy oil fraction was reduced about the same amount in both runs (see Table 9).

Fig. 28 shows HDN results of the catalyst TS-21 (4% Co, 16% Mo). HDN activity of this catalyst was slightly better than TS-11 (Co+Mo, step) but less than TS-18 (Mo+Co) (see Table 8). Water inhibited HDN activity. The effect of water on the product quality and H/C ratio was not significant. Light oil production was more than TS-11 (Co+Mo, step) but less than TS-18 (Mo+Co).

Summary, Impregnation Techniques: Activities of the Ni-Mo catalysts are not affected greatly by impregnation technique, but activities of the Co-Mo catalysts are. When Mo is impregnated first and then Co, the activity of the catalyst was improved considerably. HDN and HYC activities were affected most. When catalyst TS-18 (Mo+Co) is compared with Ni-Mo catalysts, its activity for HDN is about the same and better for HYC, but less for HYD. This gives an advantage to this catalyst over Ni-Mo catalysts. It selectively removes nitrogen and cracks high molecular-weight hydrocarbons with less hydrogen consumption. Impregnation technique has an effect only on the product quality for Ni-Mo catalysts. In general, when Mo was impregnated batchwise, light oil production was improved, basically because of improved HYC activity since HYD activity remained nearly the same (see Fig. 23).

Research octane numbers (RON) were determined for the light oil fractions from the runs without water addition (see Table 6). Results

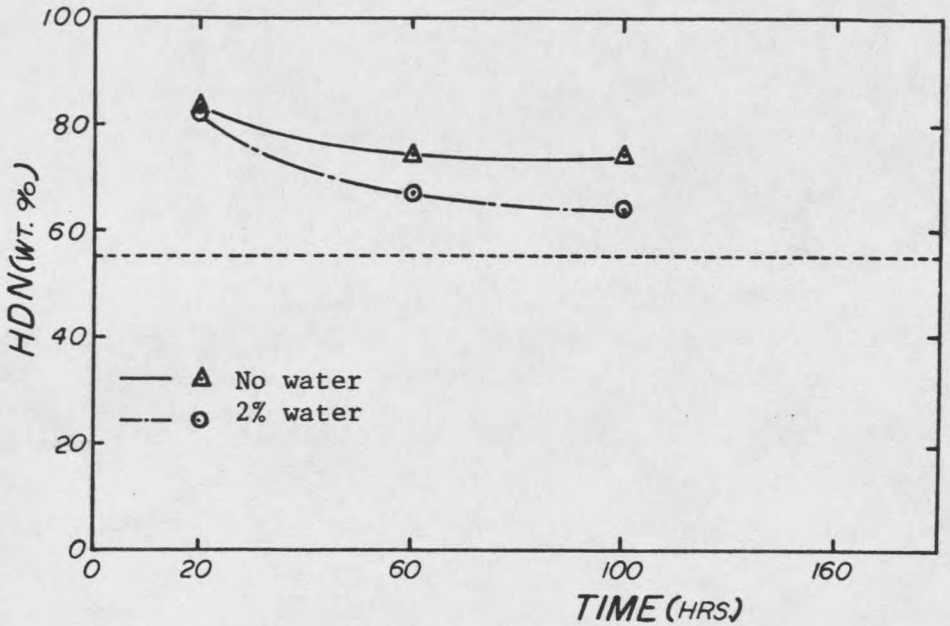

Figure 28. Hydrodenitrogenation vs. Time for the Catalyst TS-21
(4 wt% Co:s, 16 wt% Mo:b)

support the above discussion. The Co-Mo catalysts produce products with higher octane numbers than the Ni-Mo catalysts do. This shows the higher HYC activity of the Co-Mo catalysts.

THE ESCA (XPS) ANALYSIS

ESCA measurements were done for every catalyst evaluated to correlate catalytic activity with the chemical structure and distribution of metals on the support. (The peak binding energies are given in Appendix D.). First, the effect of impregnation technique on the chemical structure will be given, and then that of the metal combinations.

Effect of Impregnation Technique: Mo 3d and Ni 2p spectra of Ni-Mo catalysts are given in Fig. 29 and Fig. 30, respectively. These spectra include some reference compounds and sulfided catalysts as well as the oxide catalysts. Determining the surface structure only from the figures is difficult because of charging problems in ESCA (XPS) analyses. Although the charging was corrected by carbon 1s peak binding energy, its reliability is questionable [36, 191]. In addition to the shifts in binding energies (as shown in the figures), FWHM (Full Width at Half Maximum band) and binding energy differences between specific band peaks (such as Al 2p, O 1s and S 2p) and Ni $2p_{3/2}$ and Mo $3d_{5/2}$ will be utilized in analyzing the data. Binding energy differences (ΔE) eliminate error carried by the C 1s correction since all the spectra in question are subject to the same error source [191]. These are shown in Tables 11, 12 and 13.

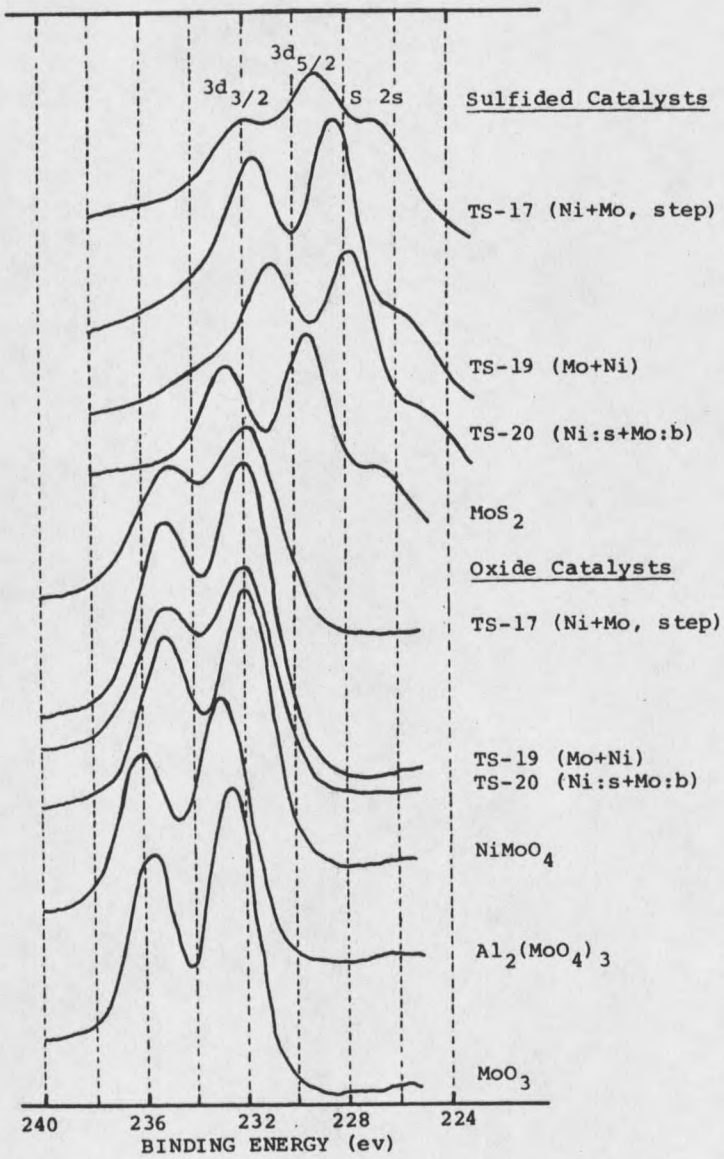

Figure 29. The Effect of Impregnation Technique on the XPS Mo 3d Spectra of the Ni-Mo Catalysts

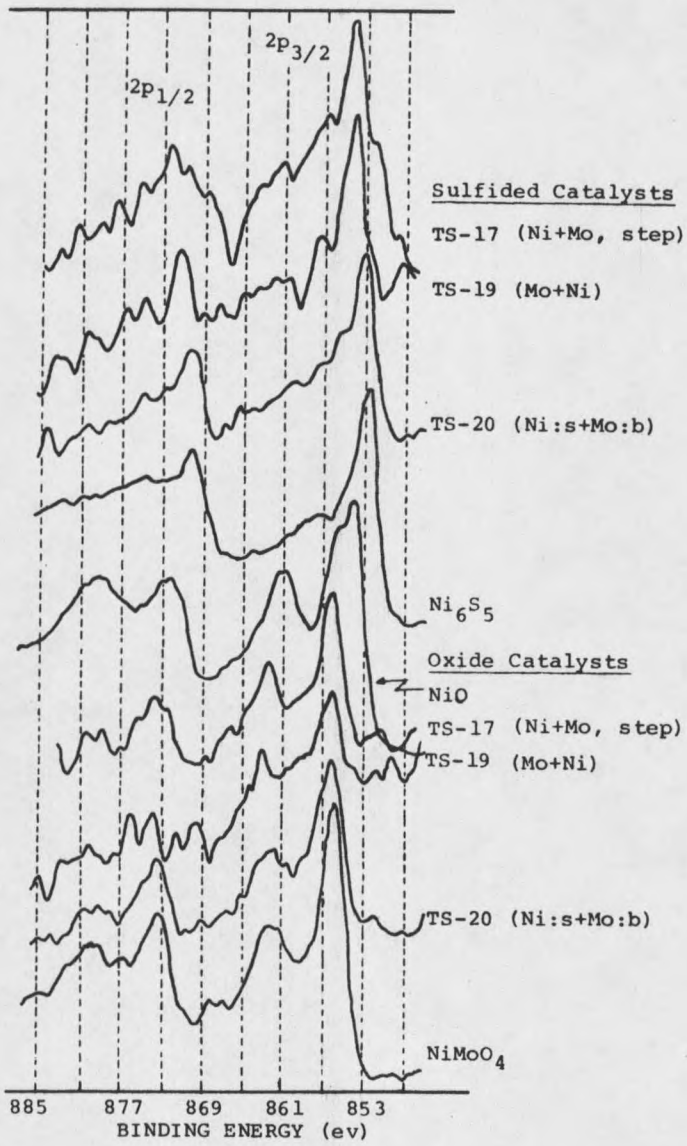

Figure 30. The Effect of Impregnation Technique on the XPS Ni 2p Spectra of the Ni-Mo Catalysts

Table 11. The Effect of Impregnation Technique on the FWHM of the Ni-Mo Catalysts

Catalyst or Compound	Mo 3d (ev)	Al 2p (ev)	Al 2s (ev)	O 1s (ev)	S 2p (ev)
TS-17 (Ni+Mo, step)	5.8	3.0	3.7	3.4	NA
TS-19 (Mo+Ni)	5.4	2.9	3.8	3.4	NA
TS-20 (Ni:s+Mo:b)	5.5	3.0	3.8	3.5	NA
$NiAl_2O_4$	NA	3.0	3.6	3.1	NA
Support	NA	3.1	4.2	3.7	NA
$Al_2(MoO_4)_3$	5.3	2.9	3.2	2.8	NA
MoO_3	5.3	NA	NA	2.4	NA
NiO	NA	NA	NA	2.7	NA
TS-17S* (Ni+Mo, step)	7.4	4.9	5.9	5.3	4.3
TS-19S* (Mo+Ni)	5.7	3.2	3.8	3.9	3.0
TS-20S* (Ni:s+Mo:b)	6.0	4.6	5.0	5.0	2.9
MoS_2	5.2	NA	NA	5.0	2.9
Ni_6S_5	NA	NA	NA	2.6	3.4

* Sulfided form
FWHM = Full Width at Half Maximum band
NA = Not available or not applicable

Mo 3d spectra of TS-17 (Ni+Mo, step) is broadened when compared with that of TS-19 (Mo+Ni) and TS-20 (Ni:s+Mo:b). Some investigators [31] attribute this broadening to the charging effect when they compare the spectra of impregnated and unimpregnated catalysts. Since both impregnated and unimpregnated catalyst samples are of the insulating type (in oxide form), they are subject to a similar charging effect. This phenomena can be seen from Table 11 when FWHM of $Al_2(MoO_4)_3$ and $NiMoO_4$ are compared with that of TS-19 (Mo+Ni) and TS-20 (Ni:s+Mo:b). They have about the same FWHM (5.3 vs. 5.4 ev).

Table 12. Specific Binding Energy Differences (ΔE) for the Ni-Mo Catalysts.

Catalyst or Compound	Mo - O $3d_{5/2}$ - 1s (ev)	Mo - Al $3d_{5/2}$ - 2p (ev)	Ni - Al $2p_{3/2}$ - 2p (ev)	Ni - Mo $2p_{3/2}$ - $3d_{5/2}$ (ev)	Ni - O $2p_{3/2}$ - 1s (ev)
TS-17*	299.2	158.2	NA	624.1	NA
TS-19*	298.2	158.1	799.8	623.9	NA
			802.1		
TS-20*	298.8	158.1	799.3	624.0	NA
			800.5	627.0	
			804.0		
$NiMoO_4$	298.0	NA	NA	624.0	326.0
NiO	NA	NA	NA	NA	325.0
MoO_3	298.0	NA	NA	NA	NA
$Al_2(MoO_4)_3$	298.6	158.6	NA	NA	NA
TS-17S**	303.0	154.3	796.2	625.4	322.4
			797.8	628.0	325.0
			800.7		320.7
TS-19S**	304.0	154.1	796.9	625.6	321.6
			800.2	629.0	325.0
			802.2		320.7
TS-20S**	304.0	153.3	796.5	625.9	321.9
			799.0	628.1	324.1
			800.2		
			801.2		
Ni_6S_5	NA	NA	NA	NA	320.6
MoS_2	302.6	NA	NA	NA	NA

* TS-17 (Ni+Mo, step), TS-19 (Mo+Ni), TS-20 (Ni:s+Mo:b).
** Sulfided form
NA = Not available or not applicable

Table 13. Specific Binding Energy Differences (ΔE) of the Sulfided Ni-Mo and Co-Mo Catalysts

Catalyst or Compound	Mo $3d_{5/2}$-S 2p (ev)	Ni $2p_{3/2}$-S 2p (ev)
TS-17S (Ni+Mo, step)	67.4	692.7
TS-19S (Mo+Ni)	66.7	692.4
TS-20S (Ni:s+Mo:b)	66.7	692.7
Ni_6S_5	NA	691.5
MoS_2		
		Co $2p_{3/2}$-S 2p
TS-11S (Co+Mo, step)	67.4	615.5
		618.1
		620.7
		621.6
TS-18S (Mo+Co)	67.0	617.3
		618.1
TS-21S (Co:s+Mo:b)	66.9	617.2
		617.7
Co_9S_8	NA	616.6

NA = not applicable

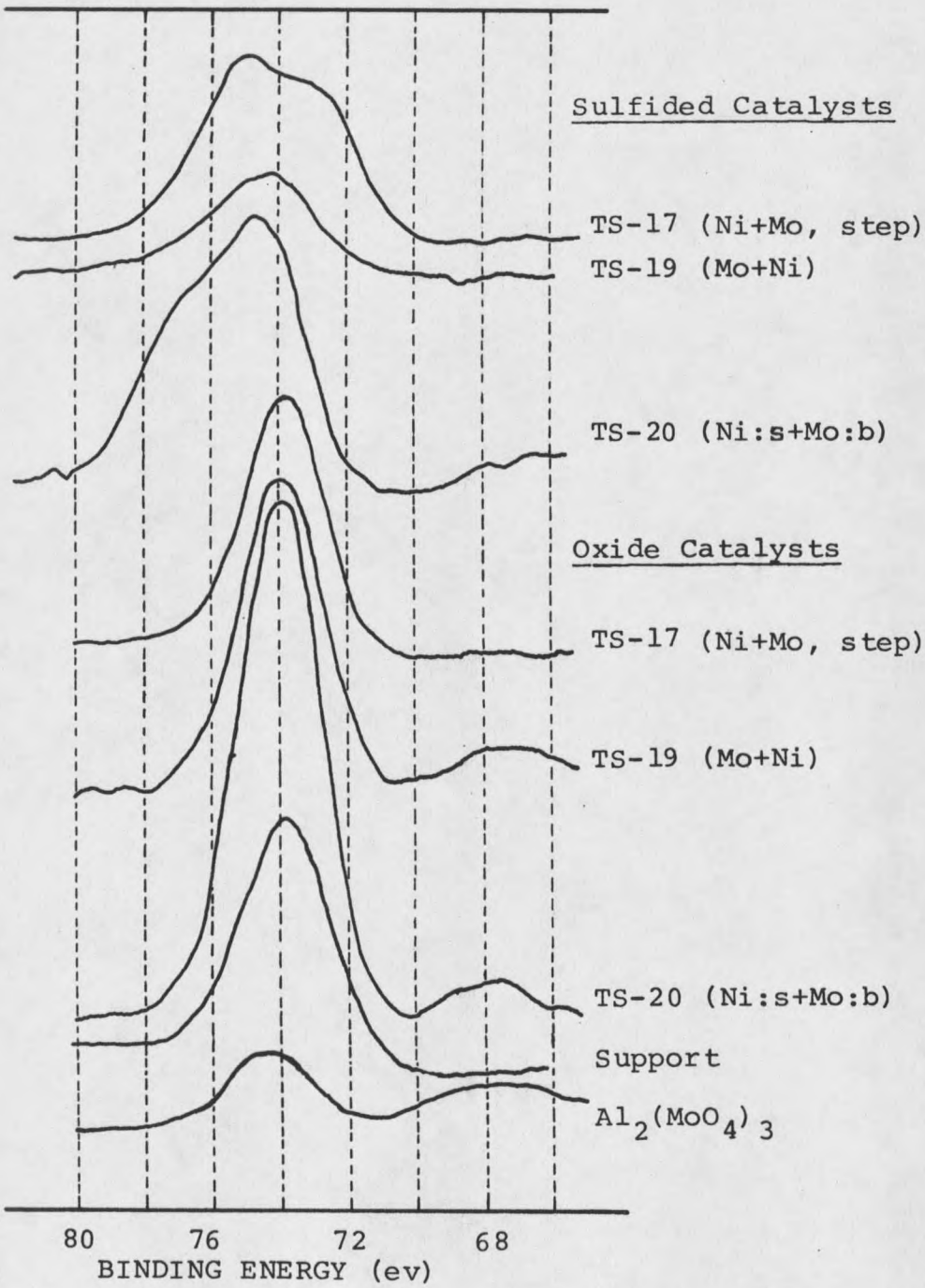

Figure 31. The Effect of Impregnation Technique on the XPS Al 2p Spectra of the Ni-Mo Catalysts

Therefore, in this study, the band broadening will be attributed to the appearance of more than one chemical [182] or geometrical state of the compound on the catalyst surface. More evidence of this will be given and discussed in the following pages. As a result, it is believed that Mo is present in more than one phase in TS-17 (Ni+Mo, step).

When the sulfided form of the TS-17 (Ni+Mo, step) catalyst is considered (upper section of Fig. 29), it has even larger FWHM (7.4 ev) than the oxide form. This is probably due to a partially sulfidable or non-sulfidable form of Mo present on the catalyst surface. Similar broadening of Mo 3d spectra occurs with TS-19 (Mo+Ni) and TS-20 (Ni:s+Mo:b) upon sulfiding. However, it is less with these latter catalysts (5.4 vs. 5.7 with TS-19 and 5.5 vs. 6.0 ev with TS-20). A similar band broadening is observed with Al 2p (see Fig. 31), Al 2s, S 2p and O 1s spectra (see Table 11). Broadening associated with these spectra is larger for TS-17 (Ni+Mo, step).

The difference between TS-17 and TS-19 is that both Ni and Mo are impregnated stepwise in TS-17, but batchwise with the reverse impregnation sequence in TS-19. In TS-20 batchwise impregnation of Mo and two-step impregnation of Ni was used (four step in TS-17). Recalling this background information, it can be postulated that the catalyst TS-17 (Ni+Mo, step) contains the most partially sulfidable phases combined with Al_2O_3. Since Mo 3d band for TS-17 (Ni+Mo, step) is broader in both the sulfided and oxide forms than these bands in TS-19 (Mo+Ni) and TS-20 (Ni:s+Mo:b), the presence of some $Al_2(MoO_4)_3$ type phase can be postulated. It is a structure probably formed by

movement of Mo into the alumina lattice. This structure gives characteristics of $Al_2(MoO_4)_3$ although the complete structure may not be in the normal molybdate form. Moreover, involvement of some Ni in this phase can not be excluded as discussed below. This phase is partially sulfidable since both Mo 3d and Al 2p bands were broadened upon sulfiding. The S 2p spectra was also broadened for this catalyst, supporting the argument above. Probably sulfur is present in a different chemical state and/or geometrical position in this structure as compared to the other sulfur structures that will be discussed below.

When Mo 3d spectra of TS-19 (Mo+Ni) and TS-20 (Ni:s+Mo:b) are compared with that of TS-17 (Ni+Mo, step), it can be said that formation of $Al_2(MoO_4)_3$ type phase in these catalysts is not likely, or insignificant if it is formed at all. The other possible structures possibilities are $NiMoO_4$, MoO_3 and a polymolybdate phase.

The presence of MoO_3 is questionable. Even if it exists, it should not be in an amount large enough to be detected by ESCA. MoO_3 would have been sulfided to MoS_2 if it had existed in significant quantity. The data from the sulfided catalysts do not give evidence of MoS_2 formation. ΔE (Mo $3d_{5/2}$-S 2p) and ΔE (Mo $3d_{5/2}$-O 1s) for TS-19 (Mo+Ni) and TS-20 (Ni:s+Mo:b) are less than that for MoS (see Tables 12 and 13). ΔE(Mo $3d_{5/2}$-S 2p) for MoS_2 comes close to the value for TS-17 (Ni+Mo, step), but it can be an anomaly of the data caused by the other phases being present on this particular catalyst or it may really represent the MoS_2 phase. The formation of MoS_2 on TS-17 (Ni+Mo, step) is possible as will be discussed below.

When ΔE (Mo $3d_{5/2}$-Ni $2p_{3/2}$) values are compared (see Table 12), formation of $NiMoO_4$ type structure is possible. However, a distinctive $NiMoO_4$ phase may not have developed under the concentration ranges of this study. It is probably a phase intermediate between a polymolybdate and $NiMoO_4$ resembling a structure close to $NiMoO_4$. This phase is probably less developed in TS-17 (Ni+Mo, step). Upon sulfiding, this phase is probably converted to a Ni-Mo-S phase well dispersed on the Al_2O_3 surface. It may contain some oxygen in its structure. In the case of TS-17 (Ni+Mo, step), this phase may be converted to Ni-Mo-S and some MoS_2 (well dispersed among the other phases) since the majority of the Ni will be in the Al_2O_3 lattice. Since the spectra of TS-19 (Mo+Ni) and TS-20 (Ni:s+Mo:b) do not give evidence for the formation of MoS_2 and Ni_6S_5 in significant quantities, the above assignment is justifiable. Under the sulfiding conditions of this study, MoS_2 and Ni_6S_5 should have formed if they were completely sulfided [201]. The formation of a similar phase (Co-Mo-S) with Co-Mo catalysts is discussed in the literature [191, 211, 212]. The Ni-Mo-S phase can be formulated as $Ni_xMo_{1-x}S_{2\pm\delta}$ by analogy to Co-Mo catalysts.

Analyses of Ni 2p spectra are more difficult than that of Mo 3d since the peak binding energies of different Ni phases differ by only 0.2 to 0.5 ev. This small difference can easily be masked by charging effects and experimental errors. Resolution of the band is a problem also.

The formation of the $NiAl_2O_4$ type phase under almost any kind of impregnation technique is possible [55]. Therefore, this phase will not be excluded in this study even though spectra for $NiAl_2O_4$ is not

available. There is always some Ni moved into the Al_2O_3 lattice occupying tetrahedral sites which is not sulfidable. When Ni $2p_{3/2}$ spectra of sulfided catalysts are compared, the secondary peaks appearing at higher binding energy level are assignable to $NiAl_2O_4$ type structure. This peak is stronger in the Ni $2p_{3/2}$ spectra of the catalyst TS-17 (Ni+Mo, step) indicating the presence of more Ni in $NiAl_2O_4$ type phase as expected. In fact, stepwise impregnation of Ni should cause movement of more Ni into the Al_2O_3 lattice similarly to the discussion by Chung and Massoth [29, 30] with Co-Mo catalysts. The presence of some Ni in the $Al_2(MoO_4)_3$ type phase is possible if the broader Ni $2p_{3/2}$ and Ni $2p_{1/2}$ bands are taken as the evidences of this involvement. However, the nature of this interaction is not clear.

Probably there is no distinct NiO phase in these catalysts since the Ni $2p_{3/2}$ peak of NiO appears at substantially lower binding energy. The rest of the Ni may be present in the $NiMoO_4$ type phase or other minor phases. The presence of Ni_2O_3 can not be excluded in these catalysts. This phase can not be distinguished from $NiMoO_4$ by ESCA since their peak binding energies are very close to each other.

Since Al 2p, Al 2s and O 1s bands are broadened for all of the Ni-Mo catalysts, the presence of some partially sulfidable Ni phase in the Al_2O_3 lattice is possible. As discussed above, the broadening of these bands is larger for the catalyst TS-17 (Ni+Mo, step). The broadening increases in the order TS-17 > TS-20 > TS-19. Since Ni was loaded in four steps on the catalyst TS-17, two steps on the catalyst TS-20 and a single step on the catalyst TS-19 (reverse sequence of

metal impregnation for this catalyst) and the stepwise impregnation of Ni causes movement of more Ni into the Al_2O_3 lattice, these band broadenings are probably caused by a partially sulfidable Ni phase associated with the Al_2O_3 structure in addition to $Al_2(MoO_4)_3$ type phase in TS-17 (Ni+Mo, step). If the phase was not associated with Al_2O_3, the Al 2p and Al 2s bands would not be effected. When the Ni-Mo catalysts are sulfided, there is a possibility of the formation of some Ni_6S_5 (a more stable form of Ni). Indeed, the shoulders appearing on the lower binding energy side of the Ni $2p_{3/2}$ spectra (see Fig. 30) coincide with Ni_6S_5 (see also Table 12). However, the amount of this phase should be small compared to the other sulfided Ni phase (Ni-Mo-S) since its peak appears as a weak shoulder. It can be speculated here that the Ni_6S_5 phase comes from the sulfidation of separate Ni phases such as Ni_2O_3 if it is assumed that Ni present in the surface $NiMoO_4$ type phase is converted only to the Ni-Mo-S phase.

In summary, stepwise impregnation of Ni and Ni+Mo (Ni first) impregnation order caused movement of more Ni into the Al_2O_3 lattice and the amount is related to the number of steps of Ni impregnation. Stepwise impregnation of Mo also caused movement of Mo into the Al_2O_3 lattice forming a phase similar to $Al_2(MoO_4)_3$, but some Ni may also present in this structure. Some of the Ni and Mo in the Al_2O_3 lattice appears to be partially sulfidable. The rest of Ni and Mo is probably present in $NiMoO_4$ type structure and in some surface Ni_2O_3. However, the assignment of Ni_2O_3 is a speculation at this stage. The $NiMoO_4$ type phase seems to be sulfidable to an intermediate phase resembling a structure like $Ni_xM_{1-x}S_{2+w}$.

The Mo 3d and Co 2p spectra of the Co-Mo catalysts are shown in Fig. 32 and Fig. 33 respectively. The Mo 3d spectra of the catalyst TS-11 (Co+Mo, step) is very similar to that of the catalyst TS-17 (Ni+Mo, step). The band is broadened to almost the same amount upon sulfiding. The Al 2p, Al 2s, O 1s and S 2p bands of the catalyst TS-11 (Co+Mo, step) are also broadened (see Fig. 34 and Table 14) more than those of the catalysts TS-18 (Mo+Co) and TS-21 (Co:s+Mo:b). However, the broadening is less when compared to the Ni-Mo catalysts. This difference can be due to the difference between Ni and Co.

As a result some Mo was moved into the Al_2O_3 lattice when it was impregnated stepwise. This is again an $Al_2(MoO_4)_3$ type structure and some Co may be involved in this structure as will be discussed below. The presence of $Al_2(MoO_4)_3$ type phase in the catalysts TS-18 (Mo+Co) and TS-21 (Co:s+Mo:b) is not likely or insignificant if it exists at all. The rest of Mo in the catalyst TS-11 (Co+Mo, step) is probably present as a surface polymolybdate phase. It may interact with some Co but the interaction seems very weak (see Table 15, WE (Co $2p_{3/2}$-Mo $3d_{5/2}$)). This is expected because most of Co is tied to Al_2O_3. The majority of Mo in the catalysts TS-18 (Mo+Co) and TS-21 (Co:s+Mo:b) is probably present as a surface phase similar to $CoMoO_4$ (it is probably less developed in the catalyst TS-21), a phase intermediate between polymolybdate and $CoMoO_4$. This assignment can be supported by WE (Mo $3d_{5/2}$-O 1s) and WE (Mo $3d_{5/2}$-Al 2p) in Table 15. Similarly to the Ni-Mo catalysts, the presence of MoO_3 is questionable because of the absence of a detectable MoS_2. However, MoO_3 may present in insignificant quantities in every catalyst.

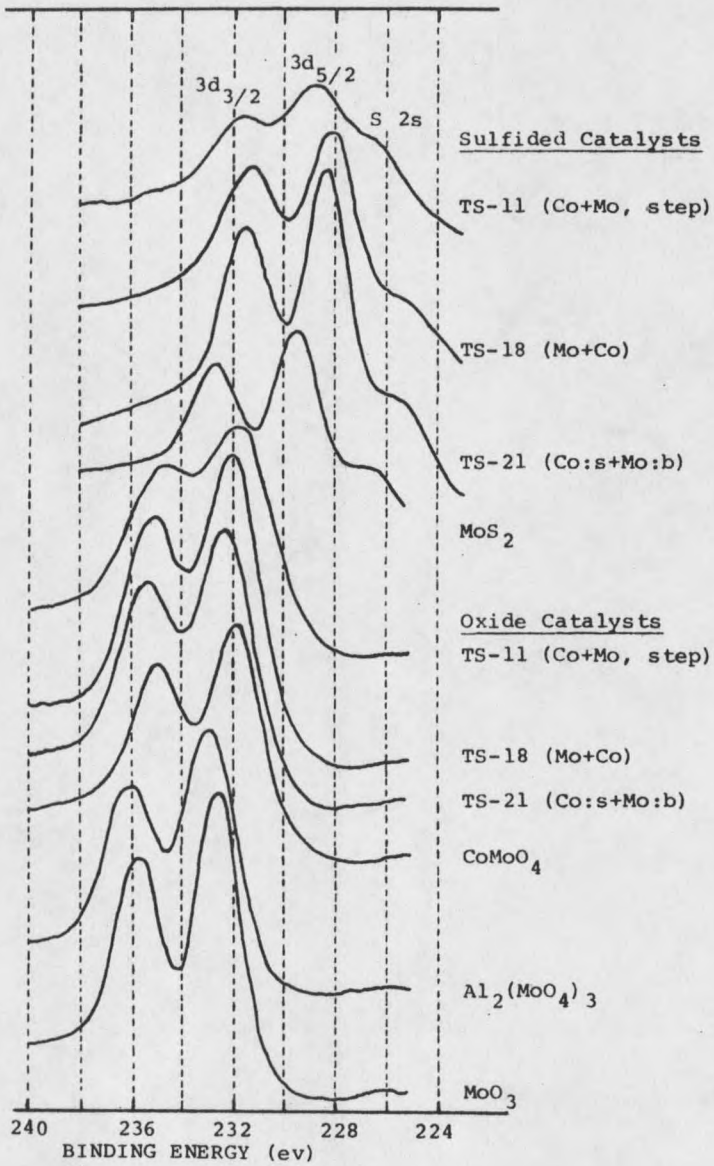

Figure 32. The Effect of Impregnation Technique on the XPS Mo 3d Spectra of the Co-Mo Catalysts

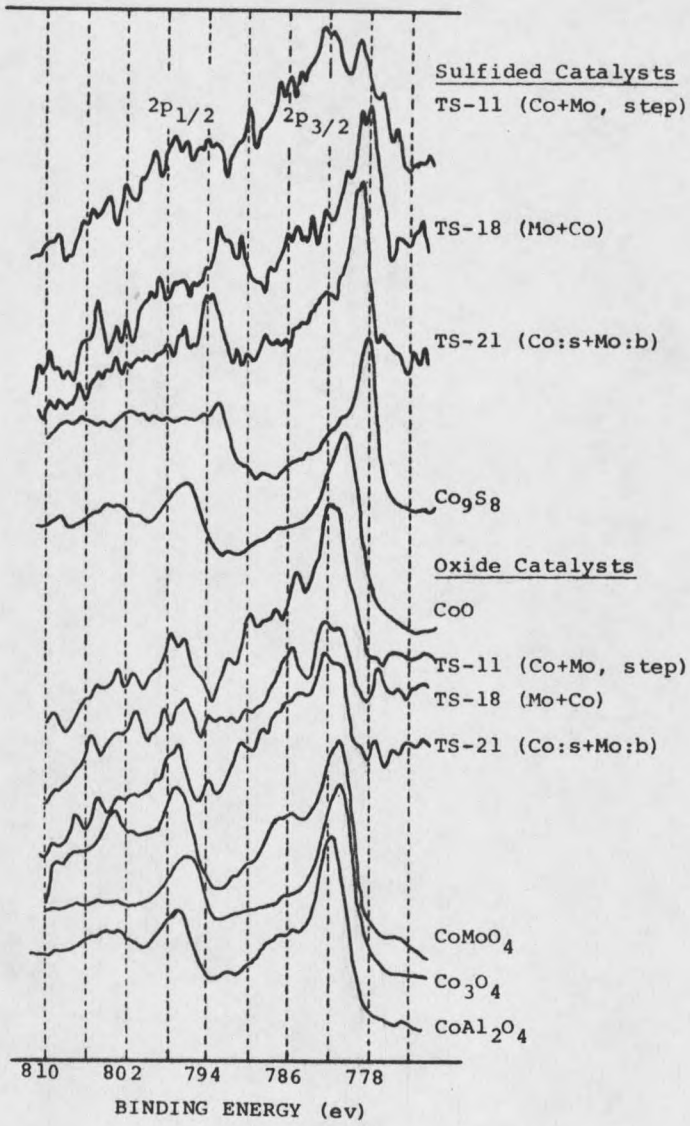

Figure 33. The Effect of Impregnation Technique on the XPS Co 2p Spectra of the Co-Mo Catalysts

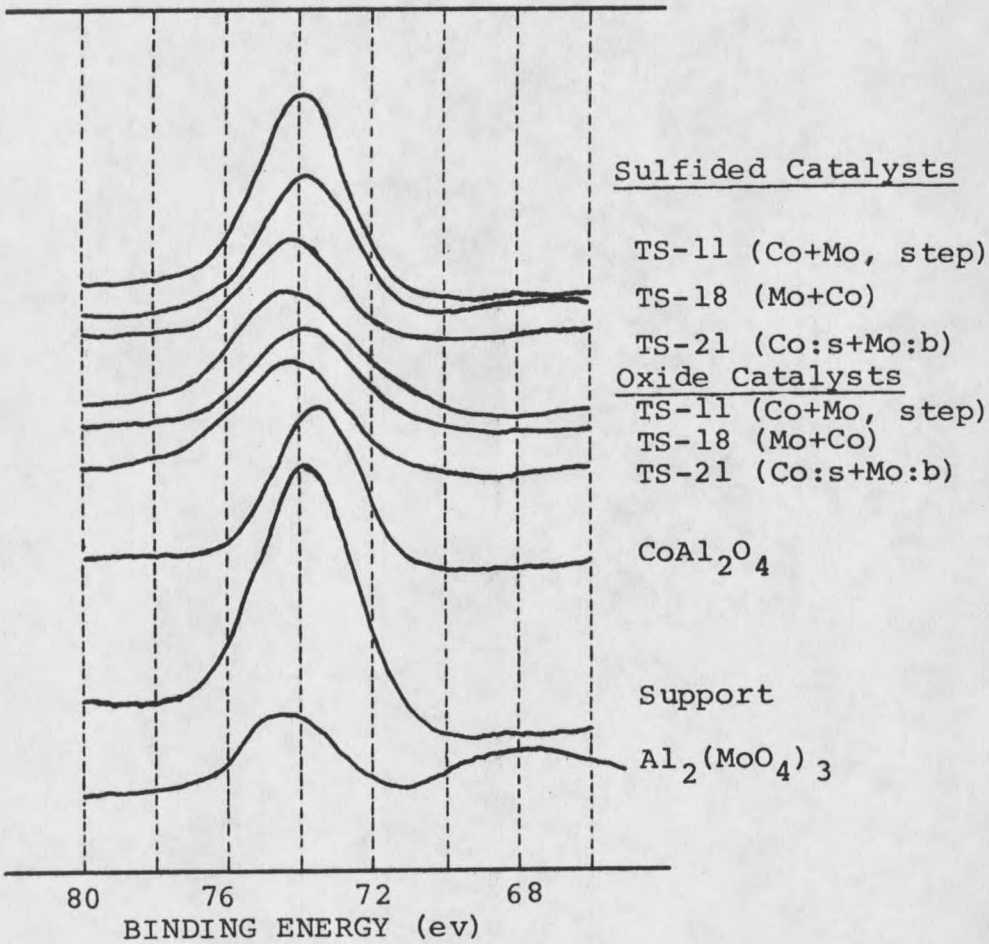

Figure 34. The Effect of Impregnation Technique on the XPS Al 2p Spectra of the Co-Mo Catalysts

Table 14. The Effect of Impregnation Technique on the FWHM of the Co-Mo Catalysts

Catalyst or Compound	Mo 3d (ev)	Al 2p (ev)	Al 2s (ev)	O 1s (ev)	S 2p (ev)
TS-11 (Co+Mo, step)	5.9	2.8	3.4	2.9	NA
TS-18 (Mo+Co)	5.4	2.9	3.5	3.0	NA
TS-21 (Co:s+Mo:b)	5.4	2.7	3.6	3.5	NA
$Al_2(MoO_4)_3$	5.3	2.9	3.2	2.8	NA
$CoAl_2O_4$	NA	2.7	3.0	3.5	NA
Support	NA	2.7	4.2	3.7	NA
MoO_3	5.0	NA	NA	2.1	NA
CoO	NA	NA	NA	4.0	NA
Co_3O_4	NA	NA	NA	2.8	NA
TS-11S (Co+Mo, step)*	7.1	3.8	4.3	3.8	3.8
TS-18S (Mo+Co)*	5.8	3.4	4.0	3.8	3.0
TS-21S (Co:s+Mo:b)*	5.5	3.5	4.1	3.8	3.0
MoS_2	5.2	NA	NA	5.0	2.9
Co_9S_8	NA	NA	NA	4.0	3.7

* Sulfided form
NA= Not applicable or not available
FWHM = Full Width at Half Maximum band

When Co-Mo catalysts are sulfided, Mo in the Al_2O_3 lattice is partially sulfidable and causes broadening in the Mo 3d, Al 2p (see Fig. 34), Al 2s, O1s and S 2p bands (see Table 14). The surface $CoMoO_4$ type phase is probably sulfidable to an intermediate phase, Co, Mo and S being attached together as reported by Topsoe et al. [191, 211, 212]. It is formulated as $Co_xMo_{1-x}S_{2\pm8}$. The less developed polymolybdate (associated with some Co) in the catalyst TS-11 (Co+Mo, step) is probably sulfided to two different phases; $Co_xMo_{1-x}S_{2\pm8}$ and MoS_2. MoS_2 may not be in a complete crystalline form. It is probably well dispersed among the other phases present.

Analyses of Co 2p spectra are more complicated than Ni 2p spectra of the Ni-Mo catalysts. The probability of forming different phases

Table 15. Specific Binding Energy Differences (ΔE) for the Co-Mo Catalysts

Catalyst or Compound	Mo - O $3d_{5/2}$ - 1s (ev)	Mo - Al $3d_{5/2}$ - 2p (ev)	Co - Mo $2p_{3/2}$ - $3d_{5/2}$ (ev)	Co - Al $2p_{3/2}$ - 2p (ev)	Co - O $2p_{3/2}$ - 1s (ev)	Co - Al $2p_{1/2}$ - 2p (ev)
TS-11*	298.8	158.5	549.6	NA	NA	NA
			550.2			
TS-18*	298.4	158.3	549.0	707.3	250.6	722.7
			550.4	708.8	252.0	723.3
						724.8
TS-21*	298.5	158.1	548.9	707.6	250.4	723.4
			550.2	708.9	251.7	724.4
						726.4
CoO	NA	NA	NA	NA	250.0	NA
Co_3O_4	NA	NA	NA	NA	250.5	NA
$CoMoO_4$	298.2	NA	549.0	NA	250.8	NA
$CoAl_2O_4$	NA	NA	NA	707.8	250.6	723.2
$Al_2(MoO_4)_3$	298.6	158.6	NA	NA	NA	NA
MoO_3	298.0	NA	NA	NA	NA	NA
TS-11S**	303.2	154.5	551.1	705.1	247.9	719.2
			553.7	707.7	250.5	720.1
			554.6	708.6	251.4	722.2
						723.3
TS-18S**	303.7	154.5	549.4	703.3	245.7	719.4
			550.7	704.6	247.0	720.7
			551.5	705.4	247.8	721.3
			552.8	706.7	249.1	723.4
TS-21S**	303.3	154.2	550.4	704.2	247.1	719.1
			550.9	704.7	247.6	722.0
			554.1	707.9	250,.8	723.4
Co_9S_8	NA	NA	NA	NA	243.9	NA
MoS_2	302.6	NA	NA	NA	NA	NA

* TS-11 (Co+Mo, step), TS-18 (Mo+Co), TS-21 (Co:s+Mo:b).
** Sulfided form
NA = Not applicable or not available

for Co is more than that for Ni. The most complicated structure exists in the catalyst TS-11 (Co+Mo, step) since Co $2p_{3/2}$ gave several peaks when sulfided. The Co $2p_{3/2}$ spectra show two major peaks for every Co-Mo catalyst (see Fig. 32).

The first Co phase to locate is the $CoAl_2O_4$ type phase (which is not a well developed compound) since it is not sulfidable. The second major peak in the Co $2p_{3/2}$ spectra of sulfided TS-11 (Co+Mo, step) catalyst and the third secondary peak in the Co $2p_{3/2}$ spectra of the sulfided TS-21 (Co:s+Mo:b) catalyst are directly assignable to the $CoAl_2O_4$ phase (see Fig. 32). Table 15 is more helpful for this assignment. ΔE (Co $2p_{3/2}$-O 1s) and ΔE (Co $2p_{3/2}$-Al 2p) reveals this information. Co $2p_{3/2}$ spectra of the sulfided TS-18 (Mo+Co) catalyst were not resolved for a $CoAl_2O_4$ peak. However, Co $2p_{1/2}$ spectra gives a weak peak at 796.3 ev which corresponds to $CoAl_2O_4$ (see Table 15 ΔE (Co $2p_{1/2}$-Al 2p)). This indicates the relatively less amount of $CoAl_2O_4$ formation in the catalyst TS-18 (Mo+Co) which agrees well with the literature [29, 30].

Since the rest of the Co phases are sulfidable to a certain degree, obtaining the information from the spectra of the sulfided catalysts will be difficult. The presence of $CoMoO_4$ type structure in the catalysts TS-18 (Mo+Co) and TS-21 (Co:s+Mo:b) is evident both from the Fig. 33 and Table 15 (ΔE (Co $2p_{3/2}$-Mo $3d_{5/2}$)). The formation of such a phase in the catalyst TS-11 (Co+Mo, step) is less likely or it may be present in small quantities. It is probably a polymolybdate structure somehow weakly associated with Co, which is more developed to a $CoMoO_4$ type structure in the catalysts TS-18 (Mo+Co) and TS-21

(Co:s+Mo:b). The formation of some Co_3O_4 and CoO can not be excluded in any of the Co-Mo catalysts. Obtaining this information is extremely difficult from the data in hand.

There is some partially sulfidable Co in the Al_2O_3 lattice in every catalyst since Al 2p, Al 2s and O 1s bands were broadened after sulfiding (see Table 14). Assigning this phase from the peak locations is not possible. There are several partially sulfided Co phases or Co phases at different sulfidation state in the catalysts TS-11 (Co+Mo, step) and TS-18 (Mo+Co) as evidenced by the peaks of Co $2p_{3/2}$ spectra. The presence of Co in the $Al_2(MoO_4)_3$ type phase is possible since Co $2p_{3/2}$ spectra of TS-11 (Co+Mo, step) is much broader than that of the other two catalysts.

In summary, stepwise impregnation of Co and Co+Mo (Co first) impregnation order caused movement of more Co into the Al_2O_3 lattice forming a $CoAl_2O_4$ type structure. The amount of Co in the Al_2O_3 lattice increased with increasing the number of impregnation steps. Some Mo was moved into the Al_2O_3 lattice forming an $Al_2(MoO_4)_3$ type structure probably in association with some Co. This phase seems to be partially sulfidable. There appears to exist some partially sulfidable Co attached to the Al_2O_3 lattice. The $CoMoO_4$ type phase and polymolybdate (with some Co association) are probably sulfided to an intermediate phase like $Co_xMo_{1-x}S_{2\pm\delta}$. The latter may form some MoS_2 in addition to $Co_xMo_{1-x}S_{2\pm\delta}$.

<u>Effect of Metal Combinations</u>: For this group of catalysts, Co 2p, Mo 3d, Ni 2p and W 4f XPS spectra were measured and are given in the Figures 35, 36, 37 and 38, respectively. FWHM for W 4f and Mo 3d

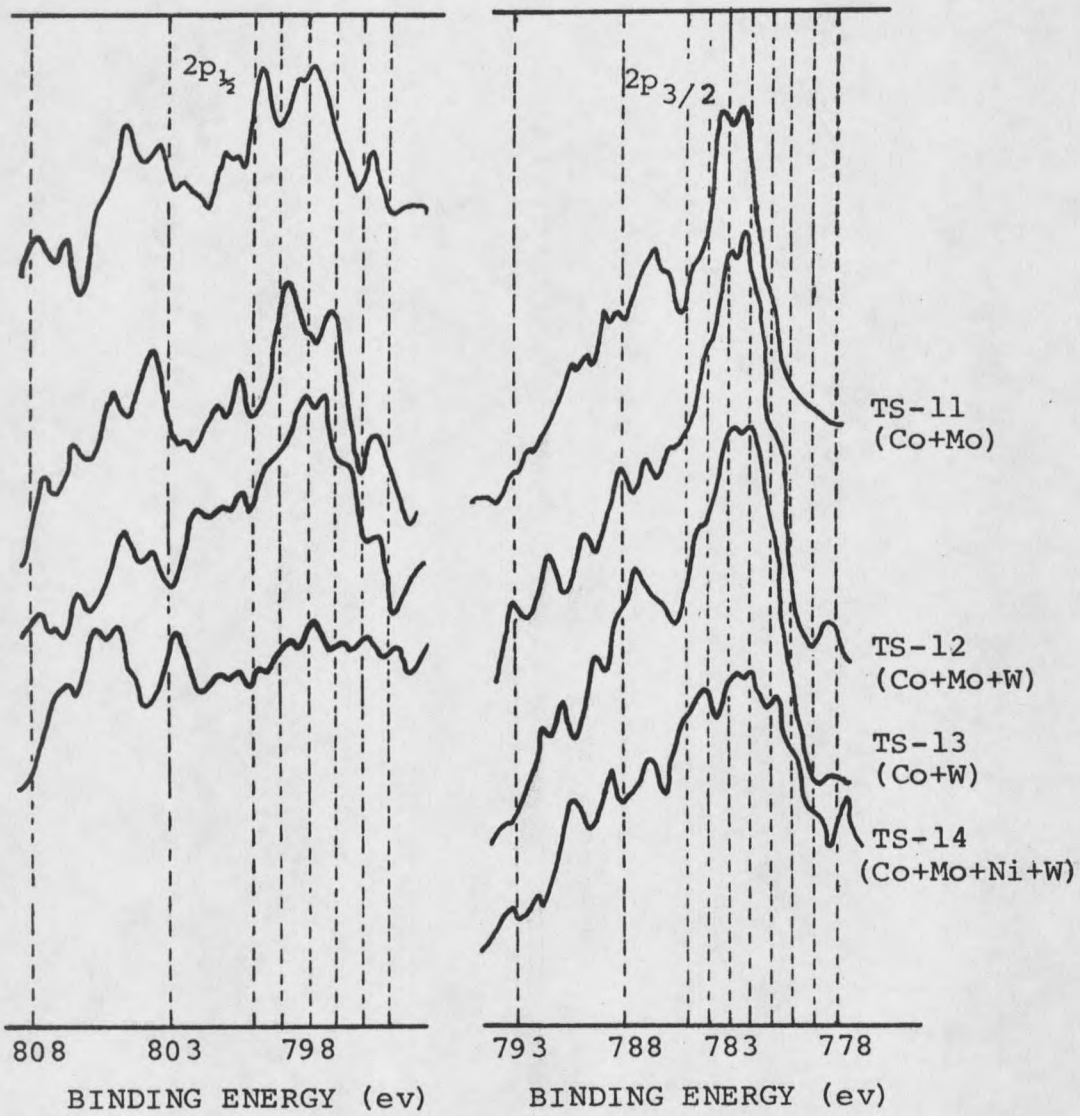

Figure 35. The Effect of Metal Combinations on the XPS Spectra of the Catalysts at the Co 2p Level

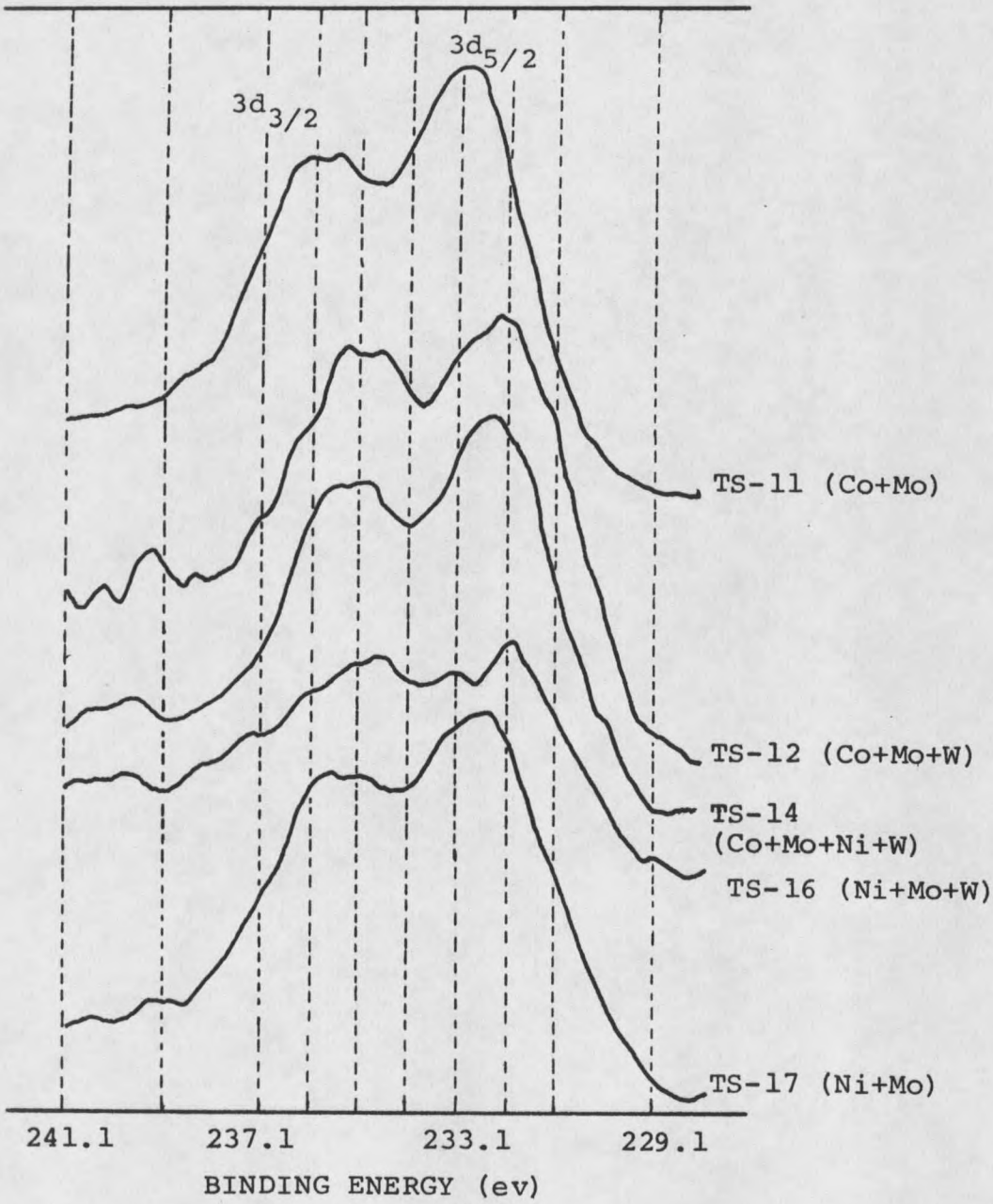

Figure 36. The Effect of Metal Combinations on the XPS Spectra of the Catalysts at the Mo 3d Level

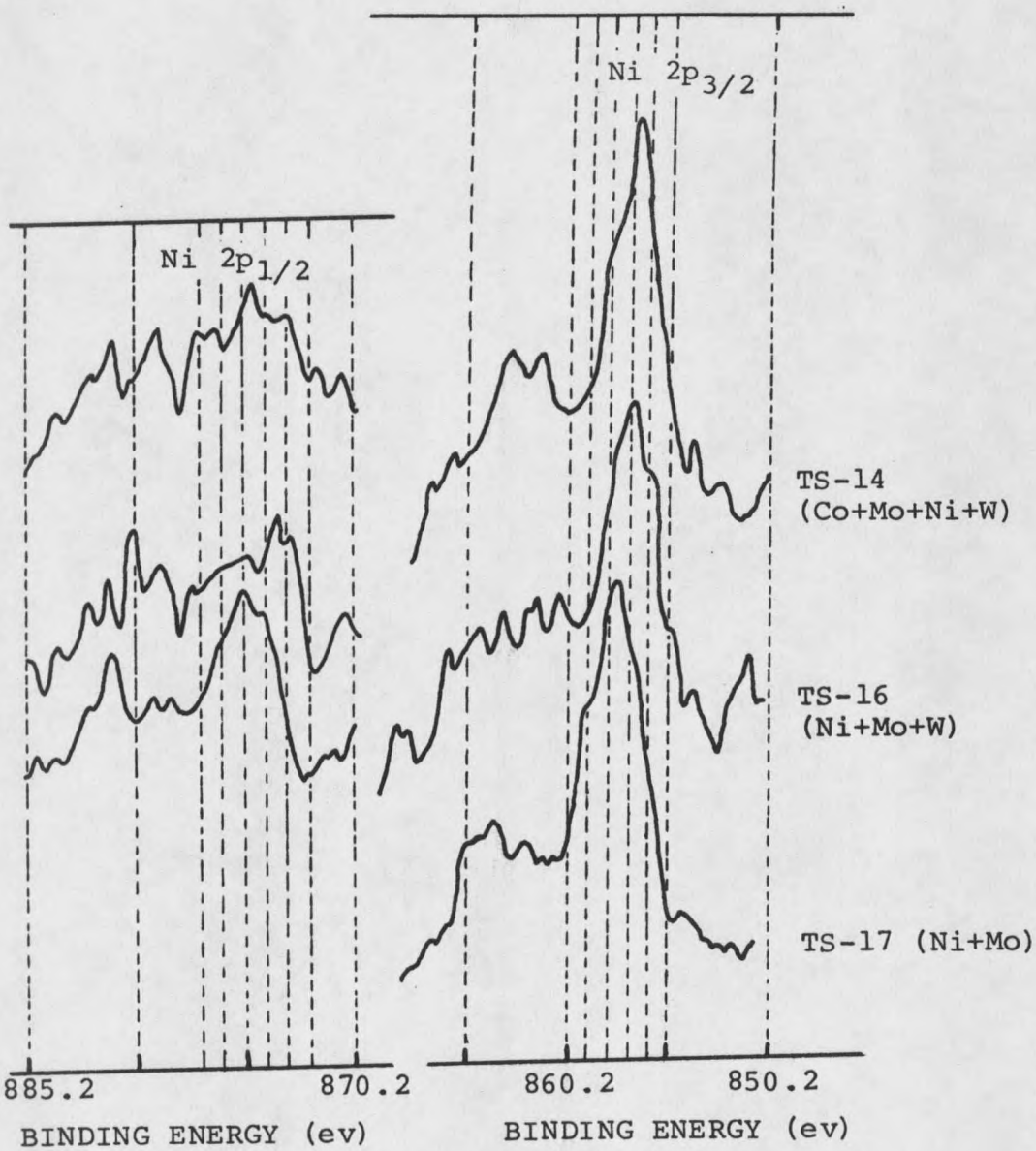

Figure 37. The Effect of Metal Combinations on the XPS Spectra of the Catalysts at the Ni 2p Level

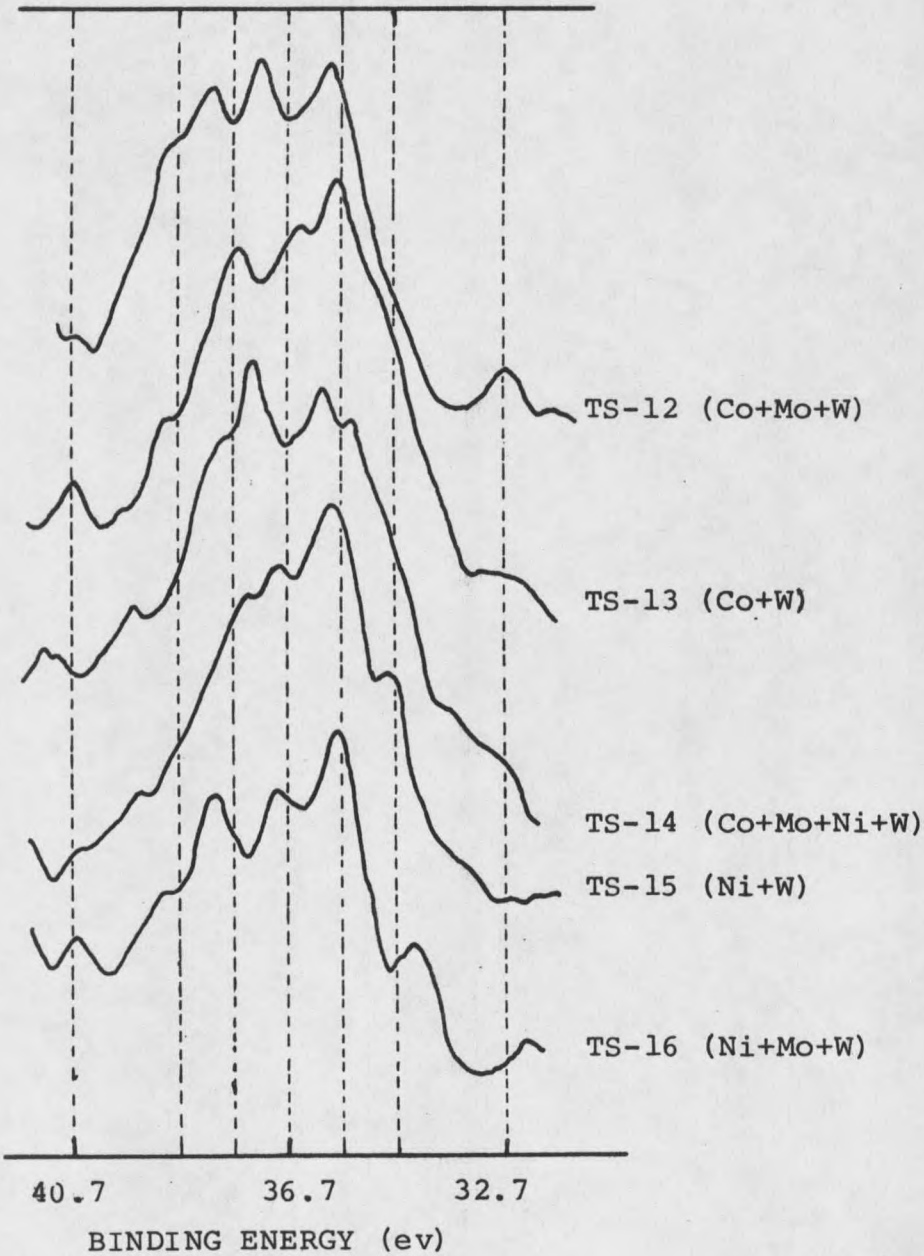

Figure 38. The Effect of Metal Combinations on the XPS Spectra of the Catalysts at the W 4f Level

spectra and specific binding energy differences (ΔE) are shown in Tables 16, 17 and 18 respectively.

Data for this group of catalysts are preliminary. That is why they will not be used to determine the true structure. They are included here to show some evidences of differences among the catalysts and a possible explanation of activity differences with them. Therefore, the results presented here and the discussion concerning this section will remain speculative until a more detailed analysis is available.

Table 16 indicates that FWHM of all catalysts for both Mo 3d and W 4f are broader than these for the reference compounds. This is evidence for the involvement of some Mo and W in the Al_2O_3 structure as discussed in the previous section. Both Mo and W probably interact with Al_2O_3. Some Ni or Co (which ever applies) may also be involved in this interaction since Ni and Co also moved into the Al_2O_3 lattice.

Analysis of the data is very complicated as can be seen from the Tables 17 and 18. Without any further study with sulfided and probably with reduced states of the catalysts, determination of the surface structure will be almost impossible. Mo and W may be present both on the surface and in the Al_2O_3 structure separately or in an interaction with each other. The same thing is true for Co and Ni when they are present together. Co-Mo-W, Ni-Mo-W and Co-Mo-Ni-W interactions are possible on the catalyst surface when they are present together. The differences between the shapes of Co 2p spectra for TS-11 (Co+Mo), TS-12 (Co+Mo+W), TS-13 (Co+W) and TS-14 (Co+Mo+Ni+W) show the presence

Table 16. The Effect of Metal Combinations on FWHM of Mo 3d and W 4f.

Catalyst or Compound	Mo 3d (ev)	W 4f (ev)
TS-11 (Co+Mo)	5.9	NA
TS-12 (Co+Mo+W)	5.7	4.6
TS-13 (Co+W)	NA	4.7
TS-14 (Co+Mo+Ni+W)	5.5	4.8
TS-15 (Ni+W)	NA	4.5
TS-16 (Ni+Mo+W)	5.7	4.6
TS-17 (Ni+Mo)	5.8	NA
WO_3	NA	3.5
MoO_3	5.0	NA
$Al_2MoO_4)_3$	5.3	NA
$NiMoO_4$	5.3	NA
$CoMoO_4$	5.2	NA

NA = Not applicable

of different Co structures in every catalyst (see Fig. 35) The same thing is true for Ni 2p spectra of TS-17 (Ni+Mo), TS-16 (Ni+Mo+W) and TS-14 (Co+Mo+Ni+W) (see Fig. 37). W 4f spectra of TS-12 (Co+Mo+W), TS-13 (Co+W), TS-14 (Co+Mo+Ni+W), TS-15 (Ni+W) and TS-16 (Ni+Mo+W) show some differences which indicate the presence of W in different forms in these catalysts. As a result, the surface structure of the catalysts in this group shows some similarities and dissimilarities. The presence of different phases or complex phases are greater with increasing the number of metals on a catalyst and analysis gets more complicated.

Table 17. Specific Binding Energy Differences (ΔE) for the Catalysts Studied for the Effect of Metal Combinations

Catalyst or Compound	Co 2p$_{3/2}$ (ev) - O 1s	Co 2p$_{3/2}$ (ev) - Al 2p	Mo 3d$_{5/2}$ (ev) - O 1s	Mo 3d$_{5/2}$ (ev) - Al 2p	Co 2p$_{3/2}$ (ev) - Mo 3d$_{5/2}$	
TS-11*	250.8	708.1	298.8	158.5	549.6	
	251.6	708.9			550.4	
TS-12*	250.3	707.9	299.4	158.2	549.7	
	250.9	708.5			550.3	
TS-13*	250.6	708.1	NA	NA	NA	
	251.3	708.8				
	252.8	710.3				
TS-14*	249.3	706.4	299.2	157.9	548.5	
	250.4	707.5	297.8	159.3	549.6	
	251.2	708.3			550.4	
	252.7	709.8			551.9	
$CoMoO_4$	250.8	NA	298.2	NA	549.0	
$CoAl_2O_4$	250.6	707.8	NA	NA	NA	
CoO	250.0	NA	NA	NA	NA	
Co_3O_4	250.5	NA	NA	NA	NA	
	Ni 2p-O 1s	Ni 2p-O 1s			Ni 2p-Mo 3d	
TS-15*	NA	NA	NA	NA	NA	
TS-16*	324.7	781.9	298.3	157.8	623.0	624.1
	325.6	782.8	299.4	158.9	623.9	625.0
	326.3	78.35			624.6	625.7
TS-17*	326.1	783.5	298.8	158.6	624.9	
			(297.9)	(159.2)	(624.3)	
TS-14*	325.4	782.5	299.2	157.9	624.6	
	326.5	783.6	297.8	159.3	625.7	
$NiMoO_4$	326.0	NA	298.0	NA	624.0	
$Al_2(MoO_4)_3$	NA	NA	298.6	158.4	NA	
MoO_3	NA	NA	298.0	NA	NA	

NA = Not applicable

* TS-11 (Co+Mo), TS-12 (Co+Mo+W), TS-13 (Co+W), TS-14 (Co+Mo+Ni+W), TS-15 (Ni+W), TS-16 (Ni+Mo+W), TS-17 (Ni+Mo).

Table 18. Specific Binding Energy Differences (ΔE) for the Catalysts Containing Tungsten

Catalyst or Compound	W O 4f 1s (ev)	W Al 4f 2p (ev)	W Mo 4f $3d_{3/2}$ (ev)	W Co 4f (ev)	W Co $2p_{3/2}$	W Ni 4f (ev)	W Ni $2p_{3/2}$
TS-12*	493.9	36.3	194.5	744.8	744.2	NA	
	494.8	37.2	195.4	745.7	745.1		
	496.2	38.6	196.8	747.1	746.5		
TS-13*	494.0	36.5	NA	746.8	745.3	NA	
	495.1	37.6		747.9	746.4		
	495.8	38.3		748.6	747.1		
				744.6			
				745.6			
				746.4			
TS-14*	493.5	36.4	195.7	746.2	744.7	820.0	
	494.0	36.9	196.2	746.7	745.2	820.5	
	495.4	38.3	197.6	748.1	746.6	821.9	
	495.9	38.8	198.1	748.6	747.1	822.4	
			194.3	743.9		818.9	
			194.8	744.4		819.4	
			196.2	745.8		820.8	
			196.7	746.3		821.3	
TS-15*	494.6	36.9	NA	NA		NA	
	495.2	37.5					
	496.2	38.5					
	497.2	39.5					
TS-16*	492.4	35.2	194.1	NA	818.7	818.0	
	493.3	36.1	195.0		819.6	818.9	
	494.5	37.3	196.2		820.8	820.1	
	495.6	38.4	197.3		821.9	821.2	
			193.0			817.1	
			193.9			818.0	
			195.1			819.2	
			196.2			820.3	
WO_3	493.0	NA	NA	NA		NA	
	495.1						

* TS-12 (Co+Mo), TS-13 (Co+W), TS-14 (Co+Mo+Ni+W), TS-15 (Ni+W), TS-16 (Ni+Mo+W).

NA = Not applicable

CHAPTER 5

DISCUSSION

The factors that will be discussed in this section are metal combinations, impregnation technique and water addition since all the other factors such as support physical properties, operating conditions, feed composition and reactor type were kept constant. The support was selected so that it would minimize the diffusion problems. Appendix B gives the detailed data for the support physical properties. The support has a large surface area (223 m^2/g), a large pore diameter (169 Å) and a large pore volume (1.1 ml/g). More than 54 % of the surface area and 74 % of the pore volume is in the 100 Å and larger pore diameter range. The adsorption and desorption isotherm shows that most of the pores are accessible (narrow hysteresis) for large molecules (less number of constraints) (see Fig. 39). From this data, it can be said that the effect of the support physical properties is minimized so that the effect of the other factors mentioned above can be analyzed.

The effect of these three factors (metal combinations, impregnation technique and water addition) on HDN, HYD and HYC will be discussed. Correlation between catalytic activity and the chemical environment and the interaction of these three factors will also be discussed. Some comparisons with the literature will be made whenever appropriate.

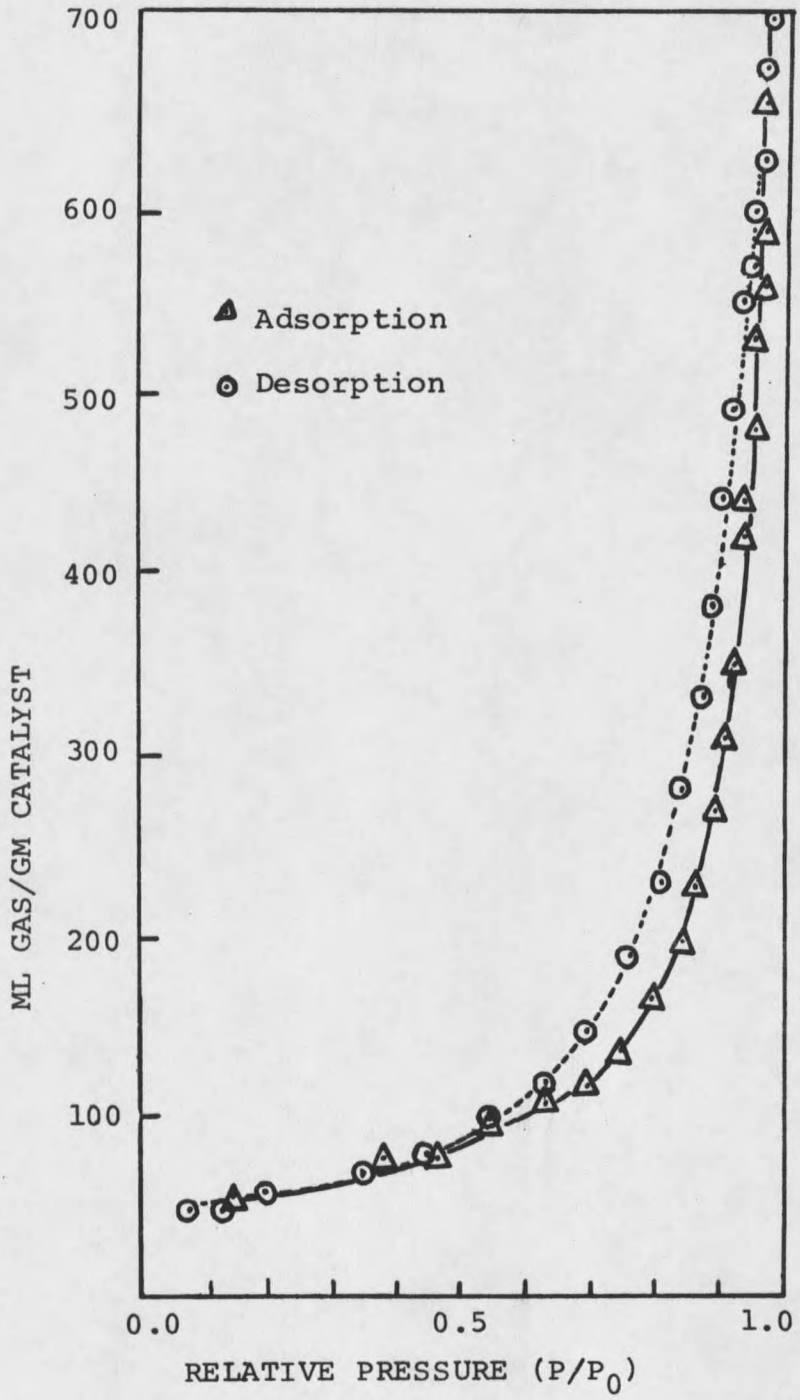

Figure 39. Adsorption-Desorption Isotherm of the Catalyst Support

EFFECT OF METAL COMBINATIONS

The cumulative results for both catalytic activity and the XPS measurements are given in the previous chapter (Chapter 4). In this chapter, some references will be made to these results to clarify the discussions. As it is reported there, every catalyst studied in this category had a different activity, and also different catalyst chemical structure (as evidenced from the XPS spectra). There should exist some relationship between the catalytic activity and the existence of a different chemical structure. In this section these relationships will be discussed for the runs without water addition.

In general, W containing catalysts had less HDN activity than their Co-Mo or Ni-Mo counterparts. This may be caused by the impregnation technique used to prepare these catalysts or some interactions (somehow related to the preparation technique) between the metals. The addition of W on Co-Mo combination reduced HDN activity (compare the catalyst TS-11 (Co+Mo) with the catalyst TS-12 (Co+Mo+W)). Similarly addition of W on Ni-Mo combination reduced HDN activity (TS-17 (Ni+Mo) vs. TS-16 (Ni+Mo+W)). This can be caused either by poorer HDN activity of W compared with Mo (see Fig. 20) or by alteration of catalyst structure by introduction of W to the Co-Mo or Ni-Mo structure. HYD activity of these two catalysts are lower than their Co-Mo and Ni-Mo counterparts. However, some uncertainty arises when Co-W and Ni-W catalysts are brought into the discussion. Co-W and Ni-Mo-W have lower HDN activity than Co-Mo-W and Ni-W, respectively. Co-Mo-W and Ni-W have higher HYD activity than Co-W and Ni-Mo-W respectively. In contrast, Co-W has higher HYC activity than Co-Mo-W.

The HYC activity of Ni-W follows a similar pattern to its HYD and HDN activity. In other words, Ni-W is more active than Ni-Mo-W for every function. This can be attributed to the muti-metallic interaction on the catalyst surface. More experimental data are necessary to confirm the nature of the interaction and the effect of chemical environment and geometrical configuration of metal atoms in this structure on the activity. The Co-Mo-W interaction is probably not as strong as the Ni-Mo-W interaction since it has higher HDN, HYD and HYC activity than Ni-Mo-W.

The uncertainty between the catalysts TS-12 (Co+Mo+W) and TS-13 (Co+W) can be cleared up when HYD and HYC activities of the catalysts TS-11 (Co+Mo) and TS-13 (Co+W) are compared. H/C ratio of the catalysts TS-11 (Co+Mo) and TS-13 (Co+W) are 1.38 and 1.33, respectively. The light oil productions are 10.9% and 8.9%, respectively for these two catalysts. Therefore, the Co-W combination has more HYC activity or at least as much as the Co-Mo combination. Then, it is reasonable for Co-W to have less HDN activity since HDN and HYD are directly related (see Chapter 2). As a result, the uncertainty between the catalysts TS-12 (Co+Mo+W) and TS-13 (Co+W) is caused by poor HYD activity of the Co-W combination.

HDN activity of the catalyst TS-14 (Co+Mo+Ni+W) is higher than that of the catalyst TS-16 (Ni+Mo+W) but lower than that of the catalyst TS-12 (Co+Mo+W). However, HYD and HYC activities of the catalyst TS-14 (Co+Mo+Ni+W) are higher than those of the catalysts TS-12 (Co+Mo+W) and TS-16 (Ni+Mo+W). The difference among these functions is probably caused by the impregnation of Ni after Mo since

this order of impregnation of Ni and Mo improved HYD and HYC activities (see Table 9). Actually the difference between HDN activities of the catalysts TS-12 (Co+Mo+W) and TS-14 (Co+Mo+Ni+W) is only 6 wt%. This may also be the result of muti-metallic interaction. In summary, even though W is less active for coal liquids upgrading (under the conditions of this study), probably the interaction of W with Mo and promoters (Ni or Co) reduced activity of either Co-Mo or Ni-Mo combinations when W added. W containing catalysts have high HYC activity despite their low HYD activity (see Table 6 column under HO). This result agrees with the literature (see Chapter 2).

Comparison of Ni-Mo and Co-Mo combinations (TS-11 (Co+Mo) and TS-17 (Ni+Mo)) shows that Ni-Mo has higher HYD activity but lower HYC activity than the Co-Mo combination. HDN activity of Ni-Mo is higher showing the interrelationship between HYD and HDN. These two combinations will be discussed in detail in the next section.

At this stage, some comparisons with the literature can be made. Kujawa [132] and Yeh [144, 153] reported the insignificant effect of Ni on HDN. In Kujawa's work, the concentration of Ni was lower than Co, and the Ni-Co-Mo combination was used in all catalysts. Probably, the effect of the low concentration of Ni was masked by the high concentration of Co or some interaction formed between these three metals. In Yeh's work, four metals (Ni, Mo, Co, W) were present in every catalyst at different concentrations, similar to the catalyst TS-14 (Co+Mo+Ni+W) in this work. This can be explained as follows. Impregnation of Ni after Co and Mo would leave most of Ni on the surface since the Al_2O_3 sites were already occupied by Co and Mo [29,

30]. Therefore, Ni on the surface would be available for W interaction. Since Ni-W or Ni-Mo-W are less active than the other combinations, the effect of Ni would be masked. As a result, the effect of Ni on HDN would be insignificant in a statistical experimental design study.

Another disagreement with some literature results is with W containing catalysts, especially Ni-W [22, 66, 70, 150]. It is well known that Ni-W is a good hydrotreating catalyst in petroleum refining [22]. The reason of the disagreement appears to be the different source of catalysts or catalyst supports [66, 70, 150] and the feed [22, 70, 66]. Since catalyst physical properties and support composition contribute to the HDN and HDS, the comparison of results from such catalysts are unreliable. The feed used in these studies differs from each other. Some investigators used model compounds [66, 70] or petroleum fractions [22]. Coal liquids have different properties and they would require different active sites or more activity. However, there is some agreement with the literature results which used the same source of catalyst support and actual coal liquids [69]. Schwager [69] studied different combinations of bimetallic catalysts, and concluded that Ni-W and Co-W catalysts were poorer than Ni-Mo and Co-Mo catalysts even though he used a different sequence of metal impregnation from the one used in this work. In this study, Co-W was poor for the HDN of SRC-II LECF although it is better than Ni-W.

The conclusion reached in this work about the better HDN and HYD activity of Ni-Mo agrees well with the literature [67, 69, 128, 132,

140]. The W containing catalysts were probably as active as Co-Mo for HYC. Comparison of H/C ratio and light oil production reveals this conclusion. This agrees with Shih et al.'s [66] model compound study and Schwager's SRC-II hydrotreating results [69].

EFFECT OF IMPREGNATION TECHNIQUE

When Ni-Mo catalysts are compared, their HDN and HYD activities do not differ much by changing the impregnation technique, however their HYC activities do. With approximately the same HYD activity, the catalysts prepared by batchwise Mo impregnation (the catalysts TS-19 (Mo+Ni) and TS-20 (Ni:s+Mo:b)), regardless of sequence of impregnation, produced more light oil. The XPS analysis of these catalysts showed some difference between the abundance of some phases present, but most of the phases were present in every catalyst. The only difference was the presence of Mo involvement in the Al_2O_3 structure and more Ni in the Al_2O_3 lattice for the catalyst TS-17 (Ni+Mo, step). The lower HYC activity of the catalyst TS-17 (Ni+Mo, step) than that of the catalysts TS-19 (Mo+Ni) and TS-20 (Ni:s+Mo:b) can be attributed to the movement of Mo into the Al_2O_3 lattice. This effect can be caused by the occupation of Al_2O_3 sites by Mo and loss of some Mo into the Al_2O_3 lattice since both factors contribute to HYC activity. Therefore, Mo-Al_2O_3 interaction is not desirable for HYC activity of the Ni-Mo catalysts. HYD and HDN activities seem not affected by this interaction. This is probably because of the different sites involved for these reactions.

Comparison of Co-Mo catalysts shows certain differences in activities of catalysts which were prepared by different impregnation techniques. The catalyst TS-11 (Co+Mo, step) is the poorest for HDN and was prepared by stepwise impregnation of both Co and Mo. The most active catalyst, TS-18 (Mo+Co), was prepared by batchwise impregnation of Co after batchwise Mo impregnation.

The XPS results showed that more Co and Mo was moved into the Al_2O_3 structure by stepwise impregnation. In addition, it was found that Co was present at different sulfidation states in the catlyst TS-11 (Co+Mo, step). Most important of all, $CoMoO_4$ type phase was more developed in the catalyst TS-18 (Mo+Co) than that in the catalyst TS-21 (Co:s+Mo:b) and Mo was present as a polymolybdate phase (probably with some weak Co association) in the catalyst TS-11 (Co+Mo, step). Interestingly, HDN activities followed the same sequence with the surface Mo phase. When sulfided, the more developed $CoMoO_4$ type phase produced more Co-Mo-S phase and the least developed polymolybdate phase produced less Co-Mo-S phase. Therefore, the formation of more surface Co-Mo-S phase makes Co-Mo catalysts more active for HDN and HYC. This phenomena was observed for HDS activities of the Co-Mo catalysts [212]. HYC activity is probably related to the presence of Mo in the Al_2O_3 structure also as discussed with the Ni-Mo catalysts.

Surprisingly, the abundance of the surface Co-Mo-S phase did not have any significant effect on HYD activity. It is probably because different phases are responsible for this activity. The formation of less Mo-Al_2O_3 interaction and $CoAl_2O_4$ phase and more surface complexes such as $CoMoO_4$ type phases (Co-Mo-S when sulfided) make the catalyst

TS-18 (Mo+Co) the most active catalyst. From this discussion, it can be concluded that less interaction of Mo and Co with the support is necessary for better catalytic activity.

The comparison of the Ni-Mo and Co-Mo catalysts shows that the catalyst TS-18 (Mo+Co) is as active as Ni-Mo catalysts (may be slightly better) for HDN and more active for HYC. It has lower HYD activity. Therefore, a good control of surface structure of the Co-Mo catalysts during the preparation stage produces a catalyst better than Ni-Mo catalysts for hydrotreating of coal liquids. Here the necessity of more research on basic science of catalysis is worth stressing.

In the literature, better HDS activity for Co-Mo and Ni-Mo catalysts when they are prepared by Co or Ni impregnation after Mo, is reported [34, 39, 60, 64]. This work shows that the same result is true for HDN and HYC.

EFFECT OF WATER ADDITION

The results of this work show that the effect of water is very complicated. In general, when it enhances HDN, it does the same for product quality, however, the reverse is not true. The reverse is true only if the effect of water is strongly inhibitive on HDN, for example the catalyst TS-14 (Co+Mo+Ni+W).

The results indicate that the effect of water depends on the metal combinations as well as impregnation technique. Therefore, discussing the material in two categories will be appropriate.

Metal Combinations: Water inhibits the HDN activities of the catlyst TS-14 (Co+Mo+Ni+W), TS-12 (Co+Mo+W), TS-15 (Ni+W) and TS-11

(Co+Mo) and enhances that of the catalysts TS-13 (Co+W) and TS-17 (Ni+Mo). The effect on the catalysts TS-11 (Co+Mo), TS-12 (Co+Mo+W) and TS-15 (Ni+Mo) is small compared with the others. When the metal contents of these catalysts are compared, some information can be obtained. The catalysts TS-11 (Co+Mo), TS-12 (Co+Mo+W) and TS-14 (Co+Mo+Ni+W) contain Co-Mo , TS-14 (Co+Mo+Ni+W) and TS-15 (Ni+W) contain Ni-W, TS-13 (Co+W) contains Co-W and TS-17 (Ni+Mo) contains Ni-Mo in their structure. As a result, water appears to have a negative effect on HDN activity of the metal combinations of Co-Mo and Ni-W, and a positive effect on the Ni-Mo and Co-W combinations. This conclusion may be true only for the catalysts prepared by the impregnation technique of this group since it is affected by the impregnation technique too.

The effect of water on HYD activity of the catalysts containing W was negative. The inhibitive effect of water is more on the catalysts containing Ni-W in their structure (TS-14 (Co+Mo+Ni+W) and TS-15 (Ni+W)). For the rest of the W containing catalysts it is very small.

The effect of water on product quality was positive for the blank support and all the other catalysts except the catalyst TS-14 (Co+Mo+Ni+W). The positive effect of water on the blank support is probably due to inhibitive effect on the condensation of light fractions. This is evident from the Fig. 9 and Fig. 10. Since the effect of water on HYD activity of the W containing catalysts is negative, the HYC activity of them is enhanced by water addition. This enhancing effect of water on HYC activity may be partially due to its effect on

the support. However, the contribution from the metals is large because of the HYC activities of all of the W containing catalysts except TS-14 (Co+Mo+Ni+W). All except the catalyst TS-14 (Co+Mo+Ni+W) showed improved HYC activity when water was added. HYC activity of Ni-Mo combination is also affected greatly. The effect of water on HYC activity of the catalyst TS-14 (Co+Mo+Ni+W) is uncertain because there is no direct way of measuring HYC activity other than comparing H/C ratio and distillation fractions. Water had a negative effect on both of these factors for this particular catalyst.

Impregnation Technique: The effect of water on the Ni-Mo catalysts did not change greatly by changing the impregnation technique. The enhancing effect of water on HDN and HYC activity of the catalyst TS-17 (Ni+Mo, step) disappeared for the other two catalysts. Water did not have a significant effect on HDN, HYD and HYC activities of the catalysts TS-19 (Mo+Ni) and TS-20 (Ni:s+Mo:b). The reason for this change can be attributed to the weakening or disappearance of support-Mo interaction for the catalysts TS-19 (Mo+Ni) and TS-20 (Ni:s+Mo:b). This interaction is very strong for the catalyst TS-17 (Ni+Mo, step). It can be speculated here that water may alter the structure of this interaction and cause the effect mentioned either by forming a weak chemical bond with it or causing some destruction in the structure. The destruction can be done if water replaces (MoO_4^{-2}) in the structure with OH^{-1} ions. This is a possibility since Mo impregnation involves ion exchange mechanism [28] between these groups. However, this point needs an experimental verification.

The effect of water on the Co-Mo catalysts is changed more than the Ni-Mo catalysts by changing the impregnation technique. The insignificant effect of water on HDN became more negative from the catalyst TS-11 (Co+Mo, step) to the catalysts TS-18 (Mo+Co) and TS-21 (Co:s+Mo:b). Although HYD activities of the catalysts TS-11 (Co+Mo, step) and TS-21 (Co:s+Mo:b) remained the same, that of the catalyst TS-18 (Mo+Co) was lower. Product quality was also affected negatively for this catalyst by water addition. The insignificant effect of water on Co-Mo combination developed into a more negative effect with batchwise impregnation of Mo for HDN activity. The reverse impregnation sequence of metals in the catalyst TS-18 (Mo+Co) made the effect of water on the product quality and HYD highly negative. When the effect of water on the product quality for the catalysts TS-11 (Co+Mo, step) and TS-21 (Co:s+Mo:b) are compared, the positive effect of water on the product quality for the catalyst TS-11 (Co+Mo, step) turned to a negative effect for the catalyst TS-21 (Co:s+Mo:b).

The less interaction between the support -Co and -Mo makes the effect of water more negative. A speculation similar to the one made to explain the behavior of the Ni-Mo catalysts can be made here for the Co-Mo catalysts. Water may alter the structure of the Al_2O_3-Mo interaction and cause the effect mentioned either by a strong chemisorption or by destroying the interaction. The negative effect of water on HDN activity of these catalysts becomes more negative with increased run time (the angle between two lines in Figures 13, 27, and 28). This may be caused by either more water chemisorption on the catalyst surface or destruction of Mo-support or Co-support

interaction by increasing run time as discussed above. An experimental verification is necessary to be certain.

When the results of this work are compared with others, some contradictions arise [154, 202, 213]. In an earlier study by the author [154, 213], water enhanced the activity of the Harshaw HT 400 Co-Mo catalyst. HDN was improved considerably. In another study [202, 213], a catalyst similar to the catalyst TS-12 (Co+Mo+W) was tested and a substantial improvement in HDN activity was obtained. In contrast, the Co-Mo catalysts (TS-11 (Co+Mo, step), TS-18 (Mo+Co), TS-21 (Co:s+Mo:b)) and Co-Mo-W catalyst (TS-12 (Co+Mo+W)) had less HDN activity when water was present. The difference between the catalyst TS-12 (Co+Mo+W) and its counterpart in the earlier study was the different impregnation technique, a different catalyst support and a different inert support used as diluent, but the same metal sequence. The difference between Co-Mo catalysts was different source of catalysts (Harshaw HT 400 is a commercial catalyst) and the inert diluent. From this information, it is evident that the effect of water on activity of a catalyst depends on the catalyst support or the source of the catalyst, as well as the impregnation technique. It may also depend on the source of the inert diluent .

To the author's knowledge, there are only two other studies concerning the effect of water on HDN activity of hydrotreating catalysts, both dealing with model compounds [214, 215]. Saterfield and Carter [214] studied the effect of water vapor on quinoline HDN using a commercial Ni-Mo catalyst, with 1/1 ratio of partial pressure of water to quinoline. They found that at low temperatures water has

an enhancing effect on the HDN but inhibiting effect at high temperatures (420°C). Also water changed the reaction path favoring more ring saturation at 375°C. Since their catalyst is a commercial one, the metal impregnation will be similar to TS-19 (Mo+Ni). The inhibiting effect of water at high temperatures is probably in agreement with the results obtained with TS-19. However, comparison of a model compound study with that of actual coal liquids may lead to an error. In addition, their work uses very high percentage of water compared with only 2% in this work.

A full explanation of the effect of water remains obscure at this point. Before it can be explained, more experimental evidence is necessary. One possible explanation is that it might be changing adsorption characteristics of the compounds on the catalyst surface as was observed by Segawa and Hall [216]. Their studies indicated that water addition altered the relative amounts of pyridine adsorbed on the Bronsted and Lewis acid sites on metal oxide catalysts, producing more Bronsted acid sites. A similar thing might be happening with metal sulfides, but to be sure, this particular point requires further study.

CHAPTER 6

SUMMARY AND CONCLUSIONS

The objective of this study was to develop improved catalysts to upgrade SRC-II Light Ends Column Feed (LECF) to a feedstock acceptable to conventional petroleum refineries. To achieve this objective, the factors studied were the effect of metal combinations, impregnation technique and water addition on the catalytic activity.

The salient findings of this work are the following:

1. The catalyst support does not have any HDN activity, and it causes condensation of light fractions to heavier ones.
2. The activities of the different metal combinations can be ranked as follows when stepwise impregnation was used;
   a) HDN activity,

      Ni+Mo > Co+Mo > Co+Mo+W > Co+Mo+Ni+W > Co+W > Ni+W > Ni+Mo+W

   b) HYD activity,

      Ni+Mo > Co+Mo > Co+Mo+Ni+W = Co+Mo+W > Ni+W > Ni+Mo+W = Co+W

   c) Light oil production,

      Co+Mo > Ni+Mo > Co+Mo+Ni+W > Co+Mo+W = Ni+W > Ni+Mo+W = Co+W
3. The effect of impregnation technique on the HDN and HYD activities of the Ni-Mo catalysts is negligible. However, their HYC

activities were affected considerably by impregnation technique. Batchwise impregnation of Mo produced more light oil.

4. The effect of impregnation technique on the activities of the Co-Mo catalysts was substantial. Again, batch-wise impregnation of Mo improved HYC activities, and HYD activities were not affected. The impregnation of Mo first and then Co produced a catalyst with the highest HDN and HYC activity.
5. Water appeared to inhibit the HDN activities of the catalysts containing Co-Mo and Ni-W combinations, but enhanced that of Ni-Mo and Co-W combinations.
6. Water slightly enhanced the HYC activities of all of the metal combinations studied except Co-Mo-Ni-W.
7. The enhancing effect of water on HDN and HYC activities of the Ni-Mo combination disappeared when both the sequence of impregnation and number of steps of impregnation of metals were changed.
8. The enhancing effect of water on HYC activities of Co-Mo catalysts disappeared and became an inhibiting effect when both the number of steps of metal impregnation and sequence of metal impregnation were changed. The effect of water on HDN became more negative.
9. The XPS analysis showed that the chemical and geometrical environment of the metals on the support can be altered by changing the impregnation technique, and the activity of a catalyst depends on this environment.

10. The XPS analysis of Ni-Mo and Co-Mo catalysts prepared by different impregnation techniques showed that the effect of water was directly related to the change in the chemical and geometrical environment of the catalyst surface.

11. A Co-Mo catalyst prepared by Mo+Co metal sequence (first Mo and then Co) seems advantageous over Ni-Mo catalysts for coal liquids upgrading since it selectively removes nitrogen and cracks heavy hydrocarbons with minimum hydrogen consumption.

CHAPTER 7

RECOMMENDATIONS FOR FUTURE STUDY

The experience gained from this study and the recent literature review suggests the following to guide the future work:

1. In order to determine the chemical environment and geometrical configuration of atoms on the catalyst surface, pure reference compounds should be analyzed by the same instrument.
2. In the future, the study of catalysts for a wide variety of purposes should be supported by a surface analysis of newly developed catalysts to contribute to the basic science of catalysis. Without this scientific background, most of the new findings will continue to be accidental findings rather than a scientific prediction. This makes catalyst research an expensive one.
3. In order to determine the true surface structure and its relationship with activity and selectivity on certain reactions taking place, several instruments should be used to make up for the weak points of the individual instrument and strengthen the findings. X-ray Photoelectron Spectroscopy (XPS), Auger Spectroscopy, Raman Spectroscopy, Secondary Ion Mass Spectroscopy (SIMS), Low Energy Ion Scattering Spectroscopy (ISS) and Mossbauer

Emission Spectroscopy are among the ones recently reported to be powerful.

4. Activity tests of the catalysts should be done with actual reaction media rather than model compounds whenever possible to avoid uncertainties. This requires more product analysis. Model compounds may be useful for mechanism studies.

LITERATURE CITED

LITERATURE CITED

1. "Steam Coal Prospects to 2000," International Energy Agency of Organizations for Economic Cooperation and Development, 1978.

2. Fryback, M.G. Chem. Eng. Progr. 1981, 77(5), 39.

3. Anderson, L.L.; Tillman, D.A. "Synthetic Fuels from Coal"; John Willey & Sons: New York, 1979.

4. Office of Fossil Energy "Energy from Coal: A State-Of-The-Art Review," Under contract No. E(49-18)-2225, I, p.1, 1976.

5. Brinkman, D.W.; Bowden, J.N. Fuel 1982, 61, 1141-8.

6. U.S. ERDA "Scientific Resources Relevant to the Catalytic Problems in the Conversion of Coal," v.3, 301-51, 1976.

7. Cheadle, G.D.; Welch, C.J.; Lappin, T.A.; Dana, P.M. Oil and Gas J. 1966, 64(29),76-82.

8. Grimes, W.G. In "Coal Science," ;Gorbaty, M.L.; Larsen, J.W.; Wender, I., Eds.; Academic Press: New York, 1982; Vol.I, pp. 21-42.

9. Meyers, R.A. In "Coal Handbook"; Meyers, R.A. Ed.; Marcel Dekker: New York, 1981; Chapter 1.

10. Davidson, R.M. In "Coal Science"; Gorbaty, M.L.; Larsen, J.W.; Wender, I., Eds.; Academic Press: New York, 1982; Vol. 1, pp. 83-155.

11. Deno, N.C. Fuel 1980, 59, 694.

12. Hayatsu, R.; Scott, R.; Moore, L.P.; Studier, M.H. Nature (London) 1975, 257, 378-80.

13. Given, P.H. Fuel 1960, 39, 147.

14. Wiser, W.H. Am. Chem. Soc. Div. Fuel Chem. Prepr. 1975, 20, 122.

15. Pitt, G.J. In "Coal and Modern Coal Processing; An Introduction"; Pitt, G.J.; Miward, G.R., Eds.; Academic Press: New York, 1980; pp. 27-50.

16. Hill, G.R.; Lyon, L.B. Ind. Eng. Chem. 1962, 54, 36.

17. Solomon, P.R. In "New Approaches in Coal Chemistry"; Blaustin, B.D.; Bockroth, B.C.; Freidman, S., Eds.; Am. Chem. Soc. Symp. Ser. 169: Washington, D.C., 1981; pp.61-71

18. Cordero, H.G.; Tarring, L.H. "Babylon to Birmingham" Quin Press: London, England, 1960.

19. O'Hara, J.B. In "Coal Handbook"; Meyers, R.A., Ed.; Marcell Dekker: New York, 1981; pp. 715-816.

20. U.S. Department of Energy, "Coal Liquefaction"; Quarterly report, April 1980; p. 7.

21. Southern California Edison "Emission Characteristics of Paraho Shale Oil as Tested in a Utility Boiler"; Southern California Edison/Paraho Oil Shale Demonstration, Inc.: Los Angeles, 1976.

22. Energy Engineering Board "Refining Synthetic Fuels From Coal and Shale"; National Academy Press: Washington, D.C., 1980; p. 51.

23. Niemark, A.V.; Kheifez, L.I.; Feneonou, V.B. Ind. Eng. Chem. Prod. Res. Dev. 1981, 20, 439-50.

24. Weisz, P.B. Trans. Faraday Soc. 1967, 63, 1801.

25. Weisz, P.B.; Hicks, J.S. Trans. Faraday Soc. 1967, 63, 1807.

26. Weisz, P.B.; Hicks, J.S. Trans. Faraday Soc. 1967, 63, 1815.

27. Harioft, P. J. Catal. 1969, 14, 43.

28. Tsigdinos, G.A.; Chen, H.Y.; Strevsond, B.J. Ind. Engr. Chem. Prod. Res. Dev. 1981, 20, 619-23.

29. Chung, K.J.; Massoth, F.E. J. Catal. 1980, 64, 320-31.

30. Chung, K.J.; Massoth, F.E. J. Catal. 1980, 64, 332-45.

31. Okamoto, Y.; Imanota, T.; Teranishi, S. J. Catal. 1980, 65, 448-60.

32. Miller, A.W.; Atkinson, W.; Barber, M.; Swift, P. J. Catal. 1971, 22, 140.

33. Knozinger, H.; Jezionowski, H.; Taglauer, E. Proc. Intl. Congr. on Catal., 7th (Tokyo, 1980); Elsevier-Kodansha: Amsterdam/Tokyo, 1981; p. 604.

34. Sultanov, A.S.; Abdurakhmanov, M.; Talipov, G.S.; Inoyatov, N.S.; Samigov, K.; Kayumov, A.A. Kinet. Katal. (U.S.S.R.) 1972, 27, 357.

35. Okamoto, Y.; Nakano, H.; Shimokoma, T.; Imanoka,T.; Terinishi, S. J. Catal. 1977, 50, 447-54.

36. Cimino, A.; De Angelis, B.A. J. Catal. 1975, 36, 11-22.

37. Massoth, F.E. In "Advances in Catalysis"; Academic Press: New York, 1978; Vol. 27, p. 265.

38. Stone, E; Tilley, R. In "Reactivity of Solids"; Schwab, G. Ed.; Elsevier: Amsterdam, 1965; p. 590.

39. Decklerck-Grimme, R.I.; Canesson, P.; Freidman, R.M.; Fripiat, J.J. J. Phys. Chem. 1978, 82, 889.

40. Grimblot, J.; Bonnelle, J.P. J. Electron. Spectrosc. Relat. Phenom. 1976, 9, 449.

41. Mone, R.; Moscou, L. Am. Chem. Soc. Div. Petrol. Chem. Prep. 1975, 20(2), 564.

42. Gajardo, P.; Grange, P.; Delmon, B. J. Catal. 1980, 63, 201-16.

43. Ratnasamy, P.; Knozinger, H. J. Catal. 1978, 54, 155.

44. Medena, J.; Van Stau, C.; de Beer, V.H.J.; Connings, A.J.A.; Konningsberger, D.C. J. Catal. 1978, 53, 386.

45. Richardson, J.T. Ind. Eng. Chem. Fundam. 1964, 3, 154.

46. LoJacono, M.; Schlavello, M.; de Beer, V.H.J.; Minelli, G. J. Phys. Chem. 1977, 81, 1583.

47. Cheng, C.P.; Schrader, G.L. J. Catal. 1979, 60, 276.

48. LoJacono, M.; Verbeek, J.L.; Schuit, G.C.A. J. Catal. 1973, 29, 463.

49. de Beer, V.H.J.; Schuit, G.C.A. In "Preparation of Catalysis"; Delmon, B.; Jacobs, P.A.; Pencelet, G., Eds.; Elsevier: Amsterdam, 1976; p. 343.

50. Lipsch, J.M.J.G.; Schuit, G.C.A. J. Catal. 1969, 15, 174.

51. Ashley, J.H.; Mitchel, P.C.H. J. Chem. Soc. (A) 1969, 2730.

52. Grimblot, J.; Bonelle, J.P.; Beufills, J.P. J. Electron Spectrosc. Relat. Phenom. 1976, 8, 437.

53. Ueda, H.; Todo, N. J. Catal. 1972, 21, 281.

54. Topsoe, H. Clemson, B.S.; Burriesci, N.; Candia, R.; Morup, S. Scientific Bases for the Preparation of Heterogeneous Catalysts, 2nd Intl. Symp.; Louvain La Neuve, Belgium, September 1978; Paper E3 (from Ref. 30).

55. Dufresne, P.; Payen, E.; Grimblot, J.; Bonelle, J.P. J. Phys. Chem. 1981, 85, 2344-51.

56. Jeziorowski, H.; Knozinger, H.; Tauglauer, E.; Vogdt, C. J. Catal. 1983, 80, 286-95.

57. Vedrine, J.C.; Hollinger, G.; Duc, T.M. J. Phys. Chem. 1978, 82, 1515-20.

58. Shelef, M.; Wheeler, M.A.Z.; Yao, H.C. Surf. Sci. 1975, 47, 697.

59. Wu, M.; Chin, R.; Hercules, D.M. Spectrosc. Lett. 1978, 11, 615 (from Ref. 53).

60. Conosa Rodrigo, B.; Jeziorowski, H.; Knozinger, H.; Wang, X.Sh.; Tauglouer, E. Bull. Soc. Chim. Belg. 1981, 90, 1339.

61. More, R. In "Preparation of Catalysis"; Delmon, B.; Jacobs, P.A.; Ponete, G., Eds.; Elsevier: Amsterdam, 1976; p.381.

62. Ng, K.T.; Hercules, D.M. J. Phys. Chem. 1976, 80, 2094-102.

63. Voorhouse, R.J.H. J. Catal. 1971, 23, 236.

64. Okamoto, Y.; Tomioha, H.; Imanaka, T.; Teranishi, S. "Proc. Intl. Congr. on Catal., 7th (Tokyo, 1980)"; Elsevier-Kodansha: Amsterdam/Tokyo, 1981.

65. Ripperger, W.; Saum, W. J. Less Common Metals 1977, 54, 353-62.

66. Shih, S.; Reif, E.; Zawadzki, R.; Katzer, J.R.; Am. Chem. Soc. Div. Fuel Chem. Prepr. 1978, 23, 99.

67. Jankowski, A.; Doehler, W.; Graer, U. Fuel 1982, 61, 1032.

68. Weisser, O.; Landa, S. "Sulfide Catalysts, Their Properties and Applications"; Pergamon Press: New York, 1973.

69. Schwager, I.; Stamires, D.N. "Development of New Catalysts for Coal Liquids Refining", DOE/ET/12103-T4, Final Report, Filtrol Corporation, Los Angeles, 1981.

70. Shaptai, J.; Veluswamy, L.; Oblad, A.G. Am. Chem. Soc. Div. Fuel Chem. Prepr. 1978, 23, 107.

71. Shaptai, J.; Veluswamy, L.; Oblad, A.G. Am. Chem. Soc. Div. Fuel Chem. Prepr. 1978, 23, 114.

72. Fitz, C.W.; Rase, H.F. Ind. Eng. Chem. Prod. Res. Dev. 1983, 22, 40-44.

73. Cecil, R.R.; Mayer, F.X.; Cart, E.N. Paper Presented at AIChE Meeting, Los Angeles, CA., 1968.

74. Berg, L.; Kim, N.K. U.S. Patent application.

75. Satterfield, C.N. AIChE J. 1975, 21, 209-28.

76. Satterfield, C.N. "Heterogeneous Catalyts in Practice"; McGraw Hill: New York, 1980.

77. Schuit, G.C.A.; Gates, B.C. AIChE J. 1973, 19, 417-38.

78. Moritz, K.H.; Savage, H.R.; Traficante, D.; Weissman, W.; Young, B.J. Chem. Engr. Prog. 1971, 67(8), 63.

79. Paradis, S.G.; Gould, G.D.; Bea, D.A.; Reed, E.M. Chem Engr. Progr. 1971, 67(8), 57.

80. Van Deemeter, J.J. In "Third European Symposium on Chemical Reaction Engineering"; Pergamon Press: Oxford, U.K., 1965; pp. 215-23.

81. Cusumano, J.A.; Dalla Betta, R.A.; Levy, R.B. "Catal-ysis in Coal Conversion"; Academic Press: New York, 1978.

82. Sonnomans, J.; Gourdiaan, F.; Mars, P. "Proc. Intl. Congr. Catal., 5th (1972)"; Elsevier: Amsterdam, 1973; Vol. 2, p.1085.

83. Sonnomans, J.; Mars, P. J. Catal. 1973, 31, 209.

84. Sonnomans, J.; Vandenberg, G.H.; Mars, P. J. Catal. 1973, 31, 220.

85. Abdul-Gheit, A.K.; Abdau, I.K. J. Inst. Pet. London 1973, 59, 188.

86. Sonnomans, J.; Neyens, W.J.; Mars, P. J. Catal. 1974, 34, 215.

87. Sonnomans, J.; Neyens, W.J.; Mars, P. J. Catal. 1974, 34, 230.

88. Mayer, J.F. Ph.D. Thesis, MIT, Cambridge, Massachusets, 1974.

89. McIlvried, H.G. Ind. Eng. Chem. Proc. Des. Dev. 1971, 10, 125.

90. Flin, F.A.; Larson, O.A.; Beuther, H. Hydrocarbon Process. Pet. Refiner 1963, 42, 129.

91. Doelman, J.; Vlugter, J.C. Proc. World Pet. Congr., 6th, Frankfurt, Germany, 1963.

92. Schreiber, G.P. Ph.D. Thesis, Montana State College, Bozeman, MT., 1961.

93. Koros, R.M.; Bank, S.; Hoffman, J.E.; Kay, M.I. Am. Chem. Soc. Div. Pet. Chem. Prep. 1967, 12, B-165.

94. Cox, K.E.; Berg, L. Chem. Engr. Progr. 1962, 58, 54.

95. Willson, W.A.; Voreck, W.E.; Malo, K.V. Ind. Eng. Chem. 1957, 59, 657.

96. Rosenheimer, M.O.; Kiovsky, J.R. Am. Chem. Soc. Div. Pet. Chem. Prepr. 1967, 12, B-147.

97. Satterfield, C.N.; Cocchetto, J.F. AIChE J. 1975, 21, 1107-10.

98. Satterfield, C.N.; Modell, M.; Mayer, J.F. AIChE J. 1975, 21, 1100-1107.

99. Satterfield, C.N.; Modell, M.; Wilkens, J.A. Ind. Eng. Chem. Proc. Des. Dev. 1980, 19, 154-60.

100. Satterfield, C.N.; Modell, M.; Hites, R.; DeClerk, J.C. Ind. Eng. Chem. Proc. Des. Dev. 1978, 17, 141.

101. Satterfield, C.N.; Cocchetto, J.F. Ind. Eng. Chem. Proc. Des. Dev. 1981, 20, 53-62.

102. Cocchetto, J.F.; Satterfield, C.N. Ind. Eng. Chem. Proc. Des. Dev. 1981, 20, 49-53.

103. Satterfield. C.N.; Gultekin, S. Ind. Eng. Chem. Proc. Des. Dev. 1981, 20, 62-68.

104. Stern, E.W. J. Catal. 1979, 57, 390-96.

105. Willson, R.L.; Kemball, C. J. Catal. 1964, 3, 1426.

106. Keiren, P.; Kemball, C. J. Catal. 1965, 4, 380.

107. Willson, R.L.; Kemball, C.; Golway, A.K. Trans. Faraday Soc. 1962, 58, 583.

108. Keiren, P.; Kemball, C. J. Catal. 1965, 4, 394.

109. Owens, P.J.; Amberg, C.H. Can. J. Chem. 1966, 44, 941.

110. Owens, P.J.; Amberg, C.H. Can. J. Chem. 1966, 44, 947.

111. Kolboe, S.; Amberg, C.H. Can. J. Chem. 1966, 44, 2623.

112. Owens, P.J.; Amberg, C.H. "Solid Surfaces and the Gas Solid Interface"; Am. Chem. Soc.: Washington, D.C., 1961.

113. Desikan, P.; Amberg, C.H. Can. J. Chem. 1963, 41, 1966.

114. Desikan, P.; Amberg, C.H. Can. J. Chem. 1963, 41, 843.

115. Satterfield, C.N.; Roberts, G.W. AIChE J. 1968, 14, 159.

116. Singhal, G.H.; Espino, R.L.; Sobel, J.E. J. Catal. 1981, 67, 446-456.

117. Singhal, G.H.; Espino, R.L.; Sobel, J.E.; Huff, G.A. J. Catal. 1981, 67, 457-68.

118. Nag, N.K.; Sapre, A.V.; Broderick, D.H.; Gates, B.C. J. Catal. 1979, 57, 509-513.

119. Kilanowski, D.R.; Gates, B.C. J. Catal. 1980, 62, 70.

120. Houalla, M.; Nag, N.K.; Sapre, A.V.; Broderick, D.H.; Gates, B.C. AIChE J. 1978, 24, 1015-21.

121. Sapre, A.V.; Broderick, D.H.; Fraenkel, D.; Gates, B.C.; Nag, N.K. AIChE J. 1980, 26, 690-4.

122. Frye, C.G.; Mosby, J.F. Chem. Eng. Progr. 1967, 63, 66.

123. Givens, E.N.; Venuto, P.B. Am. Chem. Soc. Pet. Chem. Prepr. 1970, 15, A-183.

124. Weiser, W.H.; Massoth, F.E.; Shaptai, J.; Lui, Y.; Baluswamy, K. DOE Contract No. DE-AC01-79ET14700, Quarterly Report, Salt Lake City, Utah, July-Sept. 1982.

125. Massoth, F.E.; Muralidhar, G., paper presented at Fourth Climax Intern. Conf., Chemistry and Uses of Molybdenum, Golden, Colorado, 1982.

126. Stein, R.T.; Voltz, S.E.; Collen, R.B. Ind. Eng. Chem. Prod. Res. Dev. 1977, 16, 61-8.

127. Veluswamy, L.; Shaptai, J.; Oblad, A.G. Am. Chem. Soc. Div. Fuel Chem. Prepr. 1979, 24(2), 280-8.

128. Fu, Y.C.; Batchelder, R.F.; Winslow, J.C. Am. Chem. Soc. Div. Fuel Chem. Prepr. 1978, 23(1), 81-91.

129. Cabal, A.V.; Sterling, E.V.; Stein, T.R. Ind. Eng. Chem. Prod. Res. Dev. 1979, 18, 179-85.

130. Sivasubramanian, R.; Crynes, B.L. Ind. Eng. Chem. Prod. Res. Dev. 1979, 18, 179-85.

131. Hass, G.R. Ph.D. Thesis, Montana State University, Bozeman, Montana, 1978.

132. Kujawa, S.T. Ph. D. Thesis, Montana State University, Bozeman, Montana, 1978.

133. Yeh, A.G. Master's Thesis, Montana State University, Bozeman, Montana, 1979.

134. Ramer, R.J. Master's Thesis, Montana State University, Bozeman, Montana, 1979.

135. Runnion, K.N. Master's Thesis, Montana State Univer-sity, Bozeman, Montana, 1977.

136. Scheppele, S.E.; Greenwood, G.J.; Pancirov, R.J.; Ashe, T.R. Am. Chem. Soc. Div. Fuel Chem. Prepr. 1980, 25(1), 37-46.

137. O'Rear, D.J.; Sullivan, R.F.; Staugeland, B.E. Am. Chem. Soc. Div. Fuel Chem. Prepr. 1980, 25(1), 78.

138. Sutterfield, D.; Lanning, W.C.; Rayer, R.E. Am. Chem. Soc. Div. Fuel Chem. Prepr. 1980, 25(1), 79-83.

139. Sivasubramanian, R.; Olson, J.H.; Katzer, J.R. Am. Chem. Soc. Div. Fuel Chem. Prepr. 1980, 25(1), 84-149.

140. Shih, S.S.; Angevine, P.J.; Heck, R.H.; Sawruk, S. Am. Chem. Soc. Div. Fuel Chem. Prepr. 1980, 25(1), 152-63.

141. Garg, D.; Tarrer, A.R.; Guin, J.A.; Lee, J.M. Am. Chem. Soc. Div. Fuel Chem. Prepr. 1980, 25(1), 164-75.

142. Soni, D.S.; Crynes, B.L. Am. Chem. Soc. Div. Fuel Chem. Prepr. 1980, 25(1), 176-87.

143. Fu, Y.C.; Markby, R.E.; Batchelder, R.F. Am. Chem. Soc. Div. Fuel Chem. Prepr. 1982, 27(3-4), 130-8.

144. Yeh, A.G.; Berg, L.; McCandless, F.P. Am. Chem. Soc. Div. Fuel Chem. Prepr. 1982, 27(3-4), 63-70.

145. Curtis, C.W.; Guin, J.A.; Hostings, K.E. Am. Chem. Soc. Div. Fuel Chem. Prepr. 1981, 26(2), 164-72.

146. Ternan, M.; Brown, J.R. Fuel 1982, 61, 1110-8.

147. Wailes, P.C. Fuel 1982, 61, 1051-7.

148. Armstrong, L. Fuel 1982, 61, 1051-7.

149. Chillingworth, R.S.; Hastings, K.E.; Potts, J.D. Ind. Eng. Chem. Prod. Res. Dev. 1980, 19, 34-38.

150. Sullivan, R.F.; Frumkin, H.A. "Refining and Upgrading of Synfuels From Coal and Oil Shales by Advanced Catalytic Processes. Processing of SRC-II Syncrude", DOE Report Under Contract No. AC22-76ET10132, Chevron Research Company, Richmond, CA, 1982.

151. Potts, J.D.; Chillingworth, R.S.; Unger, H. "Expanded Bed Hydroprocessing of SRC and Short Contact Time (SCT) Extracts", DOE Report Under Contract No. AC22-76ET10135, Cities Sirvice Research and Developmet Co., Tulsa, Oklahoma, 1982.

152. Kim, N.K. Master's Thesis, Montana State University, Bozeman, Montana 1981.

153. Yeh, A.G. Ph.D. Thesis, Montana State University, Bozeman, Montana, 1981.

154. Sahin, T. Master's Thesis, Montana State University, Bozeman, Montana, 1982.

155. Bhatia, H. Master's Thesis, Montana State University, Bozeman, Montana, 1982.

156. Kim, N.K. Ph. D. Thesis, Montana State University, Bozeman, Montana, 1982.

157. Tsao, I.H. Master's Thesis, Montana State University, Bozeman, Montana, 1983.

158. Pan, C.R.J. Master's Thesis, Montana State University, Bozeman, Montana, 1983.

159. Berg, L.; McCandless, F.P.; Bhatia, H.; Yeh, A.G. Energy Progress 1982, 2, 236.

160. Ross, L.D. Chem. Engr. Progr. 1965, 61(10), 77-82.

161. Hersowitz, A.A.; Smith, J.M. AIChE J. 1978, 24, 439.

162. Montagna, A.A.; Shah, Y.T.; Paraskos, J.A. Ind. Eng. Chem. Proc. Des. Dev. 1977, 16, 152.

163. Scardi, S.; Baldi, G.; Gianetto, A.; Specchia, V. Chem. Eng. Sci. 1980, 35, 67.

164. Colombo, A.J.; Baldi, G.; Scardi, S. Chem. Eng. Sci. 1976, 31, 1101.

165. Scardi, S.; Baldi, G.; Specchia, V.; Mazzarino, I.; Gianetto, A. Chem. Eng. Sci. 1981, 36, 226-8.

166. van Klinken, J.; van Dangen, R.H. Chem. Eng. Sci. 1980, 35, 59-66.

167. Carlson, T.A. " Photoelectron and Auger Spectroscopy"; Plenum Press: New York, 1975; Chap. I-V.

168. Fadley, C.S. In "Electron Spectroscopy; Theory, Techniques and Applications"; Brundle, C.R.; Baker, A.D., Eds.; Academic Press: New York, 1978; Vol. 2, Chap. I.

169. Hung, J.T.J.; Rabalais, J.W. In "Electron Spectroscopy; Theory, Techniques and Applications"; Brundle, C.R.; Baker, A.D., Eds.; Academic Press: New York, 1978; Vol. 2, Chap. III.

170. Wertheim, G.K. In "Electron Spectroscopy; Theory, Techniques and Applications"; Brundle, C.R.; Baker, A.D., Eds.; Academic Press: New York, 1978; Vol. 2, Chap. IV.

171. Briggs, D. In "Electron Spectroscopy; Theory, Techniqes and Applications"; Brundle, C.R.; Baker, A.D.,Eds.; Academic Press: New York, 1978; Vol. 3, pp. 306-359.

172. Kim, K.S.; Davis, R.E. J. Electron Spectrosc. Relat. Phenom. 1972, 1, 251-8.

173. Biloen, P.; Pott, G.T. J. Catal. 1973, 30, 169-74.

174. Carlson, T.A.; McGuire, G.E. J. Electron Spectrosc. Relat. Phenom. 1972, 1, 161-8.

175. Brinnen, J.S. J. Electron Spectrosc. Relat. Phenom. 1974, 5, 377-400.

176. Wallbank, B.; Maun, I.G.; Johnson, C.E. J. Electron Spectrosc. Relat. Phenom. 1974, 5, 259-66.

177. Kim, K.S. J. Electron Spectrosc. Relat. Phenom. 1974, 3, 217-26.

178. Grimblot, J.; D'Huysser, A.; Bonelle, J.P.; Beaufils, J.P. J. Electron Spectrosc. Relat. Phenom. 1975, 6, 71.

179. Freidman, B.M.; Declerk-Grimee, R.I.; Fripiat, J.J. J. Electron Spectrosc. Relat. Phenom. 1974, 5, 437-46.

180. Bonelle, J.P.; Grimblot, J.; D'Huysser, A. J. Electron Spectrosc. Relat. Phenom. 1975, 7, 151-62.

181. Scofield, J.H. J. Electron Spectrosc. Relat. Phenom. 1976, 8, 129-37.

182. Ratsnasamy, P. J. Catal. 1975, 40, 137-39.

183. Oku, M.; Hirokawa, K. J. Electron Spectrosc. Relat. Phenom. 1976, 8, 475-81.

184. Haber, J.; Stoch, J.; Ungier, L. J. Electron Spectrosc. Relat. Phenom. 1976, 9, 459-67.

185. Walton, R.A. J. Catal. 1976, 44, 335-37.

186. Haber, J.; Ungier, L. J. Electron Spectrosc. Relat. Phenom. 1977, 12, 305-12.

187. Mitchel, P.C.H. J. Catal. 1980, 64., 491-9.

188. Chin, R.L.; Hercules, D.M. J. Phys. Chem. 1982, 86, 360-7.

189. Suziki, K.; Soma, M.; Onishi, T.; Tamaru, K. J. Electron Spectrosc. Relat. Phenom. 1981, 24, 283-7.

190. Bresse, M.; Bennet, B.A.; Chadwick, D. J. Catal. 1981, 71, 430-3.

191. Alstrup, I.; Chorkendorff, I.; Candia, R.; Clausen, B.S.; Topsoe, H. J. Catal. 1982, 77, 397-409.

192. Salvoy, R.B.; Reucroft, P.J. J. Electron Spectrosc. Relat. Phenom. 1977, 12, 351-6.

193. Vedrine, J.C.; Hollinger, G.; Duc, T.M. J. Phys. Chem. 1978, 82, 1515-20.

194. Kerkhoff, F.P.J.M.; Moulijn, J.A. J. Electron Spectrosc. Relat. Phenom. 1978, 14, 453-66.

195. Hoste, S.; De Vondel, D.V.; Van Der Kelen, G.P. J. Electron Spectrosc. Relat. Phenom. 1979, 16, 407-13.

196. Scrocco, M. J. Electron Spectrosc. Relat. Phenom. 1980, 19, 311-9.

197. Houalla, M.; Delmon, B. J. Phys. Chem. 1980, 84, 2194-9.

198. Penn, D.R. J. Electron Spectrosc. Relat. Phenom. 1976, 9, 29-40.

199. Kerkhoff, F.P.J.M.; Moulijn, J.A. J. Phys. Chem. 1979, 83, 1612-19

200. Defosse, C. J. Electron Spectrosc. Relat. Phenom. 1981, 23, 157-73.

201. McKinley, J.B. In "Catalysis"; Emmet, P.H., Ed.; Reinhold Pub. Co.: New York, 1957; vol. 5, pp. 450-455.

202. Berg, L.; McCandless, F.P.; Sahin T. DOE Reports F.E.-2034-26, Montana State University, Bozeman, Montana, Dec.1981-Feb. 1982.

203. Sax, N.I. "Dangerous Properties of Industrial Materials", 2nd Ed.; Reinhold: New York, 1963; p. 288.

204. Norton Denston 57 Catalyst Bed Supports, Bulletine D-12, Norton Company, Calgary, Canada.

205. Instructions of Operations of Brooks Thermal Mass Flowmeter, Brooks Instrument Div., Emerson Electric Co., Hatfield, PA , April 1975.

206. Fritz, J.S.; Shenk, G.H. "Qualitative Analytical Chemistry", 3rd Ed.; : Boston, 1947.

207. Annual Book of ASTM Standards 1974, part 30, Designation D-258.

208. Lake, G.R.; McCutchen, P.; Van Meter, R.; Neel, J.C. Analitical Chem. 1951, 23(11), 1634-38.

209. Instruction Manual for Instrumental Analyzer Mod. 1106, Carlo Erba, Milano, Italy.

210. Ternan, M.; Furimsky, E.; Parsons, B.I. Fuel Process. Tech. 1979, 2, 45-55.

211. Topsoe, H.; Clausen, B.S.; Candia, R.; Wivel, C.; Morup, S. J. Catal. 1981, 68, 433-452.

212. Wivel, C.; Candia, R.; Clausen, B.S.; Morup, S.; Topsoe, H. J. Catal. 1981, 68, 453-463.

213. Berg. L.; McCandless, F.P.; Sahin, T.; Tsao, I.H. Energy Progress (to be published).

214. Satterfield, C.N.; Carter, D.L. Ind. Eng. Chem. Proc. Des. Dev. 1981, 20, 539.

215. Gourdiaan, F. Thesis, Twente University of Technology, Enchede, The Nederlands, 1974.

216. Segawa, K.; Hall, W.K. J. Catal. 1982, 76, 133.

APPENDICES

APPENDIX A- SRC-II PRODUCT PROPERTIES

PROPERTIES OF SRC-II PROCESS PRODUCTS [1]

Description Chevron Identification	Whole SRC-II WOW 3666	SRC-II Naphtha WOW 3750	400°F+ SRC-II WOW 3751
Wt % of Whole SRC-II	100	29	71
Inspections			
Gravity, °API	18.6	36.2	10.7
Aniline Point, °F	<30	56.4	-
Sulfur, Wt %	0.29	0.26	0.25
Total Nitrogen, Wt %	0.85	0.42	0.99
Basic Nitrogen, Wt %	0.7		0.82
Oxygen, Wt %	3.79	3.51	3.63
Carbon, Wt %	84.61	83.66	85.86
Hydrogen, Wt %	10.46	12.15	9.27
Hydrogen/Carbon Atom Ratio	1.47	1.73	1.29
Chloride, ppm	50	18/20	77/62/81
Pour Point, °F	Below -80	-	-50
Group Type, LV %		Low Mass/FIAM*	
Paraffins	(See Table 6)	23	(See Table 6)
Naphthenes	↓	38	↓
Olefins		5	
Aromatics		34	
Ramsbottom Carbon, Wt %	0.70	-	0.81
Hot Heptane Asphaltenes, ppm	468	-	2200
Benzene Insolubles, Wt %	<0.03	-	<0.03
Refractive Index (80°C)	1.5073	-	1.5340
Ash, Wt %	0.004	-	0.010
Molecular Weight	132	118	160
Bromine Number	70	49/52	69
Viscosity, cSt			
at 100°F	2.196	0.8933	4.213
at 130°F	1.617	-	-
at 210°F	-	-	1.238
ASTM Distillation, °F	D 86/D 1160	D 86	D 1160
St/5	154/217	151/179	393/413
10/30	281/382	197/249	427/448
50	438	290	471
70/90	484/597	332/366	506/590
95/EP	699/850	380/393	662/847
% Overhead (Excl. Trap)	98	98	99
% in Flask	0	1	1
% Trap	2	1	0
TBP Distillation, °F (Simulated by Chromatography)			
St/5	56/189	53/153	233/366
10/30	241/379	173/235	382/430
50	424	291	477
70/90	473/562	345/395	527/639
95/99	642/820	408/442	707/849
Maleic Diene Value, cg I_2/g	30.7	3.28	37.3
Water by Distillation, Vol %	0.6		
Acid Neutralization No., mg KOH/g	0.2		

*paraffins and naphthenes were determined by mass spec.; aromatics and olefins by FIAM (fluorescent indicator analytical method). Reliability of these analyses for this type of sample is uncertain.

[1] From reference 150.

COMPOSITION OF WHOLE SRC-II PROCESS PRODUCT
AND 400°F+ SRC-I PROCESS PRODUCT BY 22-COMPONENT
MASS SPECTROMETRIC ANALYSIS*

Type Chevron Identification	Whole SRC-II WOW 3666	400°F+ SRC-II WOW 3751
Composition, LV %		
Saturates		
C(N)H(2N+2), Paraffins	7.2	4.6
C(N)H(2N), Monocycloparaffins	6.9	2.3
C(N)H(2N-2), Dicycloparaffins	2.2	1.8
C(N)H(2N-4), Tricycloparaffins	4.1	3.2
Total Saturates	20.3	12.0
Monoaromatics		
C(N)H(2N-6), Alkylbenzenes	17.9	13.3
C(N)H(2N-8), Benzocycloparaffins	13.9	15.3
C(N)H(2N-10), Benzodicycloparaffins	2.0	5.2
Diaromatics		
C(N)H(2N-12), Naphthalenes	27.8	33.2
C(N)H(2N-14)	5.1	6.8
C(N)H(2N-16)	7.0	8.1
Triaromatics		
C(N)H(2N-18)	3.0	4.0
C(N)H(2N-22)	0.9	0.6
Tetraaromatics		
C(N)H(2N-24)	0.2	0.1
Total Aromatics	77.7	86.6
C(N)H(2N-4)S, Thiophenes	0.3	0.4
C(N)H(2N-10)S, Benzothiophenes	1.3	0.8
C(N)H(2N-16)S, Dibenzothiophenes	0.4	0.3
Sulfur Compounds	1.9	1.4
Calculated, Wt % Composition		
Hydrogen (Corrected for N, S, O)	9.7	9.4
Carbon (Corrected for N, S, O)	85.4	85.7

*Important note: Because the large number of heteromolecules present are not included in this analysis (except for thiophenes), results should not be regarded as quantitative. However, this analysis does serve to indicate the types of hydrocarbons present with the following qualifications:

Sample types correctly analyzed are:

1. C_{12} to C_{36}, 250°F to 1050°F hydrocarbons
2. Olefin-free hydrocarbons
3. Less than 5% oxygen, nitrogen, or sulfur compounds

Only listed types are considered; all others are ignored. Factors which contribute to an incorrect analysis are as follows:

1. Large amounts of a single hydrocarbon
2. Unusual distribution of compounds
3. Thermally unstable materials

APPENDIX B- PHYSICAL PROPERTIES OF THE CATALYST SUPPORT

KATALCO CARRIER

SAMPLE # 81-6731

96508 LC137-1901 (17-27) S 31-Aug-81

N	RELATIVE PRESSURE (P/PO)	GASEOUS N2 VOL SORBED (CC/G @ STP)	LIQUID N2 VOL SORBED (CC/G)	T	A	DV/DP
1	0.078	51.555	0.080	4.429	16.	
2	0.150	58.384	0.091	4.892	20.	0.147
3	0.210	63.289	0.099	5.217	23.	0.129
4	0.376	76.235	0.119	6.097	32.	0.121
5	0.465	84.407	0.132	6.618	38.	0.143
6	0.559	95.529	0.149	7.251	47.	0.185
7	0.635	108.035	0.168	7.876	58.	0.256
8	0.704	124.644	0.194	8.583	71.	0.375
9	0.758	143.523	0.224	9.288	87.	0.544
10	0.806	168.052	0.262	10.098	109.	0.796
11	0.845	198.921	0.310	10.966	135.	1.233
12	0.874	230.695	0.359	11.799	165.	1.737
13	0.899	267.274	0.416	12.767	204.	2.262
14	0.918	308.454	0.481	13.755	251.	3.307
15	0.934	352.523	0.549	14.803	308.	4.401
16	0.951	419.158	0.653	16.416	413.	6.036
17	0.956	444.258	0.692	17.059	461.	7.520
18	0.964	477.748	0.744	18.221	556.	6.776
19	0.971	526.385	0.820	19.653	692.	10.525
20	0.976	560.762	0.874	20.814	816.	11.902
21	0.981	593.366	0.924	22.694	1050.	9.236
22	0.993	709.652	1.106	32.400	2988.	14.730
23	0.987	680.541	1.060	25.688	1508.	6.978
24	0.983	660.895	1.030	23.522	1165.	7.848
25	0.978	631.346	0.984	21.393	884.	8.370
26	0.971	602.085	0.938	19.722	699.	7.474
27	0.963	568.041	0.885	18.003	537.	6.027
28	0.958	553.453	0.862	17.319	481.	5.051
29	0.941	487.523	0.760	15.393	344.	5.972
30	0.925	437.839	0.682	14.157	272.	4.778
31	0.905	383.404	0.597	13.064	218.	4.349
32	0.879	328.670	0.512	11.978	172.	3.230
33	0.852	282.910	0.441	11.155	142.	2.680
34	0.810	230.226	0.359	10.176	111.	1.950
35	0.764	187.265	0.292	9.374	90.	1.446
36	0.707	149.988	0.234	8.612	72.	1.014
37	0.633	119.442	0.186	7.860	57.	0.649
38	0.550	98.707	0.154	7.189	46.	0.390
39	0.455	80.736	0.126	6.558	37.	0.295
40	0.350	69.529	0.108	5.954	30.	0.165
41	0.200	57.010	0.089	5.168	22.	0.131
42	0.139	51.874	0.081	4.828	19.	0.131
43	0.080	45.907	0.072	4.444	16.	0.157

96504 LC137-1901 (17-27) S 31-Aug-81

ADSORPTION PORE VOLUME DATA
22 POINT PV AND 3 POINT SA

BET SA = 223.15 SAT PV = 1.1056 MEDIAN PD ON SA = 115.9
1200 PORE VOLUME = 0.9438 4V/A = 169.2 MEDIAN PD ON PV = 287.0

PORE DIAMETER A	PORE VOLUME (CC/G)	CUMULATIVE PORE VOLUME (CC/G)	VOL PERCENT (CC/G)		SURFACE AREA (SQ M/G)	CUMULATIVE SURFACE AREA
1200 - 600	0.1920	0.192	20.3	20.3	9.81	9.8
600 - 500	0.0628	0.255	6.7	6.7	4.57	14.4
500 - 400	0.0828	0.338	8.8	8.8	7.49	21.9
400 - 300	0.1166	0.454	12.4	12.4	13.47	35.3
300 - 200	0.1531	0.607	16.2	16.2	25.05	60.4
200 - 195	0.0085	0.616	0.9		1.72	62.1
195 - 190	0.0085	0.624	0.9		1.78	63.9
190 - 185	0.0086	0.633	0.9		1.83	65.7
185 - 180	0.0086	0.641	0.9	3.6	1.88	67.6
180 - 175	0.0086	0.650	0.9		1.94	69.5
175 - 170	0.0087	0.659	0.9		2.01	71.5
170 - 165	0.0087	0.667	0.9		2.09	73.6
165 - 160	0.0093	0.677	1.0	3.7	2.28	75.9
160 - 155	0.0096	0.686	1.0		2.44	78.4
155 - 150	0.0108	0.697	1.1		2.83	81.2
150 - 145	0.0103	0.707	1.1		2.80	84.0
145 - 140	0.0105	0.718	1.1	4.4	2.96	86.9
140 - 135	0.0107	0.729	1.1		3.12	90.1
135 - 130	0.0109	0.740	1.2		3.28	93.3
130 - 125	0.0110	0.751	1.2		3.46	96.8
125 - 120	0.0111	0.762	1.2	4.6	3.63	100.4
120 - 115	0.0112	0.773	1.2		3.80	104.2
115 - 110	0.0112	0.784	1.2		3.97	108.2
110 - 105	0.0111	0.795	1.2		4.13	112.4
105 - 100	0.0110	0.806	1.2	4.7	4.29	116.6
100 - 95	0.0108	0.817	1.1		4.44	121.1
95 - 90	0.0106	0.828	1.1	2.3	4.60	125.7
90 - 85	0.0106	0.838	1.1		4.84	130.5
85 - 80	0.0107	0.849	1.1	2.3	5.21	135.7
80 - 75	0.0109	0.860	1.2		5.64	141.4
75 - 70	0.0110	0.871	1.2	2.3	6.09	147.5
70 - 65	0.0107	0.882	1.1		6.31	153.8
65 - 60	0.0106	0.892	1.1	2.3	6.78	160.5
60 - 55	0.0102	0.902	1.1		7.10	167.6
55 - 50	0.0095	0.912	1.0	2.1	7.22	174.9
50 - 45	0.0089	0.921	0.9		7.49	182.4
45 - 40	0.0084	0.929	0.9	1.8	7.92	190.3
40 - 35	0.0077	0.937	0.8		8.18	198.5
35 - 30	0.0067	0.943	0.7	1.5	8.22	206.7
30 - 25	0.0003	0.944	0.0		0.48	207.2

KATALCO
DIGISORB 2500

SAMPLE: 96508 LC137-1901 (17-27) STA: 2 EQTIME: 3 METHOD: 3

ADSORPTION PORE VOLUME DISTRIBUTION

RANGE PORE DIAMETER,A	AVERAGE DIA.,A	PORE VOLUME (CC/G)	CUMULATIVE PORE VOLUME	SURFACE AREA (SQ M/G)	CUMULATIVE SURFACE AREA
+600-500	+550.0	+0.064137	+0.064137	+4.665	+4.665
+500-450	+475.0	+0.036491	+0.100628	+3.073	+7.737
+450-400	+425.0	+0.048089	+0.148717	+4.526	+12.264
+400-350	+375.0	+0.052491	+0.201209	+5.599	+17.863
+350-300	+325.0	+0.068451	+0.269660	+8.425	+26.287
+300-280	+290.0	+0.025409	+0.295069	+3.505	+29.792
+280-260	+270.0	+0.030833	+0.325902	+4.568	+34.360
+260-240	+250.0	+0.030862	+0.356764	+4.938	+39.298
+240-220	+230.0	+0.032065	+0.388829	+5.577	+44.874
+220-200	+210.0	+0.036473	+0.425302	+6.947	+51.822
+200-180	+190.0	+0.033072	+0.458374	+6.962	+58.784
+180-160	+170.0	+0.039692	+0.498066	+9.339	+68.123
+160-150	+155.0	+0.017239	+0.515306	+4.449	+72.572
+150-140	+145.0	+0.022395	+0.537701	+6.178	+78.750
+140-130	+135.0	+0.021957	+0.559657	+6.506	+85.256
+130-120	+125.0	+0.021440	+0.581097	+6.861	+92.117
+120-110	+115.0	+0.026052	+0.607149	+9.062	+101.178
+110-100	+105.0	+0.022905	+0.630054	+7.964	+109.142
+100 -95	+97.5	+0.008558	+0.638613	+3.511	+112.653
+95 -90	+92.5	+0.010811	+0.649424	+5.540	+118.193
+90 -85	+87.5	+0.011823	+0.661247	+5.405	+123.598
+85 -80	+82.5	+0.010291	+0.671537	+4.989	+128.587
+80 -75	+77.5	+0.012139	+0.683676	+6.265	+134.853
+75 -70	+72.5	+0.012493	+0.696170	+6.893	+141.746
+70 -65	+67.5	+0.010126	+0.706296	+6.001	+147.746
+65 -60	+62.5	+0.012341	+0.718637	+7.898	+155.644
+60 -55	+57.5	+0.011348	+0.729985	+7.894	+163.539
+55 -50	+52.5	+0.010594	+0.740578	+8.071	+171.610
+50 -45	+47.5	+0.010780	+0.751359	+9.078	+180.688
+45 -40	+42.5	+0.010261	+0.761620	+9.657	+190.346
+40 -35	+37.5	+0.010033	+0.771653	+10.702	+201.048
+35 -30	+32.5	+0.009941	+0.781594	+12.236	+213.284
+30 -25	+27.5	+0.010374	+0.791969	+15.090	+228.374
+25 -20	+22.5	+0.014483	+0.806452	+25.748	+254.121

96508 LC137-1901 (17-27) S 31-Aug-81

ADSORPTION PORE VOLUME DATA

(DELTA V/DELTA D)*1000

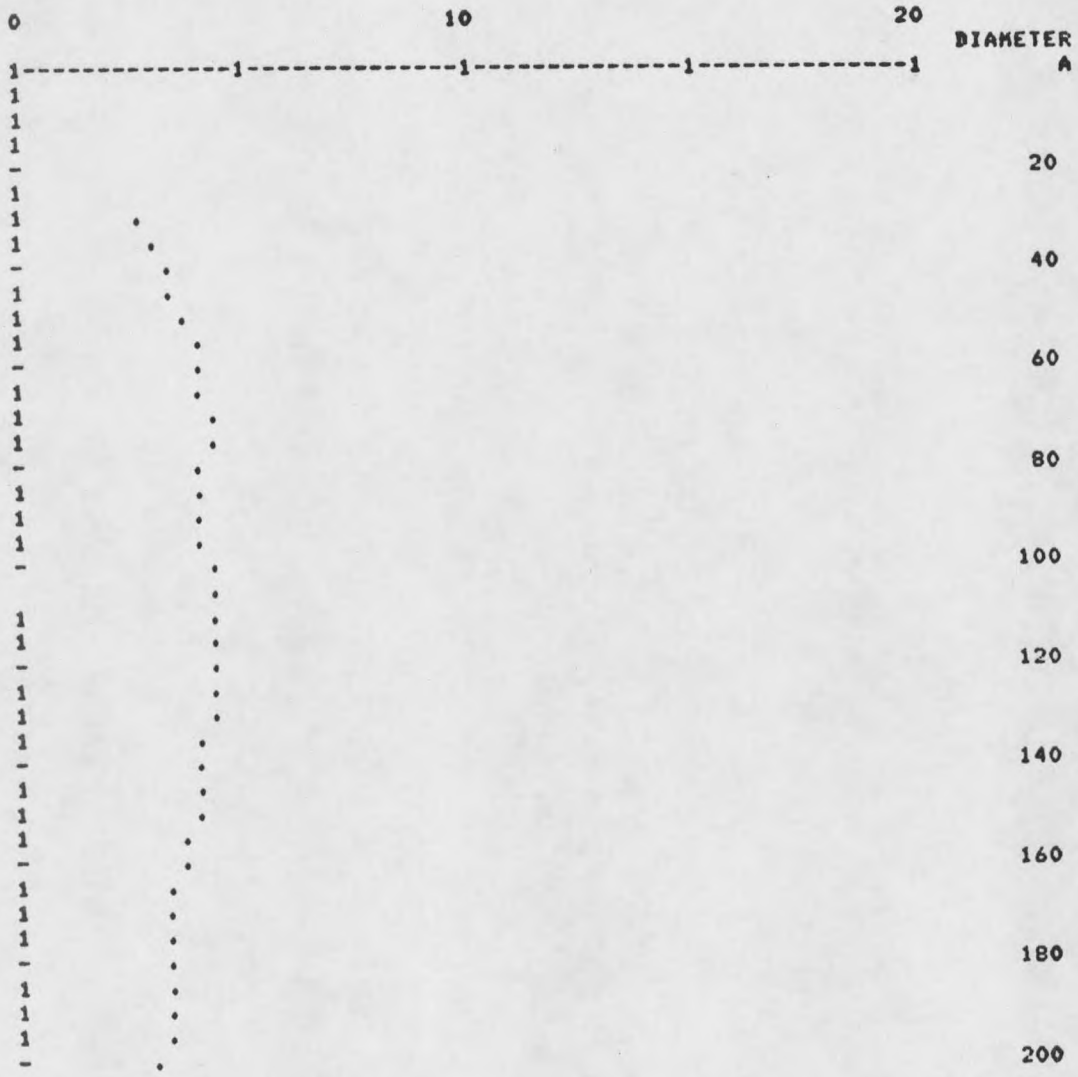

96508 LC137-1901 (17-27) S 31-Aug-81

DESORPTION PORE VOLUME DATA
22 POINT PV AND 3 POINT SA

BET SA = 223.15 SAT PV = 1.1056 MEDIAN PD ON SA = 115.5
1200 PORE VOLUME = 1.0337 4V/A = 185.3 MEDIAN PD ON PV = 210.2

PORE DIAMETER A	PORE VOLUME (CC/G)	CUMULATIVE PORE VOLUME (CC/G)	VOL PERCENT (CC/G)		SURFACE AREA (SQ M/G)	CUMULATIVE SURFACE AREA
1200 - 600	0.1388	0.139	13.4	13.4	6.80	6.8
600 - 500	0.0415	0.180	4.0	4.0	3.03	9.8
500 - 400	0.0638	0.244	6.2	6.2	5.79	15.6
400 - 300	0.1156	0.360	11.2	11.2	13.30	28.9
300 - 200	0.1786	0.538	17.3	17.3	29.51	58.4
200 - 195	0.0124	0.551	1.2		2.51	60.9
195 - 190	0.0114	0.562	1.1		2.37	63.3
190 - 185	0.0115	0.574	1.1		2.45	65.8
185 - 180	0.0116	0.585	1.1	4.5	2.55	68.3
180 - 175	0.0118	0.597	1.1		2.65	70.9
175 - 170	0.0122	0.609	1.2		2.83	73.8
170 - 165	0.0135	0.623	1.3		3.23	77.0
165 - 160	0.0141	0.637	1.4	5.0	3.46	80.5
160 - 155	0.0156	0.652	1.5		3.97	84.4
155 - 150	0.0153	0.668	1.5		4.03	88.5
150 - 145	0.0158	0.684	1.5		4.30	92.8
145 - 140	0.0163	0.700	1.6	6.1	4.58	97.3
140 - 135	0.0167	0.717	1.6		4.87	102.2
135 - 130	0.0171	0.734	1.7		5.15	107.4
130 - 125	0.0166	0.750	1.6		5.21	112.6
125 - 120	0.0173	0.768	1.7	6.5	5.65	118.2
120 - 115	0.0175	0.785	1.7		5.95	124.2
115 - 110	0.0177	0.803	1.7		6.29	130.5
110 - 105	0.0193	0.822	1.9		7.20	137.7
105 - 100	0.0208	0.843	2.0	7.3	8.11	145.8
100 - 95	0.0208	0.864	2.0		8.52	154.3
95 - 90	0.0212	0.885	2.1	4.1	9.18	163.5
90 - 85	0.0217	0.907	2.1		9.90	173.4
85 - 80	0.0219	0.928	2.1	4.2	10.61	184.0
80 - 75	0.0219	0.950	2.1		11.31	195.3
75 - 70	0.0217	0.972	2.1	4.2	11.95	207.2
70 - 65	0.0210	0.993	2.0		12.46	219.7
65 - 60	0.0200	1.013	1.9	4.0	12.80	232.5
60 - 55	0.0183	1.031	1.8		12.71	245.2
55 - 50	0.0024	1.034	0.2	2.0	1.84	247.1

KATALCO
DIGISORB 2500

SAMPLE: 96508 LC137-1901(17-27) STA: 2 EQTIME: 3 MODE: 7
METHOD:2

DESORPTION PORE VOLUME DISTRIBUTION

RANGE PORE DIAMETER,A	AVERAGE DIA.,A	PORE VOLUME (CC/G)	CUMULATIVE PORE VOLUME	SURFACE AREA (SQ M/G)	CUMULATIVE SURFACE AREA
+600-500	+550.0	+0.043961	+0.043961	+3.197	+3.197
+500-450	+475.0	+0.029866	+0.073826	+2.515	+5.712
+450-400	+425.0	+0.040548	+0.114374	+3.816	+9.528
+400-350	+375.0	+0.052316	+0.166691	+5.580	+15.109
+350-300	+325.0	+0.058604	+0.225294	+7.213	+22.322
+300-280	+290.0	+0.028096	+0.253390	+3.875	+26.197
+280-260	+270.0	+0.031599	+0.284989	+4.681	+30.878
+260-240	+250.0	+0.036114	+0.321103	+5.778	+36.656
+240-220	+230.0	+0.042991	+0.364094	+7.477	+44.133
+220-200	+210.0	+0.040011	+0.404105	+7.621	+51.754
+200-180	+190.0	+0.048256	+0.452361	+10.159	+61.913
+180-160	+170.0	+0.055122	+0.507483	+12.970	+74.883
+160-150	+155.0	+0.028655	+0.536139	+7.395	+82.278
+150-140	+145.0	+0.033893	+0.570032	+9.350	+91.628
+140-130	+135.0	+0.029842	+0.599873	+8.842	+100.470
+130-120	+125.0	+0.035352	+0.635225	+11.313	+111.783
+120-110	+115.0	+0.041524	+0.676749	+14.443	+126.226
+110-100	+105.0	+0.037706	+0.714455	+14.364	+140.590
+100 -95	+97.5	+0.018525	+0.732980	+7.600	+148.190
+95 -90	+92.5	+0.024814	+0.757794	+10.731	+158.920
+90 -85	+87.5	+0.019400	+0.777194	+8.868	+167.789
+85 -80	+82.5	+0.021159	+0.798353	+10.259	+178.048
+80 -75	+77.5	+0.024718	+0.823071	+12.758	+190.805
+75 -70	+72.5	+0.023338	+0.846409	+12.876	+203.682
+70 -65	+67.5	+0.019187	+0.865596	+11.370	+215.052
+65 -60	+62.5	+0.023145	+0.888741	+14.813	+229.864
+60 -55	+57.5	+0.020690	+0.909431	+14.393	+244.258
+55 -50	+52.5	+0.016613	+0.926044	+12.657	+256.915
+50 -45	+47.5	+0.019198	+0.945242	+16.167	+273.082
+45 -40	+42.5	+0.017634	+0.962876	+16.597	+289.678
+40 -35	+37.5	+0.014300	+0.977176	+15.253	+304.932
+35 -30	+32.5	+0.007251	+0.984427	+8.925	+313.857
+30 -25	+27.5	+0.001933	+0.986361	+2.812	+316.669
+25 -20	+22.5	+0.002392	+0.988752	+4.253	+320.921 X

96508 LC137-1901 (17-27) S 31-Aug-81

PORE VOLUME DATA

ADSORPTION		DESORPTION	
BET SA = 223.1 SQ M/G		INTERCEPT = 0.000127	SLOPE = 0.019367
CUMULATIVE SA	= 207.2	CUMULATIVE SA	= 247.1
MEDIAN PD ON SA	= 115.9	MEDIAN PD ON SA	= 115.5
MEDIAN PD ON PV	= 287.0	MEDIAN PD ON PV	= 210.2
AVERAGE PD(4V/A)	= 169.2	AVERAGE PD(4V/A)	= 185.3
SATURATION PV	= 1.106	SATURATION PV	= 1.106

DIA	CC/G	DIA	CC/G
PV 1200	= .9438	PV 1200	=1.0337
PV 1000	= .9143	PV 1000	=1.0035
PV 800	= .8610	PV 800	= .9583
PV 600	= .7518	PV 600	= .8949
PV 400	= .6063	PV 400	= .7896
PV 300	= .4897	PV 300	= .6741
PV 200	= .3366	PV 200	= .4954
PV 100	= .1377	PV 100	= .1908

PV 1200 - 200 PD = 0.607	PV 1200 - 200 PD = 0.538
PV 1200 - 100 PD = 0.806	PV 1200 - 100 PD = 0.843
PERC PV 100-200 A	PERC PV 100-200 A
DIAM ON 600 TPV = 26.5 (.199)	DIAM ON 600 TPV = 34.0 (.305)
PERC PV 200-400 A	PERC PV 200-400 A
DIAM ON 600 TPV = 35.9 (.270)	DIAM ON 600 TPV = 32.9 (.294)

96508 LC137-1901 (17-27) S 31-Aug-81

SORPTION PORE VOLUME DATA

(DELTA V/DELTA D)*1000

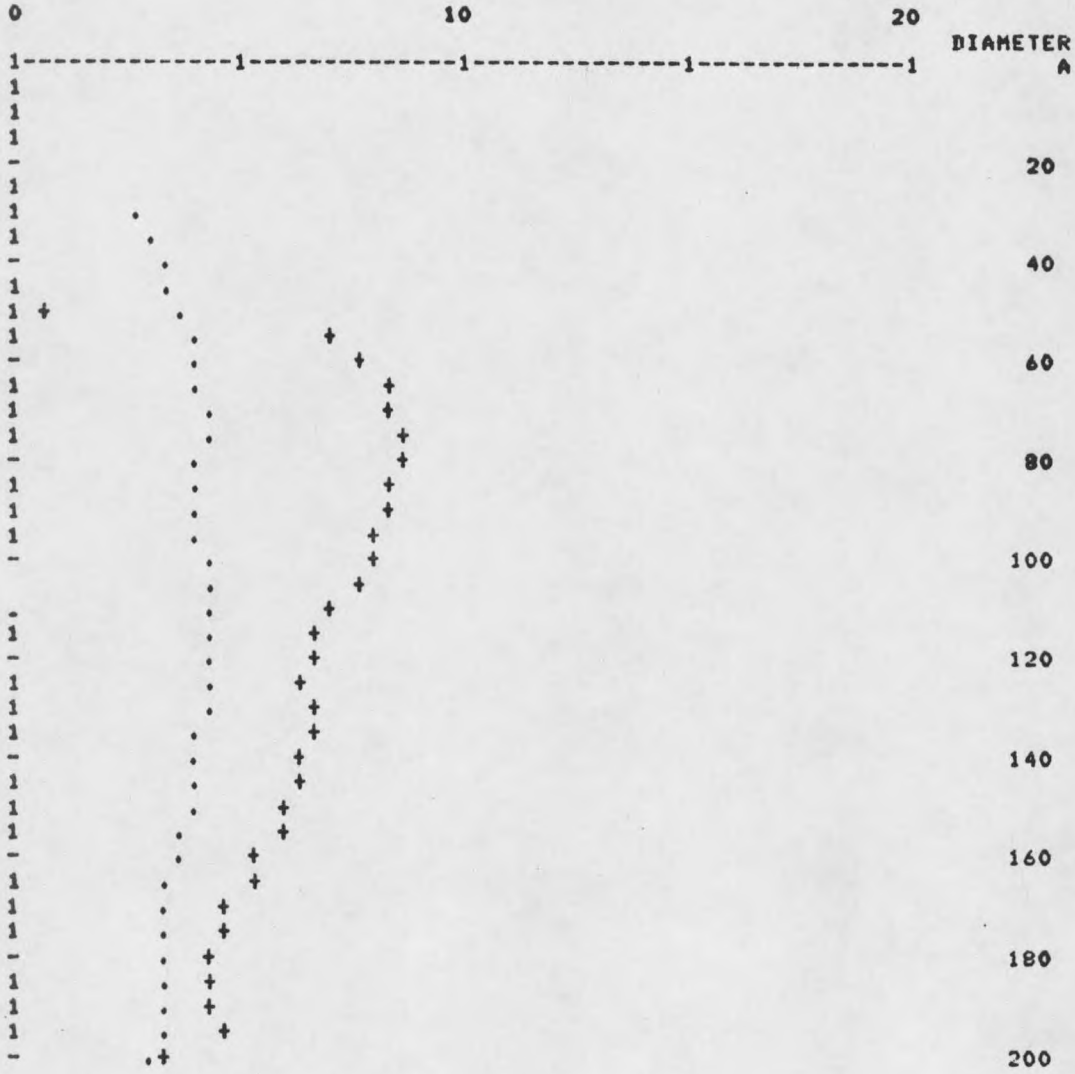

96508 LC137-1901 S 31-Aug-81

(DELTA PORE VOLUME/DELTA LOG PORE DIAMETER)

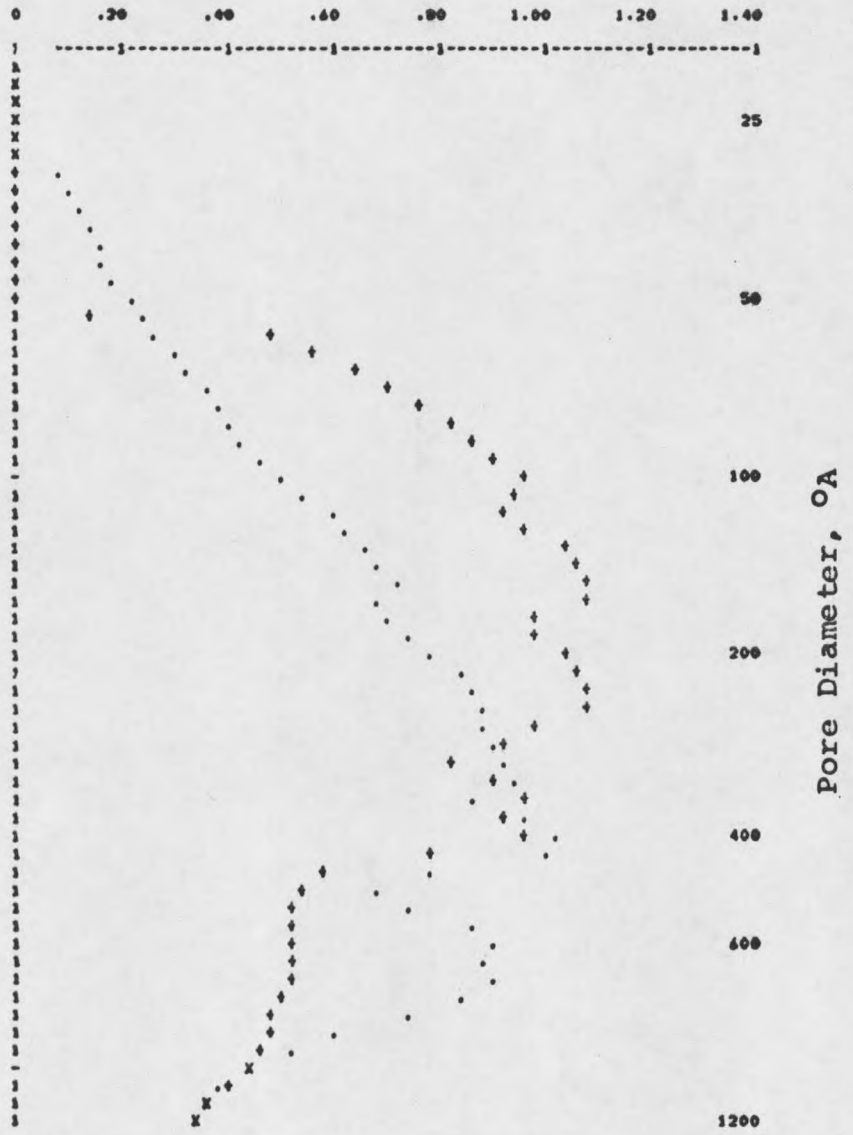

APPENDIX C- X-RAY PHOTOELECTRON SPECTROSCOPY SMOOTHING PROGRAMS

```
10 PRINT "smoothing routines"
11 PRINT "Choose 3-pt (1), 5-pt (2), gaus1 (3), or
        gaus2 (4).";
12 PRINT "G"
13 INPUT L1
14 PRINT "G"
15 DELETE S2
16 DIM S2(N)
17 S2=0
18 S2(1)=A(1)
19 S2(2)=A(2)
20 S2(N-1)=A(N-1)
21 S2(N)=A(N)
22 FOR I=3 TO N-2
23 GO TO L1 OF 24, 26, 28, 30
24 S2(I)=0.4*A(I)+0.2*(A(I+1)+A(I-1))+0.1*(A(I+2)+A(I-2))
25 GO TO 31
26 S2(I)=0.564*A(I)+0.207*(A(I+1)+A(I-1))+0.011*(A(I+2)+
        A(I-2))
27 GO TO 31
28 S2(I)=0.402*A(I)+0.244*(A(I+1)+A(I-1))+0.055*(A(I+2)+
        A(I-2))
29 GO TO 31
30 S2(I)=0.5*A(I)+0.25*(A(I+1)+A(I-1))
31 NEXT I
32 A=S2
33 PRINT "G"
34 RETURN
```

APPENDIX D- X-RAY PHOTOELECTRON SPECTROSCOPY PEAK BINDING ENERGIES

THE EFFECT OF METAL COMBINATIONS

Element	TS-11	TS-18	TS-21	TS-12	TS-13	TS-14
			BINDING ENERGIES			
Co $2p_{1/2}$	799.4 797.7	797.4 796.7	798.2 796.7 796.0 795.4	798.3 797.8	798.8 797.9 797.1 796.3	798.4 797.4 796.4 795.4 794.6
Co $2p_{3/2}$	782.9 782.1	784.1 782.5 781.8 780.3	782.8 782.0 780.9 779.6	782.4 781.8	784.0 782.5 781.8	783.8 782.3 781.5 780.4
Mo $3d_{3/2}$	235.8 235.1	235.3	235.4	235.2 234.5		235.2 234.7
Mo $3d_{5/2}$	232.5	231.4	232.4	232.1		233.3 231.9
O 1s	531.3		531.0	531.5	531.2	531.1
Al 2s	119.1	118.4	119.0	118.8	118.8	118.7
Al 2p	74.0	73.6	74.0	73.9	73.7	74.0
C 1s	284.6	284.6	284.6	284.6	284.6	284.6
W $4f_{7/2}$				37.6 36.7 35.3	37.2 36.2 35.4	37.6 37.1 35.7 35.2
Ni $2p_{1/2}$						879.0 878.1 874.5 872.8
Ni $2p_{3/2}$						857.6 856.5

THE EFFECT OF METAL COMBINATIONS (CONTINUED)

Element	TS-15	TS-16	TS-17	TS-19	TS-20
		BINDING ENERGIES			
Ni $2p_{1/2}$		874.8 873.5 872.7	875.7 874.8 873.9	875.5 874.5 873.3	874.4 873.9
Ni $2p_{3/2}$		857.4 856.7 855.2	857.2	858.2 856.8	856.9 856.4
Mo $3d_{3/2}$		234.9 234.3	235.6 235.1	235.4	235.3
Mo $3d_{5/2}$		232.8 231.7	232.3	232.3	232.3
O 1s	531.7	531.1	531.1	530.7	531.1
Al 2s	118.8	119.0	118.5	118.7	118.9
Al 2p	74.0	73.9	73.7	73.8	78.9
C 1s	284.6	284.6	284.6	284.6	284.6
W $4f_{7/2}$	37.1 36.5 35.5 34.5	38.7 37.8 36.6 35.5			

THE EFFECT OF IMPREGNATION TECHNIQUE

Element	TS-17	TS-17S*	TS-19	TS-19S*	TS-20	TS-20S*
			BINDING ENERGIES			
Ni $2p_{1/2}$	872.5 873.8 875.5	872.4 870.8 875.3	873.8 876.1	871.4 874.7 876.7	873.4 874.6 878.1 879.4	870.6 873.1 873.3 874.3
Ni $2p_{3/2}$	856.0	854.3 852.0 856.9	856.0	854.1 857.5	856.1 859.1	853.3 855.7
Mo $3d_{5/2}$	231.9	228.9	232.1	228.5	232.1	227.6
Mo $3d_{3/2}$	234.9	231.6	235.1	231.5	235.1	230.6
Al 2s		119.5		119.1 119.8		119.2 121.2
Al 2p		74.6 72.6	74.0	74.5	73.8	74.1 75.3
S 2p		161.6		161.7		160.8
O 1s		531.9		532.5		531.6
C 1s	289.1	287.3	288.7	284.6	289.1	285.4

* Sulfided form.

REFERENCE COMPOUNDS

Element	Ni_6S_5	$NiMoO_4$	$Al_2(MoO_4)_3$	MoS_2	MoO_3	NiO
Ni $2p_{3/2}$	852.5	855.9				853.9
Ni $2p_{1/2}$	870.1	873.3				871.9
Mo $3d_{5/2}$		231.9	232.8	229.4	232.6	
Mo $3d_{3/2}$		235.0	235.0	232.5	235.8	
O 1s	531.9	529.9	530.3	532.0	530.6	528.9
Al 2s			119.2			
Al 2p			74.4			
S 2p	161.0			162.2		
S 2s	225.0			226.6		

THE EFFECT OF IMPREGNATION TECHNIQUE (CONTINUED)

Element	TS-11	TS-11S*	TS-18	TS-18S*	TS-21	TS-21S*
			BINDING ENERGIES			
Co $2p_{3/2}$	781.3 781.9	779.1 781.7 782.6	780.8 782.2	778.1 778.9 780.2	781.0 782.3	778.6 779.1 782.3
Co $2p_{1/2}$	796.2 797.5	793.2 794.2 796.1 797.3 799.3	796.2 796.8 798.3	790.6 792.1 792.9	796.8 797.8 799.2	793.5 794.1 796.4 796.9
Mo $3d_{5/2}$	231.7	228.0	231.8	227.4	232.1	228.2
Mo $3d_{3/2}$	234.5	231.1	234.9	230.5	235.2	231.1
Al 2s		118.6 119.0 119.8	118.4	118.6	118.8	119.3
Al 2p		74.0	73.5	73.5	73.4	74.4
S 2p		161.0		160.8		161.4
O 1s		531.2	530.2	531.1	530.6	531.5
C 1s	289.3	287.1	289.2	285.6	289.0	284.8

*Sulfided form.

REFERENCE COMPOUNDS

Element	Co_9S_8	CoO	$CoMoO_4$	$CoAl_2O_4$	C_3O_4
Co $2p_{3/2}$	778.1	780.3	780.8	781.6	780.7
Co $2p_{1/2}$	793.4	796.1	797.0	797.0	796.0
Mo $3d_{5/2}$			231.8		
Mo $3d_{3/2}$			232.5		
O 1s	532.2	530.3	530.0	531.0	530.2
Al 2s				118.6	
Al 2p				73.8	
S 2p	161.5				
S 2s	225.6				

Sahin, T.
Catalytic hydrotreating of solvent refined coal (SPC-II)

DATE	ISSUED TO
2 WEEKS USE	INTERLIBRARY LOAN